THE UNIVERSITY *of* BIRMINGHAM

Development of a Tube-Ball Mill Mathematical Model for Mill Condition and Safety Monitoring

THESIS

Paschalis Zachariades

Supervisor: Prof. Jihong Wang

Department of Electronic, Electrical and Computer Engineering,

University of Birmingham,

Edgbaston, Birmingham B15 2TT

UNIVERSITY OF
BIRMINGHAM

University of Birmingham Research Archive

e-theses repository

This unpublished thesis/dissertation is copyright of the author and/or third parties. The intellectual property rights of the author or third parties in respect of this work are as defined by The Copyright Designs and Patents Act 1988 or as modified by any successor legislation.

Any use made of information contained in this thesis/dissertation must be in accordance with that legislation and must be properly acknowledged. Further distribution or reproduction in any format is prohibited without the permission of the copyright holder.

ACKNOWLEDGWEMNTS

First, I would like to express my appreciation and acknowledgment to my supervisor, Professor Jihong Wang, for her valuable guidance, advices, encouragement and support.

Furthermore, I would like to express my appreciation Dr. Jianlin Wei for the valuable guidance and advices through the daily discussions we had.

Finally I would like to thank to Mr. Dave Williamson and Mr. Lee Taylor from EDF Energy and Mr. Mike Garwood from E·ON UK.

ABSTRACT

The PhD research project is to examine if it is possible to minimize the mill faults and fires in the Tube Ball mill operation by using a model based approach. The research outcome proves that the risks of mill fault can be monitored and alerted by implementing the model based on-line condition monitoring software that developed through the PhD project.

The main sources of fuel used in power stations across in the UK (UK Energy Statistics, 2005) to generate electricity are: Gas 40%, Coal 33%, Nuclear 19%, Electricity Imports 2.5%, Oil 1%, Hydro 1% and Other Fuels (e.g. Wind, Biomass) 3.5%. Coal-fired power stations in the UK generate around 35% of electricity. Coal fired power stations nowadays regularly use coal with higher volatile contents and Biomass materials to satisfy the government regulations on sustainable and renewable energy. This greatly increases the risks of explosions or fires in milling plants. However, there are no acceptable measurement methods available at the present and it is difficult to identify if there will be a fire in the mill. Therefore, the project is carried out from the study mill mathematical model to mill condition monitoring.

Monitoring the mill operation conditions only based on currently available on-site measurement without requiring any extra hardware is a cost effective solution and will pose a great challenge. A mathematical model of coal mills is developed using computational intelligent algorithms for prediction of potential mill faults. To achieve the objective, the following tasks were performed:

- developing a mathematical model using evolutionary computation techniques based on the on-site measurement data and to extend the model from E-Type vertical spindle mill to other types of coal mills
- on-line implementation of the mill model in collaboration with the researcher working on the BCURA sponsored project
- o identifying coal quality variations through recognizing the variation patterns of mill model parameters and dynamics
- estimating the quality of deposit coal in the mill, which is essential for predicting potential mill fires

The thesis reports the work completed and the main contributions of the thesis are summarized as follows:

- The pulverized coal mill mathematical model for E-Type vertical spindle mills has been analysed and refined which was developed through a previous research project.
- A multi-segment mathematical model for Tube-Ball mill is developed and the unknown parameters were identified using on-site measurement data from Cottam power plant, in which evolutionary computation techniques are adopted.
- The mill model has been verified by comparing the model predicted and measured mill variable values.
- Two associated computer programs were developed for mill parameter optimization and identification using intelligent algorithms. Two intelligent algorithms – Genetic Algorithms and Particle Swarm Optimization were implemented.

INDEX

ACKNOWLEDGWEMNTS ....

ABSTRACT II

ABBREVIATION LIST IX

1. INTRODUCTION 1

1.1. BACKGROUND 1

1.2. OVERVIEW OF POWER PLANT COALL MILL MODELLING 3

1.3. PROJECT OBJECTIVE 4

1.4. THESIS OUTLINE 4

1.5. PAPERS 5

2. THE OPERATION PRINCIPLE OF POWER PLANT COAL MILLS AND INTRODUCTION TO EVOLUTIONARY ALGORITHMS 7

2.1. OVERVIEW OF COAL MILLS 10

2.1.1. Low Speed Mills 10

2.1.2. Medium Speed Mills 11

2.1.3. High Speed Mills 13

2.2. STUDY OF TUBE BALL MILLS 13

2.2.1. Introduction....................14

2.2.2. Mill Ball spectrums and Tonnages....................15

2.2.3. Classifer 15

2.2.4. Dynamic Classifier Operation 17

2.2.5. Seal Air System 18

2.2.6. Instrumentation and Controls 18

2.2.7. Classifier Reject Dampers 18

2.2.8. M.E.L Aerodynamic Classifier 18

2.2.9. Fire Detection System 19

2.3. EVOLUTIONARY ALGORITHMS....................20

2.4. SUMMARY 21

3. MATHEMATICAL MODEL OF TUBE BALL MILLS 22

3.1. MATHEMATICAL MODEL OF VERTICAL SPINDLE MILL....................23

3.2. COMPARISON OF TUBE BALL MILLS WITH VERTICAL SPINDLE MILLS 26

3.3. MATHEMATICAL MODEL OF TUBE BALL MILL 27

3.3.1. Introduction 27

3.3.2. Mass Flow Analysis 28

3.3.3. Mill Product Pressure....................30

3.3.4 Power Consumption Analysis 31

3.3.5. Thermodynamic process *31*
3.4. MODEL MODIFICATION FOR THE TUBE-BALL MILL (1) 34
3.5. MODEL MODIFICATION FOR THE TUBE-BALL MILL (2) 36
3.5.1. New Equation for estimating coal flowing into the mill *36*
3.5.2. New equation for pulverised coal flow out the mill *37*
3.5.3. Formula for calculating air into the mill *38*
3.5.4. Last version of the model *39*
3.6. SUMMARY 41

4. PARTICLE SWARM OPTIMIZATION 42

4.1. INTRODUCTION 42
4.2. COMPUTATIONAL INTELLIGENCE 44
4.3. AN APPLICATION EXAMPLE OF PARTICLE SWARM OPTIMISATION 45
4.3.1. Introduction *45*
4.3.2. Particle swarm optimization algorithm *46*
4.3.3. Demos of PSO *49*
4.4. SUMMARY AND DISCUSSION 52

5. MILL PARAMETER INDEFICATION USING PSO AND COMPARISON WITH THE RESULTS USING GAS 54

5.1. INTRODUCTION 54
5.2. MODEL UNKNOWN PARAMETER IDENTIFICATION 55
5.3. MODEL MODIFICATION FOR THE TUBE-BALL MILL (1) 63
5.4. MODEL MODIFICATION FOR THE TUBE-BALL MILL (2) 67
5.4.1. New Equation for estimating coal flowing into the mill *67*
5.4.2. New equation for pulverised coal flow out the mill *69*
5.4.3. Formula for calculating air into the mill *69*
5.4.4. The modified version of the tube-ball mill model *70*
5.5. PARAMETER IDENTIFICATION USING GENETIC ALGORITHMS 74
5.6. SUMMARY AND DISCUSSION 78

6. MULTI-SEGMENT COAL MILL MODEL 79

6.1. INTRODUCTION 79
6.2. START-UP AND SHUT-DOWN SEQUENCES 79
6.3. MULTI-SEGMENT COAL MILL MATHEMATICAL MODEL 89
6.3.1. Model Segment I *90*
6.3.2. Model Segment II *92*
6.3.3. Model Segment III *93*

6.3.4. Model Segment IV *94*
6.3.5. Model Segment V *95*
6.4. PARAMATER IDENTIFICATION AND SIMULATION STUDY OF THE MULTI-SEGMENT MODEL 96
6.5. MODEL BASED MILL CONDITION MONITORING AND FAULT DETECTION 101
6.6. SUMMARY 108

7. SUMMARY AND RECOMMENDATION FOR FUTURE WORK 109

7.1. SUMMARY 109
7.2 RECOMMENDATIONS FOR FUTURE WORK 110

REFERENCE 111

APPENDIX 1 DATA LIST 119

FIGURE 2.1: COAL-FIRE POWER GENERATION PROCESS (BRITISH ELECTRICITY INTERNATIONAL, 1991)......... 9
FIGURE 2.2: LOW SPEED MILL – TUBE BALL MILL USED BY EDF ENERGY 10
FIGURE 2.3: MEDIUM SPEED MILL – PULVERISED FUEL MILL USED BY RWENPOWER 12
FIGURE 2.4: HIGH SPEED MILL (WEI PHD THESIS 2007) 13
FIGURE 2.5: CLASSIFIER (EDF MILL OPERATION MANUAL) 17
FIGURE 3.1: DYNAMIC PROCESS OF COAL FLOW PROCESS 29
FIGURE 3.2: THERMODYNAMIC PROCESS 32
FIGURE 3.3: SKETCH OF THE AIR FLOW IN THE TUBE BALL MILL 35
FIGURE 3.4: INLET RAW COAL FLOW CALCULATED BY EQUATION (3-25) 37
FIGURE 3.5: CALCULATED MASS FLOW RATE OF INLET AIR 39
FIGURE 4.1: SCHEMATIC OF THE MODEL'S COEFFICIENTS IDENTIFICATION 49
FIGURE 4.2: GIVEN CURVE OF THE F(T) VALUE 50
FIGURE 4.3: PSO RUNNING PERFORMANCE 51
FIGURE 4.4: EVOLUTION PROGRESS OF THE PSO...52
FIGURE 5.1: SCHEMATIC OF THE MODEL'S COEFFICIENTS IDENTIFICATION 55
FIGURE 5.2: CASE 1 OF MEASURED AND SIMULATED MILL RESPONSES 57
FIGURE 5.3: CASE 1 OF MILL INTERMEDIATE VARIABLES 57
FIGURE 5.4: CASE 2 OF MEASURED AND SIMULATED MILL RESPONSES 58
FIGURE 5.5: CASE 2 OF MILL INTERMEDIATE VARIABLES 58
FIGURE 5.6: CASE 3 OF MEASURED AND SIMULATED MILL RESPONSES 59
FIGURE 5.7: CASE 3 OF MILL INTERMEDIATE VARIABLES 59
FIGURE 5.8: CASE 4 OF MEASURED AND SIMULATED MILL RESPONSES 60
FIGURE 5.9: CASE 4 OF MILL INTERMEDIATE VARIABLES 60
FIGURE 5.10: CASE 5 OF MEASURED AND SIMULATED MILL RESPONSES 61
FIGURE 5.11: SKETCH OF THE AIR FLOW IN THE TUBE BALL MILL 64
FIGURE 5.12: MEASURED AND SIMULATED RESULTS CASE I (FIGURE 5.2) 65
FIGURE 5.13: INTERMEDIATE VARIABLES FOR THE CASE I DATA...65
FIGURE 5.14: MEASURED AND SIMULATED RESULTS FOR CASE 5...66
FIGURE 5.15: INTERMEDIATE VARIABLES FOR CASE 5 STUDY 66
FIGURE 5.16: INLET RAW COAL FLOW CALCULATED BY EQUATION (5-2) 68
FIGURE 5.17: CALCULATED MASS FLOW RATE OF INLET AIR 70
FIGURE 5.18: MEASURED AND SIMULATED RESULTS USING THE MODIFIED MODEL 73
FIGURE 5.19: INTERMEDIATE VARIABLES OF THE MILL USING THE MODIFIED MODEL.....................................73
FIGURE 5.20: MEASURED AND SIMULATED OUTPUT FOR THE DATA COLLECTED ON 9TH MARCH 2008, 00:00:00 ~ 12:00:00 (12 HOURS) 75

FIGURE 5.21: MODEL INTERMEDIATE VARIABLES FOR THE DATA COLLECTEDON 9TH MARCH 2008, 00:00:00 ~ 12:00:00 (12 HOURS) 75
FIGURE 5.22: MEASURED (SOLID LINES) AND SIMULATED (BROKEN LINES) USING PSO 76
FIGURE 5.23: MEASURED (SOLID LINES) AND SIMULATED (BROKEN LINES) USING GA 76
FIGURE 6.1: A TYPICAL START-UP SEQUENCE 79
FIGURE 6.2: A TYPICAL SHUT-DOWN SEQUENCE 80
FIGURE 6.3: VALUES OF A1 A2 EXHAUSTER MOTOR CURRENT AT THE STARTING-UP STAGE 81
FIGURE 6.4: VALUES OF MILL MOTOR CURRENTS WHILE STARTING-UP 82
FIGURE 6.5: VALUES OF A1 A2 FEEDERS MOTOR CURRENTS WHILE STARTING-UP 83
FIGURE 6.6: VALUES OF A1 A2 FEEDERS MOTOR CURRENTS WHILE STARTING-UP 84
FIGURE 6.7: VALUES OF A1 A2 EXHAUSTERS' MOTOR CURRENTS WHILE SHUTTING-DOWN 85
FIGURE 6.8: VALUES OF A1 A2 FEEDERS' MOTOR CURRENTS WHILE SHUTTING-DOWN 86
FIGURE 6.9: VALUES OF MILL MOTOR CURRENTS WHILE SHUTTING-DOWN 87
FIGURE 6.10: VALUES OF A1 A2 FEEDER MOTOR CURRENTS WHILE SHUTTING-DOWN 88
FIGURE 6.11: VALUES OF A1 A2 EXHAUSTER' MOTOR CURRENTS WHILE SHUTTING-DOWN 89
FIGURE 6.12: MULTI-SEGMENT COAL MILL MODEL 90
FIGURE 6.13: MODEL SIMULATED AND MEASURED OUTPUT USING DATA SET 1 98
FIGURE 6.14: MODEL INTERMEDIATE VARIABLES USING DATA SET 1 99
FIGURE 6.15: MODEL SIMULATED AND MEASURED OUTPUT USING DATA SET 2 99
FIGURE 6.16: MODEL INTERMEDIATE VARIABLES USING DATA SET 2 100
FIGURE 6.17: MODEL SIMULATED AND MEASURED OUTPUT USING DATA SET 3 100
FIGURE 6.18: MODEL INTERMEDIATE VARIABLES USING DATA SET 2 101
FIGURE 6.19: COMPARING THE MEASURED AND SIMULATED MILL OUTPUTS FOR THE DATA COLLECTED ON 9TH MARCH 2008, 00:00:00 ~ 24:00:00 (24 HOURS) 103
FIGURE 6.20: MODEL SIMULATED OUTPUTS WITH $\hat{K}_{17}$ RE-IDENTIFIED IN EVERY 5 MINUTES, ...104
FIGURE 6.21: MODEL SIMULATED OUTPUTS, WITH $\hat{K}_{17}$ RE-IDENTIFIED IN EVERY 5 MINUTES, WITH THE DATA COLLECTED ON 2ND MARCH 2008, 00:00:00 ~ 12:00:00 (12 HOURS) 104
FIGURE 6.22: MODEL SIMULATED OUTPUTS, WITH $\hat{K}_{17}$ RE-IDENTIFIED IN EVERY 5 MINUTES, WITH THE DATA COLLECTED ON 9TH MARCH 2008, 00:00:00 ~ 12:00:00 (12 HOURS) 105
FIGURE 6.23: MODEL SIMULATED OUTPUTS, WITH $\hat{K}_{17}$ RE-IDENTIFIED IN EVERY 5 MINUTES, WITH THE DATA COLLECTED ON 9TH MARCH 2008, 00:00:00 ~ 24:00:00 (24 HOURS) 107
FIGURE 6.24: THE SIMULATION RESULTS FOR DATA OBTAINED ON THE DAY OF THE INCIDENT HAPPENING 108

ABBREVIATION LIST

AC	Alternative Current
BCURA	British Coal Utilization Research Association
CO	Carbon Monoxide
CV	Calorific Value
EA	Evolutionary Algorithms
EDF Energy	Electricité de France
E.ON	Energy On - German Energy Company
GA	Genetic Algorithms
IEEE	Institute of Electrical and Electronic Engineers
kV	kilovolts
kW	kilowatt
M.E.L.	Maximum Exposure Limit
MW	Megawatt
PA	Primary Air
PF	Pulverized Fuel
PSO	Particle Swarm Optimization
R & D	Research and Development
RPM	Revolutions Per Minute
RWE	Rheinisch Westfälische Elektrizitätswerke
UK	United Kingdom
US	United States
VFD	Variable Frequency Drive
SO	Self-Organization

1. INTRODUCTION

1.1. BACKGROUND

Coal-fired power plants nowadays '*are required to operate more flexibly with more varied coal specifications*' and regularly use coal with higher volatile contents and biomass materials; this greatly increases the risks of explosions or fires in milling plants. *'The power stations are also obliged to vary their output in response to the changes of electricity demands, which results in more frequent mill start-ups and shut-downs'. Frequent start-ups and shut-downs of mills will also have an impact on power plant operation safety* (Scott, 1995, Fan *et al* 1994, Hamiane 2000). Although the increased risks are currently being mitigated by R&D work and the implementation of increased operational controls. Often coal mills are shut down and then restarted in a short period of time, even before the mill is cooled. Those shutdowns and restarts causes a fire hazard in the mill. Nevertheless fire can be cause from the lack of coal fed inside the mill as the temperature increases. '*in many cases, coal mills are shutdown and then restarted before they have cooled adequately, which creates a potential fire hazard within the mill. Mill fires could occur if the coal stops flowing in the mill and the static deposit is heated for a period*'. During the start stage of a mill from out-of-service mills fires can occur, in extreme cases, cause explosions can happen. Similarly, fires can be triggered in running mills which may lead to explosions on shut-downs. The result of a study indicated that as many as 300 "explosions" were occurring annually in the US pulverized coal industry (Scott, 1995). The UK PF Safety Forum had recently reported an increase in the frequency of mill incidents in the UK.

However, it is difficult to identify if there will be a fire in the mill. Outlet temperature and CO measurement are established methods of detecting fires in mills, but at present, they are not very effective for detecting small fires. The CO detection system becomes ineffective when the mill is in service due to dilution effects caused by primary air flow and associated oxygen content in the mill.

Nowadays in most of the coal-fired power plants are installed and operate advanced control and monitoring systems. Those systems helps the companies to collect data from different components and equipment such as boilers, generators etc. Furthermore those systems provide on-site data e.g. Coal Mills Inlet/Outlet Temperature, Primary Air Differential Pressures, Volume Flow Rate of coal into the mills and Primary Airflow into the mill etc. For a long period, the data has been captured and stored in archived databases that represent the history of the mills. The data recorded a number of events of failures and accidents, which the mill experienced during a certain period". From the current available on-site measurement data, combustion engineers have already noticed that the mill process data tends to have been slightly different where the fires have occurred in mills. The availability of such a large volume of data presents a challenge as to how to extract the useful, task-oriented knowledge from the data. Therefore, the project is proposed to develop a on-line model based mill condition monitoring method using evolutionary computation techniques.

1.2. OVERVIEW OF POWER PLANT COALL MILL MODELLING

Coal-fired power stations and generally power plants in order to satisfy the electricity demands with all the changes, they vary their outputs. Therefore power plants have to operate more flexible. *All plants must be capable of operating at partial load, frequently changing load and even starting up and shutting down daily'* (Rees *et al.* 2002). So the whole coal mill system needs to respond efficiently to plant load and coal quality. One of the major factors that is affecting the power plant performance during load changes is the coal delivery in the burner.

However, the coal mill has received much less attention from modelling and control specialists (Rees *et al.* 2003). Even to control and operate the Coal-Mill efficiently, many control issues must be solved, such as to get a exact quantity of the mill PF flow, CV fuel, any possible mill or coal choking at any stage of the operation procedure and the level of the mill wear. Operational safety and efficient combustion require better understanding to the milling process.

The study of the Tube Ball Mill and the Vertical Spindle Mill is going on for over 10 years, from the research team in the University of Birmingham under the supervision of Professor Wang.

Historically the research starts back in 1940s when many researchers worked on mathematical modelling for the mill and developing grinding theory. In the last 40 years there is a significant improvement. Starting with the work and research that was carried out by Austin back in 1971 and carried on from Neal at 1980. Neal work was focus on boiler complex and steam pressure. This work helped to identify the transfer functions of the coal-mill system. In the same Bollinger and Snowden, in 1983, based their research on the transfer functions.

Furthermore Austin in 1982 investigated the internal dynamics of the pulverising process and Kersting in 1984 in his research divided the process into 3 submodels. Finally in 1985, Robinson and Corti introduced a model based on 76 ordinary differential equations and a model treating the breakage phenomena as continuous process respectively.

In the last 20 years many researchers such as Fan and Rees in 1994, Palizban in 1995, Sato in 1996, Shoji in 1998, Fan and Rees in 1998, Zhang in 2002 and Wei in 2007 presented improved and different control-oriented models and steady-transient operations.

The work from Dr Zhang and Dr Wei were concentrating on Vertical Spindle mills. By following the previous work conducted by Dr Zhang and Dr Wei, my work in this project will focus on model challenging type of mill – Tube-Ball Mills.

1.3. PROJECT OBJECTIVE

The objective is to develop a mathematical model of Tube-Ball mills using intelligent algorithms for prediction of potential mill faults. The mathematical model for the coal mill is required in order to monitoring the differential pressure, mill temperatures and mass flow rate of pulverized coal and air flow in different operating conditions. There are three operating stages, the start-up, the steady state and the shut-down.

1.4. THESIS OUTLINE

The thesis is divided in seven chapters as briefly described below:

Chapter 1 gives the background, objectives and motivation of the research project.

Chapter 2 is divided in two parts. First part gives a background theory of the coal mills and power stations. A brief explanation of the principles of operations and the mechanical structure of the coal mills presented the first part. In the second part gives a detail description of vertical coals in order to relate the research to the previous work.

Chapter 3 is divided in two parts. The first part shows the mathematical model of vertical spindle mill where the research project was based. The second part is the mathematical model of the Tube Ball mill including the evolution of the mille model structure.

Chapter 4 presents the intelligent parameter identification and optimization method. Particle Swarm Optimization (PSO) is introduced and the detailed explanation of this method follows the introduction. The chapter finally gives a simple example of application of PSO.

Chapter 5 shows the results using the PSO method for the tube ball mill parameter identification. Also there is a comparison between PSO and GA method in the chapter.

Chapter 6 dedicates to the work of multi-segment coal mill model and test. The initial work for mill condition monitoring and fault detection is given in this chapter as well.

Chapter 7 contributes to concluding remarks and discussion for potential future work.

1.5. PAPERS

Here is a list of all the papers:

1. J L Wei, P Zachariades, J Wang, Further Study on Coal Mill Modelling for On-line Implementation, *2007 International Conference on Coal Science and Technology*, Nottingham, U.K. August 2007.

2. P. Zachariades , J. L. Wei, J. Wang, Development of a Tube-Ball Coal Mill Mathematical Model Using Intelligent Computation Techniques, *The 13th International Conference on Automation and Computing*, Stafford, U.K., Sept. 2007.

3. P. Zachariades , J. L. Wei, J. Wang, Development of a Tube-ball Coal Mill Mathematical Model Using Particle Swarm Optimization (P.S.O.), *World Congress on Engineering 2008, London*, UK, July 2008.

4. Jihong Wang, Jianlin Wei, and Paschalis Zachariades, Mathematic Modelling of Power Station Mill Systems for Condition Monitoring, *23rd IAR Workshop on Advanced Control and Diagnosis 2008*, PP246 – PP251, Coventry, UK, Nov. 2008.

5. Jianlin Wei, Jihong Wang, and Paschalis Zachariades, Mathematic Modeling and Condition Monitoring of Power Station Tube-ball Mill Systems, *American Control Conference 2009*, St. Louis, Missouri, USA, June 2009.

On a regular basis I have attended the meetings with the experiences engineers from Cottam power plant to review the progress of the research project work. Once we completed some milestones of the research work, we summarized them and presented them at the conferences.

Also every three months a technical report was submitted to the engineers of EDF Energy, E.On and to the project supervisor from BCURA.

2. THE OPERATION PRINCIPLE OF POWER PLANT COAL MILLS AND INTRODUCTION TO EVOLUTIONARY ALGORITHMS

Coal-fired power stations produce electricity by burning coal in a furnace through a boiler to heat water to produce high temperature and high pressure steam. The steam pushes a turbine rotating, which then drives a generator to produce electricity. Afterwards, the steam is cooled, condensed back into water and return to the boiler to start the process again. So the preparation of coal is the first step towards efficient and safe power generation. The raw coal will be fed into a mill and the coal will be grinded to fine powder which will be mixed with oxygen to burn in a furnace. In this chapter, the operation principles of coal mills will be explained, which include low, medium and high speed mills respectively.

For this project, data were collected from Cottam Power Station, which has a 2000 MW generation capacity owned by EDF Energy UK. The station is located in Retford, Nottinghamshire. So the tube-ball mill operation principle is described based on the mills used by Cottam Power Station.

'The coal-fired power generation process (British Electricity International, 1991) is shown in Figure 2.1 and explained below:

- Coal is feed (14) into the pulverised fuel mill (16).
- Coal is mixed with preheated air (24) with the aid of the draught fan (20).
- With the aid of high pressure the air-fuel mixture moved to the boiler.
- Then water flows inside the boiler to create steam

- The steam passes through to the pendant superheater (19). This steam increases the pressure and the temperature around 200 bar and 570°C respectively.
- The steam passes to the high-pressure turbine (11).
- There is a steam governor valve (10) providing the auto/manual option.
- Then the steam is returned back in the boiler reheater (21) where is reheated in order to build back again pressure and temperature.
- Then the steam is moved forward to the intermediate pressure turbine (9) and then to the low pressure turbine (6). Those are the 3 stages of the turbine process.
- After the completion of the above 3 stages the pressure and the temperature are low. With the aid of the cooling tower, cold water is coming in thermal contact with the steam in the condensor (8).
- The condensed water then passed through a feed pump (7) and through a deaerator (12). It is pre-warmed, first in a feed heater (13) and then in the economiser (23), before is return back to the boiler.
- The cooling water goes back into the cooling tower (1) and then is starting again the cooling water cycle by pumping the water into the condensor (8).
- The three turbines are connected to a 3-phase electrical generator (5) which generates intermediate level voltage, around 20-25kV.
- Then with the aid of a step-up transformer (4) the voltage is increase to 200-250kV for transmission and then is sent to the transmission system (3).
- An induced draft fan (26) drives the exhaust gas from the boiler to the chimney stack (27) The exhaust gas is passing through a electrostatic precipitator (25).

A diagram of a coal-fire power station is shown in Figure 2.1:

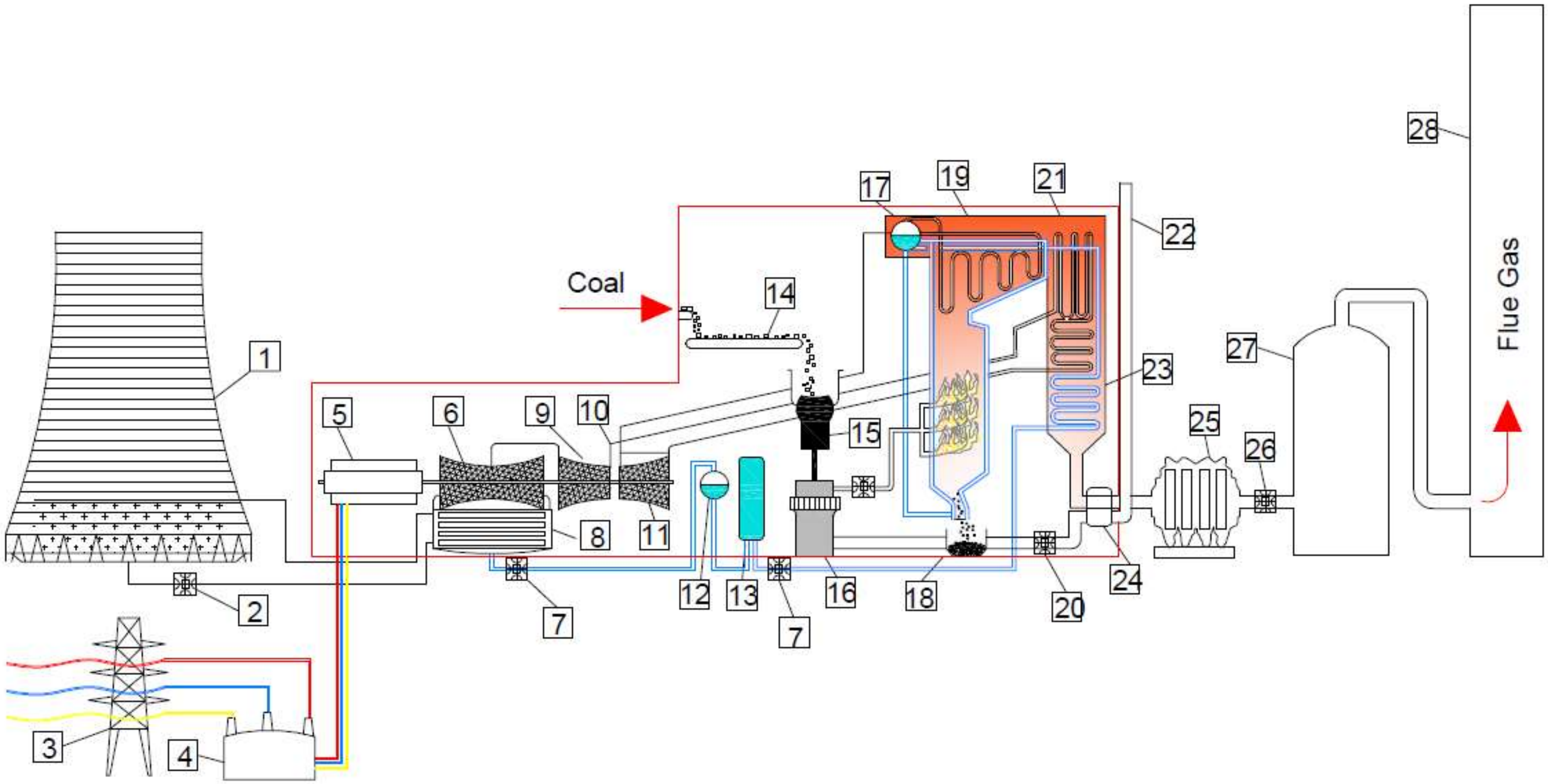

Figure 2.1: Coal-fire power generation process (British Electricity International, 1991)

2.1. OVERVIEW OF COAL MILLS

2.1.1. LOW SPEED MILLS

'The low speed mills are known as tube ball mills that operate at 15 to 20 RPM and mostly under suction'. The tube ball mill that is currently used in EDF Energy, at Cottam Power Station is shown on Figure 2.2.

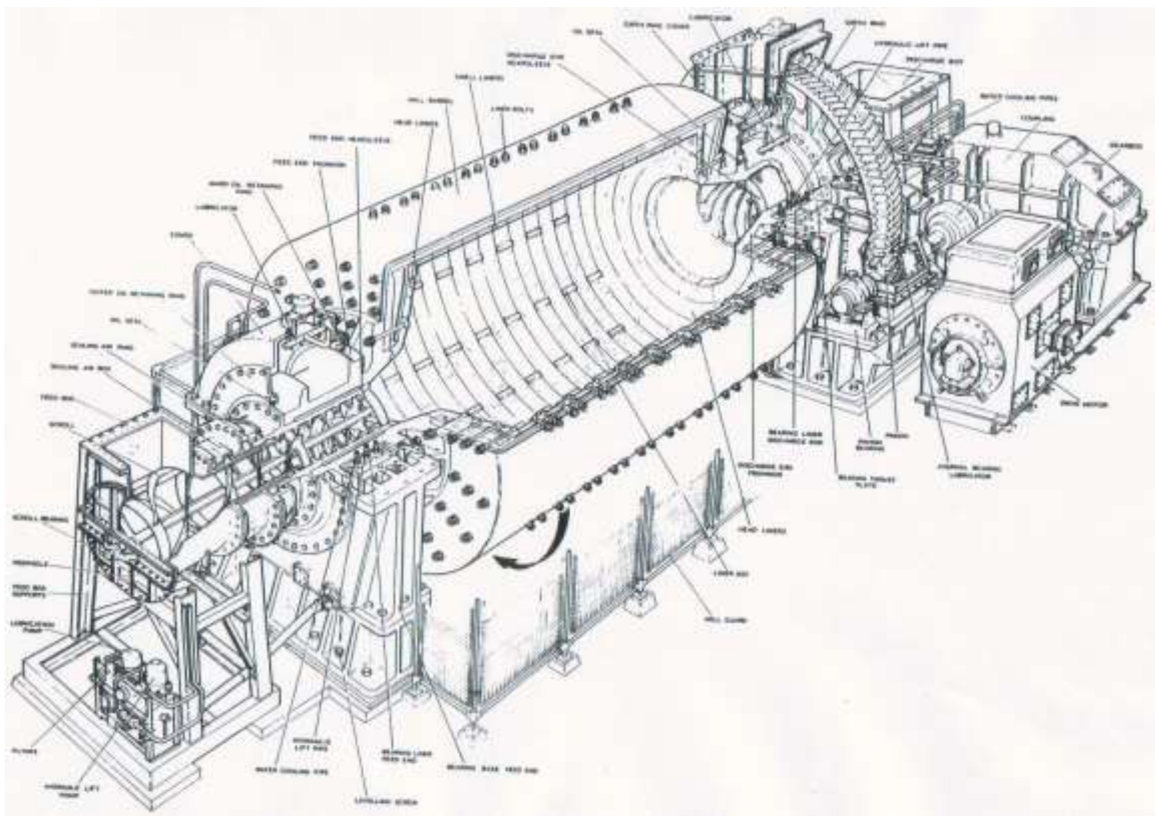

Figure 2.2: Low Speed Mill – Tube Ball Mill used by EDF Energy

'This mill is a motor driven barrel charged with steel balls. The barrel rotates horizontal. Coal is fed into the mill from the feed box. With the aid of the steel ball the coal crushes and the powder is extracted from the mill through the hot air flow.

2.1.2. MEDIUM SPEED MILLS

Nowadays most of the power generation companies are using medium speed mills to produce electricity. This kind of mills are known as vertical spindle mill. They operate in similar way as the low speed mills. Figure 2.3 shows a medium speed vertical spindle E-type mill that is used at the power stations of the RWEnpower.

'The medium speed mills are the most widely used in power generation industry nowadays, which are also known as vertical spindle mills. The principle of operation is similar with the principle of operation of the low speed mills. Again the coal is crushed between two plates one over the other. To explain the working principle, the medium speed vertical spindle E-type mill equipped at the power stations of the RWEnpower is used as shown in Figure 2.3.

The main structure of the mill is divided in three sections as follows:

- A base which supports the whole mill including the mill drive gear box
- A centre sections that covers the rotary grinding elements
- An upper section that contains the outlet turret, the classifier and the hydro-pneumatic units of the mill loading gear.

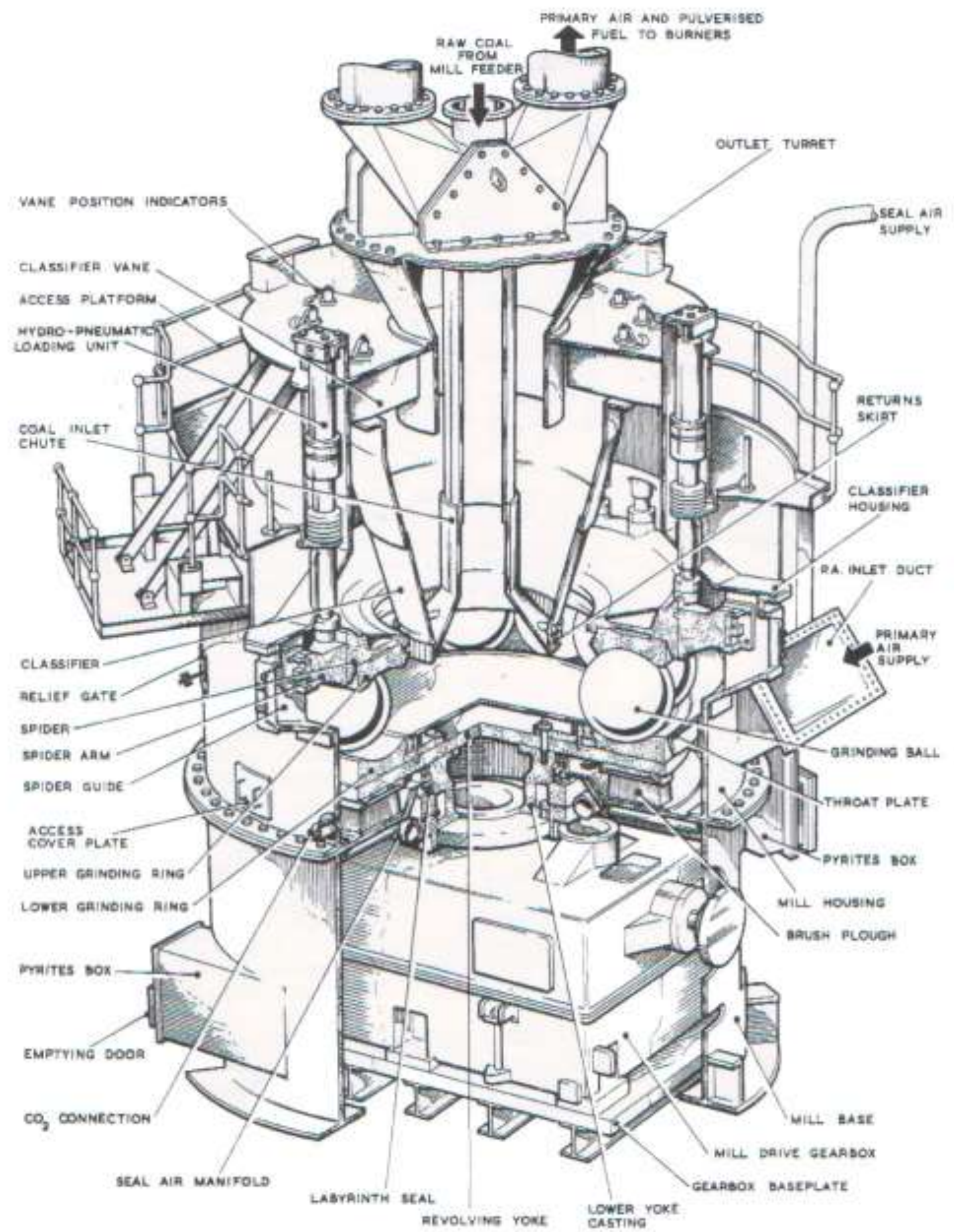

Figure 2.3: Medium Speed Mill – Pulverised Fuel Mill used by RWEnpower

2.1.3. HIGH SPEED MILLS

'The high-speed mills use hammer beaters that revolve in a chamber equipped with high wear resistant liners. In earlier days of the pulverized fuel firing, a number of high-speed mills developed, such as the Beater mill, the Impax mill and the Attrition mill. However, due to the rapid wear of hammer tips and the heavy maintenance required, the high-speed mills are not widely used for pulverized coal systems'.(Wei PhD Thesis 2007)

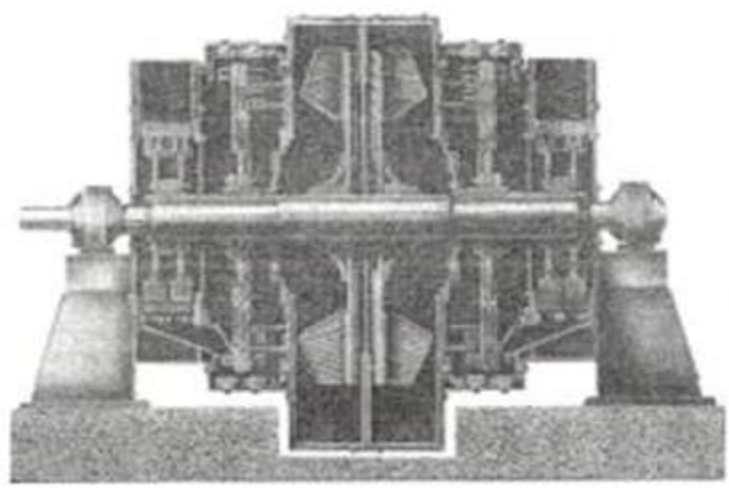

Figure 2.4: High Speed Mill (Wei PhD Thesis 2007)

2.2. STUDY OF TUBE BALL MILLS

The coal is stored in the bunker. The coal is delivered to a coal feeder. In order to control the flow of coal there is a discharge valve. Then the coal is discharged into the mill inlet chute.

There are 2 feeders for each mill and four mills for each boiler. The pulverised fuel (p.f.) that is produced in the mill moves to the classifier. The classifier is a separating chamber where with the aid of the air separates the overweight and oversized p.f. particles. Those particles are returned into the mill after passing through the rejects valve. There are two classifiers for each mill.

The p.f. is drawn from the classifier by a speed fan and is delivered to the burners. There are 4 burners that p.f. is delivered. There is a division point where separates the p.f. equally.

As the main objective of the project is to develop a coal mill model for Tube-Ball Mills, it is essential to understand the whole process of tube-ball mill operation. To achieve, three tube-ball operation manuals (EDF Energy Internal Report 1983, PF Systems Manual from EDF Energy, EDF Energy PF Code of Practice 2004) were provided by EDF Energy. The background study of the Tube-Ball mills was based on those three manuals.

2.2.1. INTRODUCTION

'The Tube Ball mill used by EDF is a motor driven tumbling barrel charged with steel grinding balls as shown in Figure 2.2. The mill drive is via a 1.6MW, 740 RPM, 3.3KV 3ph 50 Hz constant speed electric motor through a reduction gearbox. The speed of the mill barrel is 15 RPM being 75% of the critical speed.

Raw coal is delivered to the mill through the coal feeders. There are two exhauster fans that supply hot air to the mill. Usually the temperature is around 280^{O}C with a possibility to raise up the temperature up to 500^{O}C. Pulverised fuel (p.f.) flows through the discharge end of the mill to the M.E.L. classifiers. From there the p.f. is delivered to the burners with the aid of the exhausters. As it is mentioned above there 4 burners and the p.f. is equally divided for each burner.

2.2.2. MILL BALL SPECTRUMS AND TONNAGES

'The mills were balled up with their normal 120 Tone ball charge comprising of 60 tonnes of 50mm diameter balls and 60 tonnes of regarded balls which were in size range 29mm to 50mm'. The details of the specification are listed in Table 2.1.

Details of 4A Mill	
Ball charge	120 Tones of Balls (67 Tones 50mm & 53 Tones 32mm)
No. of Balls	660 000
Exhausters	A1 and A2, 1.75m impellers
Motors	A1 and A2, 95Amp. Rated
Liners	All liners changed to wavy chrome iron
Seals	Discharge end seals changed to face sealing type. Mill inlet relief damper soft lagged

Table 2.11: Details of 4A Mill

2.2.3. CLASSIFER

'The classifier is fitted directly on top of the mill outlet box. It controls the size of the particles of pulverised fuel passed to the burner (Figure 2.5). It is separating out oversized and overweigh particles and returning them to the mill via a rejects valve. The rest of the particles are carried to the burners. Particles below the size are carried suspended in air to the burners.

The classifier (dynamic style) consists of:

- *an outer housing with coal distribution control vanes,*
- *a vertical rotor assembly,*
- *a ring of fixed flow directing vanes,*
- *a reject hopper,*
- *a modular shaft and bearing assembly*
- *a drive system complete with drive belt,*
- *sprockets,*
- *an AC electric motor*
- *variable frequency inverter drive*.’

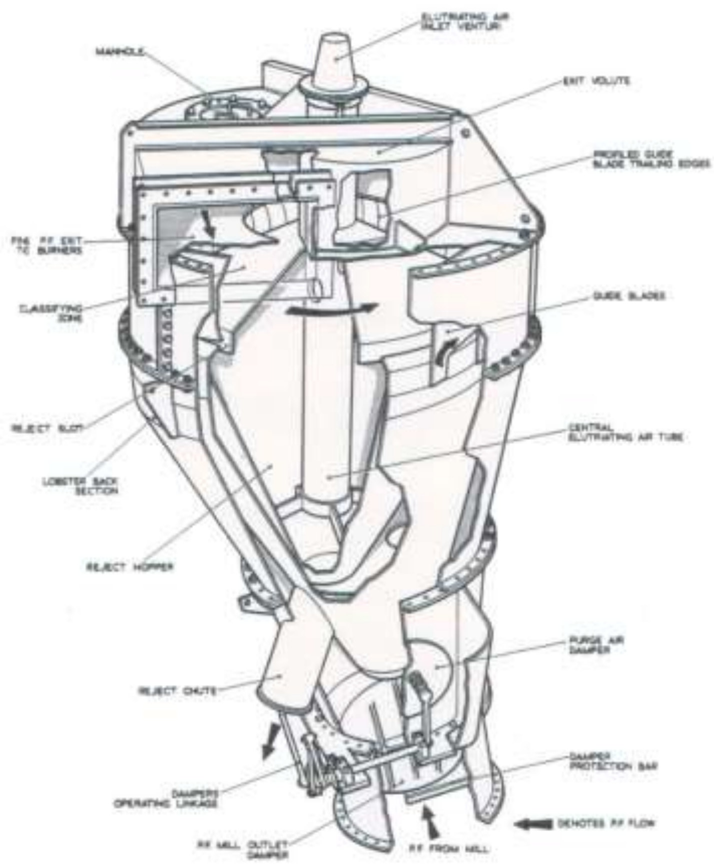

Figure 2.5: Classifier (EDF Mill operation Manual)

2.2.4. DYNAMIC CLASSIFIER OPERATION

The pulverised coal-air mixture enters the classifier. The mixture flows through a ring of fixed vanes and is directed to the rotor. Then the particles are separated based on their size. This separation is a result of the rotor external force that is produced according to rotors' speed. The higher the speed (rpm) the finer p.f. particles are through. The speed of the rotor is controlled by a variable speed drive motor. This motor operates based on the mill coal flow or mill airflow. Usually the rotor speed is between 75 to 150 RPM.

2.2.5. SEAL AIR SYSTEM

Seal air is used to seal between the classifier and the mill grinding section when the pulverizers are operating under pressure. The use of the system is to prevent any contamination inside the classifier or the opposite, escaping outside the classifier.

2.2.6. INSTRUMENTATION AND CONTROLS

Each classifier has its own instrumentation and control system. The classifier operation is controller via a variable drive controller (VFD). When the VFD operates outside the set up parameters an alarm is generated.

2.2.7. CLASSIFIER REJECT DAMPERS

Before the coal is fed into the classifier is pass though the classifier reject damper. Any over-sized coal particles that are rejected are moving back to the raw feed inlet conveyor from the classifier. The classifier reject damper can be set up on-line during the process.

2.2.8. M.E.L AERODYNAMIC CLASSIFIER

The original classifiers were removed and replaced with M.E.L. type classifiers. The original classifiers were install on the bottom but now the M.E.L. type classifiers mounted directly on the mill outlet box. There were some modifications as a result to improve the reject handling capacity of the system:

- Increasing the outlet scroll flight size

- The reject return pipework arrangement was modified to reduce the entry velocity of the rejects into the mill outlet scroll
- The mill outlet scroll centre tube was extended into the mill to cause a low velocity area where the rejects returned into the mill barrel
- ‘Blinker plates’ fitted to mill outlet scroll end to prevent recirculation of rejects into the mill outlet box

There are two main disadvantages as follows:

- Loss of boiler efficiency by allowing atmospheric cold air to enter the system and by-pass the air heater
- A 5% reduction in hot air flow through the mill with the consequential reduction in mill drying and carrying capacity.

2.2.9. FIRE DETECTION SYSTEM

The fire detection system is used to detect any sparks or flames during the operation of the pulverizing mill. It is a state of art electronic and computer integrated system. The principle of operation is to detect any light emissions in the visible to near infrared spectrum. Electronic circuit responds to the light emissions and the resulting signal is reviewed from a microprocessor system. This microprocessor is connected with the control system.

2.3. EVOLUTIONARY ALGORITHMS

There are four paradigms in evolutionary computation: Genetic Algorithms, Evolutionary Programming, Evolution Strategies and Genetic Programming.

The main fundamentals that are used for the design and implementation in Evolutionary computation are computational models of evolutionary processes. Many different evolutionary computational models have been studied in the past and they are known as evolutionary algorithms. The concept behind the evolutionary algorithms is to simulate the evolution of individual structures through the process of selection and perturbation. A key factor of the performance (fitness) of the individual structures is defined by an environment.

A population of P individual structures is initialized and then evolved from generation t to generation $t + 1$ by repeated applications of fitness evaluation, selection, recombination and mutation. The population size P is generally constant in an evolutionary algorithm, although there is no a priori reason to make this assumption.

Normally an evolutionary algorithm initializes its population. Then the evolutionary measures the fitness of each individual based its importance in some environment. There are two steps in selection, the parent selection and survival. In parent selection is decides who will become parent and how many children they can have e.g. higher-fitness individuals, higher possibilities to be parents and have more children. The children is a result of recombination and mutation, which is the information exchange between parents and further perturbs the children respectively. In the end the children are evaluated. In the survival step is decided who will survive in the population.

Particle Swarm Optimization (PSO) was initially introduced from Eberhant and Kennedy and is a new evolutionary computation technique. The optimization technique was based on the social behaviour of the birds in a flock. As it is already known each bird - particle (individual) flies according its own experience and its companions flying experience. There are three different versions in PSO, the Individual Best, Global Best and the Local Best. In the Individual Best each particle (individual) compares its own position with its best position. It is not using any other information except its own - individual. In the Global Best the particle - individual it is taking under consideration the position of the best particle from the entire swarm together with its own best position thus far. In Local Best the particle - individual is a combination of its own position with its neighbourhood particle position. This optimization technique (PSO) can solve different and difficult problems faster rather than the other evolutionary methods.

2.4. SUMMARY

This chapter has two parts. The first part includes a general description of the coal fire power stations with the principle of operation of coal mills. The second part of this chapter is an introduction to the evolutionary algorithms and the method that is used in the project, the Particle Swarm Optimization (PSO). The chapter is therefore served as an introduction to the background knowledge required for the project and read through the whole thesis.

3. MATHEMATICAL MODEL OF TUBE BALL MILLS

A wide range of literature survey shows that there are only a few reports on mathematical models of milling processes. A detailed milling process description can be found in Scott *et al.* 1995. '*An approximated linear transfer function model was*' obtained by Bollinger *et al*, in 1983. '*Mill modelling using system identification method was reported in 1984*' (Corti, L. *et al.* 1984). *With specially designed input signals, a linear discrete time model was obtained by Cheetham*, *et al* in 1990, *in which system time-delay was considered. An approximated linear time varying mill model was derived by Fan, G.Q. et al.* in 1994. *A polynomial matrix model was recently reported in 2000'* (Hamiane, M. *et al.* 2000). However, almost all the reported work describes the milling process by approximated linear mathematical models, which can not reflect the nonlinear features of coal mill systems. The complex nature of a milling process, together with the complex interactions between coal quality and mill conditions lead to immense difficulties for obtaining an effective mathematical model of a milling process.

Different from the early reported mill modelling work, the research team at Birmingham has developed a nonlinear mathematical model for vertical spindle coal mills using on-site measurement data and an evolutionary computation technique (Zhang *et al.* 2002, Wei *et al.* 2007). The team has also demonstrated a realistic technique for implementation of the model in real-time which could be used for on-line condition monitoring (Wei *et al.* 2006). Compared with the vertical mills, Tube-Ball mills are more complex in structure and have a much higher grinding capacity. The work for the E-type Spindle mill served the starting point for the work conducted in this project. At the same time, the previous work in vertical mill has been improved.

3.1. MATHEMATICAL MODEL OF VERTICAL SPINDLE MILL

The mathematical model for the vertical spindle mill has been developed from the previous research (Wei 2007, IEEE Trans Energy Conversion). It is described below.

$$W_{air} = 10 \cdot \sqrt{\Delta P_{pa}(t) \cdot \rho(t)} \tag{3-1}$$

$$\rho(t) = \frac{273}{273 + T_{in}(t)} \cdot \frac{28.8}{22.4} \tag{3-2}$$

$$W_c(t) = K_{fs} \cdot F(t)_s \tag{3-3}$$

$$W_{pf}(t) = K_{16} \cdot \Delta P_{pa}(t) \cdot M_{pf}(t) \tag{3-4}$$

$$\dot{M}_c(t) = W_c(t) - K_{15} \cdot M_c(t) \tag{3-5}$$

$$\dot{M}_{pf}(t) = K_{15} \cdot M_c(t) - W_{pf}(t) \tag{3-6}$$

$$P(t) = K_6 \cdot M_{pf}(t) + K_7 \cdot M_c(t) + K_8 \tag{3-7}$$

$$\Delta P_{mill}(t) = K_9 \cdot \Delta P_{pa}(t) + \Delta P_{mpd}(t) \tag{3-8}$$

$$\Delta \dot{P}_{mpd}(t) = K_{11} M_{pf}(t) + K_{12} M_c(t) - K_{13} \Delta P_{mpd}(t) \tag{3-9}$$

$$\begin{aligned}\dot{T}_{out}(t) &= [K_1 T_{in}(t) + K_2]\cdot W_{air}(t) - K_3 W_c(t) + K_{14} P(t) \\ &\quad - [K_4 T_{out}(t) + K_5]\cdot[W_{air}(t) + W_c(t)] + K_t T_{out}(t)\end{aligned} \tag{3-10}$$

where:

ρ: Primary air density (kg/m3)

M_c: Mass of coal in mill (kg)

M_{pf}: Mass of pulverized coal in mill (kg)

T_{out}: Outlet temperature of coal mill (°C)

ΔP_{mill}: Mill differential pressure (mbar)

ΔP_{mpd}: Mill product differential pressure (mbar)

W_{pf}: Mass flow rate of pulverized coal outlet from mill (kg/s)

P: Mill current (A)

ΔP_{pa}: Primary air differential pressure (mbar)

W_c: Mass flow rate of coal into mill (kg/s)

T_{in}: Inlet temperature of coal mill (°C)

W_{air}: Primary air flow rate into coal mill (kg/s)

$K_1,...K_{16}$: Unknown coefficients to be determined

EQUATION (3-1)& (3-2): It represents that the PA (primary air) flow rate is equation the rate at which air delivered by the primary fans, which has a square relation with the PA differential pressure and the density of air at mill inlet temperature.

EQUATION (3-3): It represents that the flow rate of coal mill is equal to the rate at which coal delivered by feeder.

EQUATION (3-4): It represents that the flow rate of PF (pulverized fuel) out of mill is equal to the rate at which Pf carried out of mill by the primary air flow.

EQUATION (3-5): It represents that the changes of mass of coal in mill is proportional to the coal flow into mill and disproportional to the fraction of coal.

EQUATION (3-6): It represents that the changes of mass of pulverized fuel in mill is proportional to the fraction of coal converted into pulverized but disproportional to the pulverized coal flow outlet from the mill.

EQUATION (3-7): It represents that the total amount of mill current consumed to run the mill motor is equal to the sum of the mill currents required to grid over surface area, to pulverized coal, and to run empty mill.

EQUATION (3-8): It represents that the mill differential pressure is proportional to the primary air fan produced differential pressure and proportional to the mill product differential pressure.

EQUATION (3-9): It represents that the changes in the mill product differential pressure is proportional to the pressure due to coal in mill and disproportional to the pressure at the last time step.

EQUATION (3-10): It represents the changes in mill outlet temperature is proportional to the heat contributed by hot primary air entering mill, disproportional to the heat lost to cool and moisture entering mill, disproportional to the heat lost to hot primary air and pulverized fuel leaving mill and proportional to the heat generated by grinding. In total this equation represents the heat balance model of the coal mill system.

3.2. COMPARISON OF TUBE BALL MILLS WITH VERTICAL SPINDLE MILLS

To adapt the above model for mathematical description of Tube Ball mills, a few issues need to be addressed.

- Feeder: The feeding system is different from the vertical mill or different from the system used in RWEnpower. There are no feeding coefficients available to be used as the system input. Equation (3-3) would be different. It is necessary to discuss with the engineers at EDF or other industrial partners to identify the way of calculation of the mass flow of raw coal into the mill.

- Extractor: There is an extractor at the outlet of the mill. It may be equivalent to an extra input force to the mill. It is essential to identify the mathematical description of the effect of the extractor. It is anticipated that Equations (3-5), (3-6) and (3-9) would be modified accordingly. And also, extra differential equations may be added to the original model.

- Heat balance: As the result of different mechanical structures, the heat balance equation may not be able to represent the tube ball mill accurately.

The first step to take the mathematical modelling work forward would be to solve the first problem above and run the original model with GAs to identify the necessary modification for the model.

3.3. MATHEMATICAL MODEL OF TUBE BALL MILL

3.3.1. INTRODUCTION

The procedure for coal mill modelling can be broken down into the following steps:

1) To derive the basic mill model dynamic equations through analyzing the milling process, applying physics and engineering principles and integrating the knowledge of experienced engineers
2) To identify unknown parameters using PSO techniques based on-site measurement data
3) To analyze the simulation results and interpret the parameters identified through the discussions between the researchers and experienced engineer
4) To return back to step 2 if any modification is required in order to improve the mill model or to conduct further simulation in order to validate the model.

The variables are divided into three groups, the inputs, intermediates and outputs.

Coal Mill Variables		
Input Variables	**Intermediate Variables**	**Output Variables**
- A1 feeder Actuator Position A_{P1} (%) - A2 feeder Actuator Position A_{P2} (%) - Mill outlet pressure ΔP_{Out} - Primary air temperature inlet the mill T_{in}	- Mass of coal in mill M_c - Mass of pulverised coal in mill M_{pf} - Mill product pressure ΔP_{mpd} - Mass flow rate of pulverized coal out of mill W_{pf}	- Mill inlet pressure ΔP_{In} - Mill outlet temperature T_{out} - Mill power consumed P

Table 3.1: List with Tube-Ball Mill Variables

With this organization of the data sets, the modelling study for the Tube-Ball mill has been carried out. The initial results are described in the following subsections.

3.3.2. MASS FLOW ANALYSIS

In the tube ball mill system, two feeders are equipped for providing raw coal flow into the mill. Each feeder is driven by a variable speed electric motor operating on a 415V, 3phase 50Hz supply. Right before the feed hopper, a banker discharge valve is installed to control the flow. In the system, both the feeder motor current and discharge valve actuation position are measured. Based on the available measurement, the feeder current could be converted to the equivalent coal mass flow rate into the mill. It is proposed that the mass flow rate is calculated by the following equation:

$$W_c(t) = K_{f1} \cdot A_{P1}(t) + K_{f2} \cdot A_{P2}(t) \tag{3-11}$$

where A_{P1} is the A1 feeder actuation position (%), A_{P2} is the A2 feeder actuation position (%), the K_{f1} and the K_{f2} are the converting coefficients for the A1 and A2 feeders. As the total mass of coal fed into the mill per hour is given in the manual from EDF [5], these two coefficients can be estimated to be 51.6 kg/s and 25.8kg/s.

From the fluid mechanism, the air blowing into the coal mil can be calculated by the following equation:

$$W_{air}(t) = K \cdot \sqrt{\Delta P_{In}(t) \cdot \rho(t)} \tag{3-12}$$

where ρ(t) denotes the primary air density (kg/m3), ΔP_{in} is the mill inlet differential pressure and K is a constant. Combining with the ideal gas law $\rho(t)$ at the temperature $T_{in}(t)$ can be represented by

$$\frac{273}{273+T_{in}(t)}\cdot\frac{28.8}{22.4}.$$

The hot air flow into the coal mill inlet into the coal mill can therefore be calculated by the following equation:

$$W_{air}(t)=10\cdot\sqrt{\Delta P_{In}(t)\cdot\frac{273}{273+T_{in}(t)}\cdot\frac{28.8}{22.4}} \tag{3-13}$$

To simplify modelling the coal mass quantity in mill, the coal in mill is classified as pulverized and un-pulverized two categories only. The dynamic process of coal mass flow during the mill operation can be schematically illustrated by Figure 3.1. The raw coal is fed into the mill by the feeders for pulverizing at a mass flow rate of W_c. By tumbling the raw coal M_c with a charge of steel balls, the pulverized coal M_{pf} is produced and carried out by the warm air flow at the mill outlet with a mass flow rate of W_{pf}. From the mass balance point of view (see Figure 3.1), the total mass of the pulverized coal output from the mill at the flow rate W_{pf} should be equal to the total mass of the raw coal mill flowing into the mill at the flow rate W_c eventually.

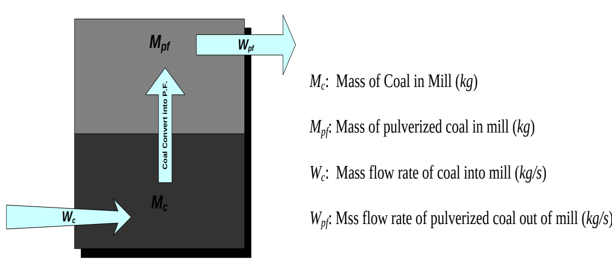

Figure 3.1: Dynamic Process of Coal Flow Process

Based on the principle of mass balance, Equations (3-14) ~ (3-16) are derived.

$$W_{pf}(t)=K_{16}\cdot\Delta P_{out}(t)\cdot M_{pf}(t) \tag{3-14}$$

$$\dot{M}_c(t) = W_c(t) - K_{15} \cdot M_c(t) \tag{3-15}$$

$$\dot{M}_{pf}(t) = K_{15} \cdot M_c(t) - W_{pf}(t) \tag{3-16}$$

where K_{15} and K_{16} are the unknown coefficients to be identified.

Equation (3-14) represents that the flow rate of PF (Pulverized Fuel) out of mill $W_{pf}(t)$ by the exhausters is proportional to the mass of pulverized coal in mill $M_{pf}(t)$ and the mill outlet differential pressure produced by the two exhauster fans $\Delta P_{Out}(t)$.

Equation (3-15) represents that the changes of mass of coal in the mill $\dot{M}_c(t)$ is proportional to the difference between the coal flow into mill $W_c(t)$ and a fraction of the coal pulverized $K_{15}M_c(t)$.

Equation (3-16) describes that the changes of mass of pulverized fuel in mill $\dot{M}_{pf}(t)$ is proportional to the difference between the fraction of pulverized coal $K_{15}M_c(t)$ and the pulverized coal flow out from the mill $W_{pf}(t)$.

3.3.3. MILL PRODUCT PRESSURE

While pulverizing the coal, the mill barrel rotates at around 15 rev./min. Due to the influence of aerodynamics, the mill product pressure ΔP_{mpd} is generated. The dynamic characteristics of the pressure variations are like the behaviours of a first order linear system. The pressure value is influenced by the pulverized coal in mill and the raw coal fed into the mill. The relationship can be described by equation:

$$\Delta \dot{P}_{mpd}(t) = K_{11} M_{pf}(t) + K_{12} M_c(t) - K_{13} \Delta P_{mpd}(t) \tag{3-17}$$

where K_{11}, K_{12} and K_{13} are unknown coefficients to be identified.

As mentioned above, there are two variable speed exhauster fans equipped at the outlet of the mill to extract the coal flow out to the burner. By combining the mill product pressure ΔP_{mpd} with the mill outlet pressure ΔP_{out}, we can derive the mill inlet pressure ΔP_{in}. The pressure is proportional to the mill outlet pressure ΔP_{in} and the mill product pressure ΔP_{mpd}, which can be modeled by the following equation:

$$\Delta P_{In}(t) = K_9 \Delta P_{pa}(t) + \Delta P_{mpd}(t) \tag{3-18}$$

where K_9 is an unknown coefficient to be identified.

3.3.4 POWER CONSUMPTION ANALYSIS

The power consume by the coal mill is normally considered as an indicator to the amount of load (raw coal and pulverized coal) of the coal mill, which is measured by the mill current for tumbling. It consists of three terms:

- Mill current required to tumble the M_{pf} inside of the coal mill
- Mill current required to pulverize the raw coal in mill;
- Mill current to run empty mill (using the term of K_8). The following equation describes the relationship:

$$P(t) = K_6 M_{pf}(t) + K_7 M_c(t) + K_8 \tag{3-19}$$

where K_6 and K_7 are the unknown coefficients to be identified and the empty mill current K_8 needs to be identified as well.

3.3.5. THERMODYNAMIC PROCESS

Distinguishing from the mineral pulverizers, the coal mills in power plants are involved with thermodynamics. How air is swept through the mill by two variable speed exhauster fans, and this air acts as both the drying and transporting agent for the coal. If the coal mill heating process is treated as happening in an isolated environment (see Figure 3.1), the heat input into the coal mill and the heat output from the coal mill complies with the heat balance rule. The heat into the coal mill Q_{in} includes the heat from raw coal Q_{coal}, the heat from the hot air Q_{coal} and the heat generated by the power consumes in tumbling and steel ball crashing Q_P. The heat out from the coal mill Q_{out} includes: the heat outlet in the pulverized coal Q_{PF} and the heat emitted from the mill body to the environment Q_e.

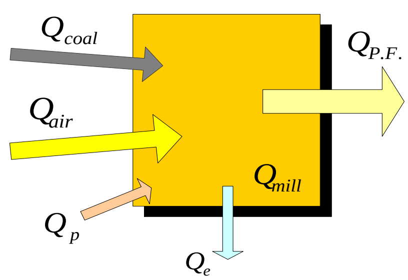

Figure 3.2: Thermodynamic Process

The heat into the coal mill Q_{in} can be obtained through equation (3-20), where the heat of hot air into the mill Q_{air} is calculated by the terms $K_1T_{in}W_{air} + K_2W_{air}$; the heat generated by the coal grinding process Q_P is represented by the term $K_{14}P$; and the heat of raw coal bringing into the mill Q_{coal} is described by the term K_3W_c.

$$\begin{aligned} Q_{in} &= Q_{air} + Q_p + Q_{coal} \\ &= [K_1T_{in}(t) + K_2]W_{air}(t) + K_{14}P(t) + K_3W_c(t) \end{aligned} \tag{3-20}$$

The heat output from the coal mill Q_{coal} can be obtained by equation (3-21), where the heat lost from the pulverized coal Q_{PF} is described by $K_4T_{out}(t)\cdot[W_{air}(t) +$

$+K_5 \cdot [W_{air}(t)+W_c(t)]$, and the heat emitted from the mill body to the environment Q_e is ignored at the moment as it has little effects onto the heart balance comparing with the other terms.

$$\begin{aligned} Q_{out} &= Q_{P.F.} + Q_e \\ &= K_4 T_{out}(t) \cdot [W_{air}(t)+W_c(t)] + K_5 \cdot [W_{air}(t)+W_c(t)] \end{aligned} \tag{3-21}$$

From the knowledge of thermodynamics, the difference between the input and output heat will cause changes in mill temperature. The rate of the temperature change is proportional to the unbalanced heat and also shows the characteristics of thermo inertias, which can be modeled by the following equation:

$$\dot{T}_{out} \propto K_t T_{out} + Q_{in} - Q_{out} \tag{3-22}$$

Substituting Q_{in} and Q_{out} into equation (3-22), we have:

$$\begin{aligned} \dot{T}_{out} = &[K_1 T_{in}(t) + K_2] W_{air}(t) + K_{14} P(t) - K_3 W_c(t) - \\ &[K_4 T_{out}(t) + K_5] \cdot [W_{air}(t) + W_c(t)] + K_{17} T_{out} \end{aligned} \tag{3-23}$$

where the notation of K_3 has a negative sign to indicate that the input coal W_c absorbs the heat from the mill instead of radiating heat. K_1, K_2, K_3, K_4, K_5, K_{14}, and K_{17} are the unknown coefficients to be identified.

Following the above analysis, the complete coal mill model can be described as follows, which does not cover the start up and shut down processes, where

A_{P1}: A1 feeder actuator position (%)

A_{P2}: A2 feeder actuator position (%)

ρ: Primary air density (kg/m^3)

M_c : Mass of coal in mill (kg)

M_{pf} : Mass of pulverized coal in mill (kg)

T_{out} : Outlet temperature of coal mill (^oC)

ΔP_{Out} : Mill outlet differential pressure (mbar)

ΔP_{mpd} : Mill product differential pressure (mbar)

W_{pf} : Mass flow rate of pulverized coal outlet from mill (kg/s)

P : Mill current (Amp)

ΔP_{In} : Mill inlet differential pressure (mbar)

W_c : Mass flow rate of coal into mill (kg/s)

T_{in} : Inlet temperature of coal mill (^oC)

W_{air} : Primary air flow rate into coal mill (kg/s)

K_{f1}, K_{f2} : A1 A2 feeder coefficients

$K_1, ...K_{17}$: Unknown coefficients to be identified

3.4. MODEL MODIFICATION FOR THE TUBE-BALL MILL (1)

The equations (3-17) and (3-18) are developed based on the working principle of a vertical spindle mill. The grinding wheels/mechanisms inside of a vertical spindle mill spin at high speed to grid raw coal which will be fed into grinding bowl. This rotating mechanism acts like a paddle spinning inside the mill and the mill product pressure ΔP_{mpd} is generated due to influences of aerodynamics. Equation (3-17) represents the dynamic characteristic of this mill produced pressure inside the mill, which is similar to a first order linear system and also the pulverized coal in mill and the raw coal fed into the mill contribute to the variation of the pressure.

From the working principle of a Tube-Ball mill (PF System Manual from EDF Energy), it is known that there is actually no rotation mechanism like paddles spinning inside of the mill. The mill product pressure can be ignored in this system. And from the air flow diagram shown below Figure 3.3, the mill outlet pressure is a compromised aerodynamic result among the mill inlet pressure, suction pressures generated by the Exhauster Fans A_1 and A_2, mass of raw coal inside of the mill and mass of pulverized coal inside of the mill. So the mill pressure model is modified and presented below in equation (3-24).

$$\begin{aligned} \Delta \dot{P}_{out} &= K_9 \cdot P_{E1} + K_{10} \cdot P_{E2} + K_{11} \cdot M_{pf} + K_{12} \cdot M_c \ldots \\ &\ldots + K_{13} \cdot \Delta \dot{P}_{in} + K_{18} \cdot \Delta P_{out} \end{aligned} \tag{3-24}$$

Where P_{E1} is the mill A_1 exhauster motor current, P_{E2} is the mill A_2 exhauster motor current, $K_9 \sim K_{18}$ are the coefficients to be identified, and the other symbols represent the same variables are explained above.

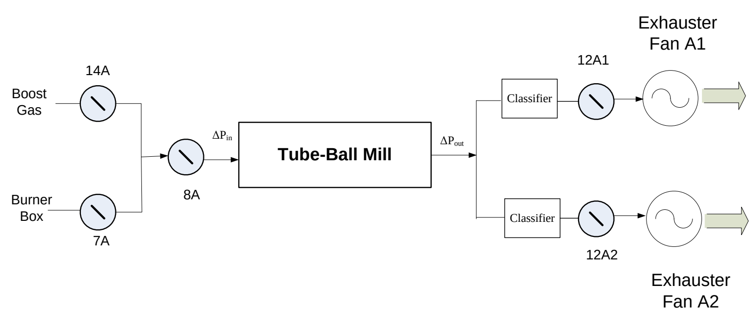

Figure 3.3: Sketch of the air flow in the tube ball mill

So using the data and doing the modifications to the tube ball mill model we can identified the unknown parameters.

3.5. MODEL MODIFICATION FOR THE TUBE-BALL MILL (2)

In 4th February 2008 a meeting was held in E.On Technology Centre in Nottinghamshire. In the meeting the engineers of E.On and EDF Energy proposed some changes in the modelling.

3.5.1. NEW EQUATION FOR ESTIMATING COAL FLOWING INTO THE MILL

Following the discussion, the zero values of actuation position of the feeders do not indicate coal feeders are off. A further conditional variable needs to be included to judge the situation of the feeder's operation, which is the mill feeder motor current. When the feeder motor is off (say the feeder motor current equals to 0 Amp or less than 1 Amp), zero value of the feeder actuation position (0%) represents the feeder is off. However, when the feeder motor is on (say the feeder motor current bigger than 1 Amp), zero value of the feeder actuation position (0%) represents the feeder is working on its minimum speed. So, two Boolean variables C_{f1} & C_{f2} are introduced into model for the modelling of the inlet coal flow W_c. The model equation is shown as follows:

$$W_c(t) = C_{f1}[K_{f1}A_{P1}(t) + 3.3] + C_{f2}[K_{f2}A_{P2}(t) + 3.3] \qquad (3\text{-}25)$$

where

A_{P1} is the A1 Feeder Actuation Position (%)

A_{P2} is the A2 Feeder Actuation Position (%)

$K_{f1} = 32.60$ and $K_{f2} = 31.64$

$C_{f1}=1$ if mill A1 feeder current $P_{F1}>1\ Amp$, else $C_{f1}=0$;

$C_{f2}=1$ if mill A2 feeder current $P_{F2}>1\ Amp$, else $C_{f2}=0$;

A simulation result of the inlet coal flow estimated by equation (3-25) is shown on Figure 3.4. From the figure, we can see the A1 Feeder and A2 Feeder work together for some periods and then works alone by itself. By judging the value of the feeder motor currents, the inlet coal flow is estimated correctly, and it matches the estimations from the engineers in power plant. For a certain period of time the A2 Feeder Actuation Position drops down close to zero. The mass flow inside to the mill drops also. Immediately the A1 Feeder motor starts. Nevertheless, the A1 Feeder Motor is on, around 20 Amps, zero value of the feeder actuation position (0%) represents the feeder is working on its minimum speed.

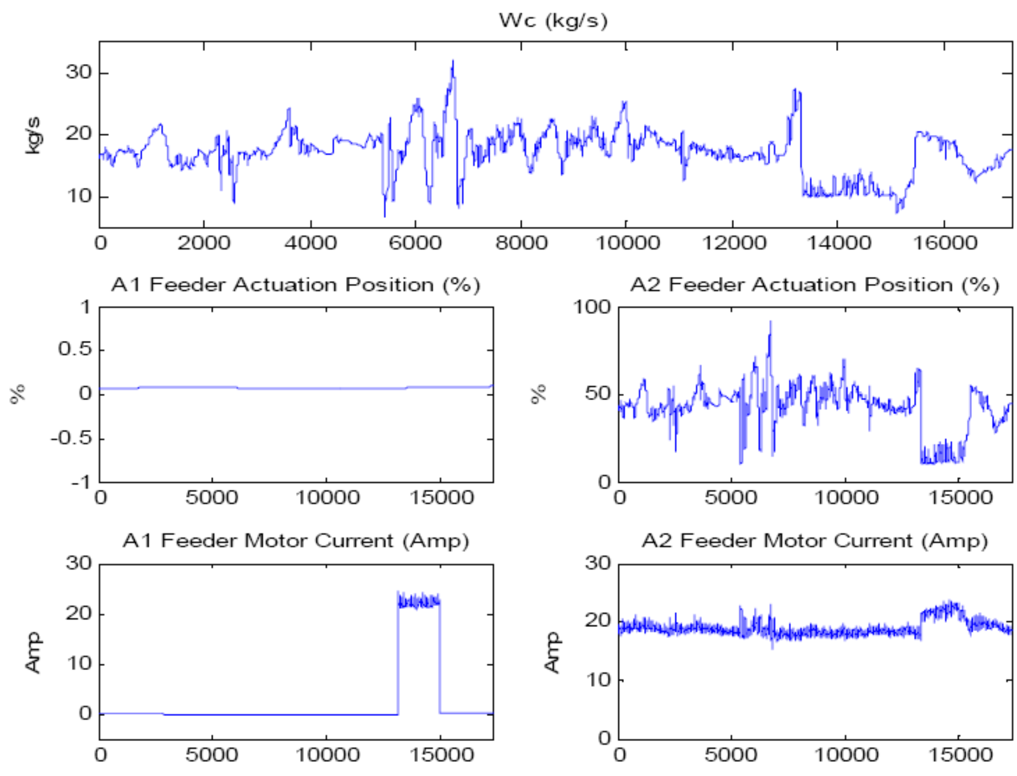

Figure 3.4: Inlet raw coal flow calculated by equation (3-25)

3.5.2. NEW EQUATION FOR PULVERISED COAL FLOW OUT THE MILL

Learning from the empirical formula of W_{pf} from E.On, the W_{pf} equation has now modified. The threshold value of P_{E1} & P_{E2} are set to be 22 Amps, and the offset value C is set to be 0.9kg/s at the moment.

$$W_{pf}(t) = K_{16}\Delta P_{out}(t) M_{pf}(t) + [C_{E1}P_{E2} + C_{E1}P_{E2}]K_{19} + 0.9 \qquad (3\text{-}26)$$

where

$C_{E1} = 1$ if mill A1 Exhauster current $P_{E1} > 22\ Amp$, else $C_{E1} = 0$

$C_{E2} = 1$ if mill A1 Exhauster current $P_{E2} > 22\ Amp$, else $C_{E2} = 0$

3.5.3. FORMULA FOR CALCULATING AIR INTO THE MILL

Following the empirical air flow formula from E.On, the inlet air flow is modified to be as shown below:

$$W_{air} = 12.42 \cdot \sqrt{\Delta P_{in\_Diff}} + 4.01 \qquad (3\text{-}27)$$

where:

ΔP_{in_Diff} is the mill inlet differential pressure (mbar)

W_{air} is the mass flow rate of inlet air (kg/s)

A simulation value of the inlet air flow equation (3-27) is shown on Figure 3.5 the value of the air flow is around 20kg/s

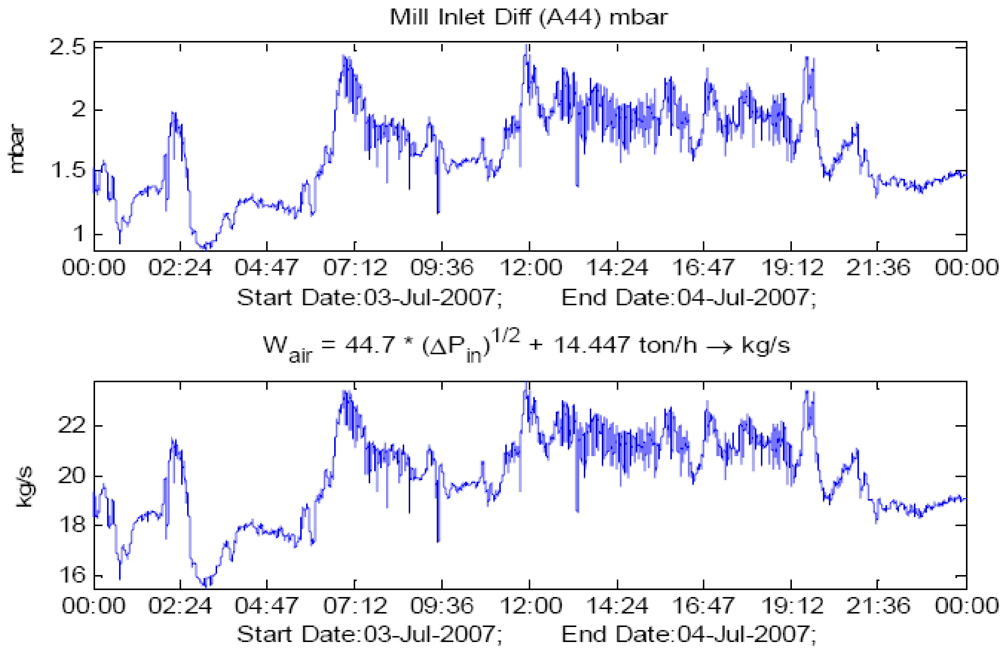

Figure 3.5: Calculated mass flow rate of inlet air

3.5.4. LAST VERSION OF THE MODEL

Based on simulation studies and consulting with the industry supervisors and engineers, the new version of the coal mill model is shown below:

$$W_{air} = 12.42 \cdot \sqrt{\Delta P_{in\_Diff}} + 4.01 \tag{3-28}$$

$$W_c(t) = C_{f1}[K_{f1}A_{P1}(t) + 3.3] + C_{f2}[K_{f2}A_{P2}(t) + 3.3] \tag{3-29}$$

$$W_{pf}(t) = K_{16}\Delta P_{out}(t)M_{pf}(t) + [C_{E1}P_{E2} + C_{E1}P_{E2}]K_{19} + 0.9 \tag{3-30}$$

$$\dot{M}_c(t) = W_c(t) - K_{15} M_c(t) \tag{3-31}$$

$$M_{pf}(t) = K_{15} \dot{M}_c(t) - W_{pf}(t) \tag{3-32}$$

$$\begin{aligned} \Delta \dot{P}_{out} &= K_9 \cdot P_{E1} + K_{10} \cdot P_{E2} + K_{11} \cdot M_{pf} + \\ &K_{12} \cdot M_c + K_{13} \cdot \Delta P_{in\_Diff} + K_{18} \cdot \Delta P_{out} \end{aligned} \tag{3-33}$$

$$\begin{aligned} \dot{T}_{out} &= K_1 T_{in}(t) + K_2 W_{air}(t) - K_3 W_c(t) + K_{14} P(t) - \\ &K_{20} T_{out} T_{in} + K_{17} T_{out} \end{aligned} \tag{3-34}$$

where:

A_{P1}: A1 feeder actuator position (%)

A_{P2}: A2 feeder actuator position (%)

ρ: Primary air density (kg/m^3)

M_c: Mass of coal in mill (kg)

M_{pf}: Mass of pulverized coal in mill (kg)

T_{out}: Outlet temperature of coal mill (^{o}C)

ΔP_{Out}: Mill outlet differential pressure (mbar)

ΔP_{mpd}: Mill product differential pressure (mbar)

W_{pf}: Mass flow rate of pulverized coal outlet from mill (kg/s)

P: Mill current (Amp)

ΔP_{In}: Mill inlet differential pressure (mbar)

W_c: Mass flow rate of coal into mill (kg/s)

T_{in} : Inlet temperature of coal mill (^oC)

W_{air} : Primary air flow rate into coal mill (kg/s)

P_{E1} : A1 Exhauster Motor Current (Amp)

P_{E2} : A2 Exhauster Motor Current (Amp)

C_{f1}, C_{f2} : A1 A2 feeders Boolean control coefficients

C_{E1}, C_{E2} : A1 A2 exhauster Boolean control coefficients

K_{f1}, K_{f2} : A1 A2 feeder coefficients

$K_1, ... K_{20}$: Unknown coefficients to be identified

3.6. SUMMARY

The mathematical mill model of the vertical spindle mill is shown in the beginning of this chapter. Based on this model, that was developed from the University of Liverpool; the mathematical mill model for tube ball mill was developed. Afterwards all the modifications of the tube ball mill mathematical model are presented up to the final version.

4. PARTICLE SWARM OPTIMIZATION

The mathematical model for the Tube-Ball mill has been derived in Chapter 3. It has been seen that there are around 20 unknown parameters to be determined. From the nature of the model, it is impossible to apply the traditional analytic parameter or optimization methods to obtain all the parameters. '*Then the numerical and data driven methods are searched. From the analysis, Genetic Algorithms and Particle Swarm computational evolutionary methods are suitable. Wei has applied the Genetic Algorithms to Vertical Spindle mill optimization'* (Wei 2007, PhD thesis). In this project, alternative method – Particle Swarm Optimisation, is investigated and compared with the Genetic Algorithms. So this chapter is dedicated to introduction of Particle Swarm Optimisation method. The study of Particle Swarm Optimization based on two books written by Kennedy J, Eberhart R and Clerc M (Kennedy & Eberhant 2001, Kennedy & Eberhant *et al* 1995).

4.1. INTRODUCTION

As we know for many years now the insects are living in colonies. Insects such as ants and bees are living in social insect colonies and they are organize. Each insect has its own duties and activities that it has to carry out every day. This daily basis individual work is done without any supervision.

In this social insect colony, each insect has specific tasks according to their morphology, age or chance. This specialization of the insects and performing individual together with their cooperative between them in the same time help them to live as an organism. The result of this combination is to be more efficient.

In some social insect colonies the insects-workers are vary according to their morphology. For example in ants there are different types of workers, the minors and the majors. The minor workers are performing different tasks and they have different specialization and duties comparing with the majors.

As it is mention above the insects are divided due to their size – morphology and none of these different subcategories of insects has a supervisor. This division of the insects in subcategories help them to organise the labour in the colony or nest. There are self-organized (SO). *Theories of self-organization (SO), originally developed in the context of physics and chemistry to describe the emergence of macroscopic patterns out of processes and interactions defined at the microscopic level.*

The self-organization of the insects offer to us powerful tools to transfer knowledge to the field of intelligent system design. As we know in daily basis the colony has many problems to solve such as finding food, extend their nest, to divide labour among the individuals efficiently, feeding the brood, respond to external challenges etc. Similar problems we face in engineering science section every day.

The colony can solve this problems in a flexible and robust way. Flexibility allows them to adapt any changes in the environment, robustness gives to the colony the ability to function even though some individual insects fail to perform or to complete their task and duties. Sometimes is necessary for the insects to design some robotic agents to behave in the same way like them at some level.

The modelling of social insects by means of SO can help design artificial distributed problem-solving devices that self-organize to solve problem-swarm intelligent systems. Until now only few applications of swarm intelligence are developed.

The swarm intelligence is difficult to program because the paths to problem solving are not prefined but are developing in the system from the interactions among individuals and between the individuals, and their environment. Hence using a swarm intelligence to solve a problem requires detailed knowledge of all the interactions that are important for such global behaviour.

4.2. COMPUTATIONAL INTELLIGENCE

Generally optimization methods are intensive, especially if the algorithms are not design and controlled properly. They require intelligent monitoring otherwise can give false results.

The easiest way to global minimization problems is to calculate all possible values of all of the parameters and is called enumeration. It is simple but not productive.

The main concept that stands behind the Gradient-based methods is first to select a point and estimating the local gradient. Then is selecting a new point for maximization or largest negative gradient for minimization. These methods are good for finding minima or maxima. Unfortunately are taking under consideration only local properties of the function. The only way to find global extremum is when is initialized close to the optimum solution.

Genetic Algorithms (GAs): Genetic Algorithms is a group of optimization modelling techniques which is based on the natural genetics and the theory of evolution by using a computational framework. *GAs are based on the Darwinian doctrine natural selection.* The main structure is called population and it is a number of individuals. Each individual has a dual representation. It has its own genotype, which contains the genome or chromosome information. Also it has its own phenotype. In Genetic Algorithms these genetic characteristics are simplified in a single chromosome. The main components in Genetic algorithms are as follows:

i. *Genetic coding*
ii. *Population*
iii. *Evaluation function/fitness value*
iv. *Reproduction*
v. *Crossover*
vi. *Mutation*

4.3. AN APPLICATION EXAMPLE OF PARTICLE SWARM OPTIMISATION

For future on-line implementation and more robust parameter identification and optimization method, an alternative optimization method has been studied, that is, Particle Swarm Optimization.

4.3.1. INTRODUCTION

Particle Swarm Optimization (PSO) was initially introduced from Eberhant and Kennedy and is a new evolutionary computation technique. The optimization technique was based on the social behavior of the birds in a flock. As it is already known each bird - particle (individual) flies according its own experience and its companions flying experirence. There are three different versions in PSO, the Individual Best, Global Best and the Local Best. In the Individual Best each particle (individual) compares its own position with its best position. It is not using any other information except its own - individual. In the Global Best the particle - individual it is taking under consideration the position of the best particle from the entire swarm together with its own best position thus far. In Local Best the particle - individual is a combination of its own position with its neighborhood particle position. This optimization technique (PSO) can solve different and difficult problems faster rather than the other evolutionary methods. Another advantage of PSO is that it has very few parameters to adjust which makes it particularly easy to implement.

In the previous project, the genetic algorithm (GA) has been employed for the coefficients identification while modelling the vertical spindle coal mill. As an intelligence search algorithm, the GA was first introduced in 1950s, and it offers fast converge and pretty good results. For the newly born PSO algorithm, it ages younger than 10 years, and has make great influence in the computational intelligence engineering. The author anticipates that this newly algorithm will offer great help to our current project. Theoretical and simulation studies of the PSO algorithm are carried out in this chapter.

4.3.2. PARTICLE SWARM OPTIMIZATION ALGORITHM

As mentioned in the above section, PSO is a population-based optimization algorithm. The population of PSO is called a swarm and individual in the population of PSO is called a particle, where each particle represents a potential solution. While applying PSO, the particles are flown through the hyperspace, and the position of each particle changes according to its own experience and that of its neighbors. Let $\vec{x}_i(t)$ denote the position of particle Pi in hyperspace, at time step t. The position of Pi is then changed by adding a velocity $\vec{v}_i(t)$ to the current position, i.e.

$$\vec{x}_i(t) = \vec{x}_i(t-1) + \vec{v}_i(t) \tag{4-1}$$

Depend on different velocity updating scheme which reflects how the social information exchange, the PSO can be divided into three different algorithms, which are the Individual Best PSO, Global Best PSO, and the Local Best PSO. Simulation studies show that the Global Best PSO offers the best performance and fastest convergence. The evolutionary process of the Global Best PSO is described below:

1) Initialize the swarm, $P(t)$ of particles such that the position $\vec{x}_i(t)$ of each particle $P_i \in P(t)$ is random within the hyperspace, with $t = 0$. Each particle represents a possible solution.

2) Evaluate the objective function ObjF of each particle, using its current position $\vec{x}_i(t)$.

3) Compare the performance of each individual to its best performance. If $ObjF\left(\vec{x}_i(t)\right)$ is less than its own best performance $pbest_i$, then: $pbest_i$ is set to be $ObjF\left(\vec{x}_i(t)\right)$, and its own best position $\vec{x}_{pbest_i}$ is set to be $\vec{x}_i(t)$.

4) Compare the performance of each particle to the global best particle. If $ObjF\left(\vec{x}_i(t)\right)$ is less than the global best performance $gbest$ then: $gbest$ is set to be $ObjF\left(\vec{x}_i(t)\right)$, and the global best position $\vec{x}_{gbest}$ is set to be $\vec{x}_i(t)$.

5) Change the velocity vector for each particle $\vec{v}_i(t)$ using the formula:

$$\vec{v}_i(t) = \omega * \vec{v}_i(t-1) + \rho_1\left[\vec{x}_{pbest_i} - \vec{x}_i(t)\right] + \rho_2\left[\vec{x}_{gbest} - \vec{x}_i(t)\right] \tag{4-2}$$

where, the ρ_1 and ρ_2 are random variables defined as $\rho_1 = r_1 c_1$ and $\rho_2 = r_2 c_2$, with $r_1, r_2 \in U(0,1)$, and the cognitive acceleration c_1 and the social acceleration c_2 are positive constants; ω is velocity weight, which is linearly decreased from a relatively large value ω_{start} to a small value ω_{end} through the course of the PSO run. If the velocity $\vec{v}_i(t)$ is bigger than the upper limit of the velocity $\vec{v}_{\max}$, then $\vec{v}_i(t)$ is set to be $\vec{v}_{\max}$.

6) Move each particle to a new position using the following formulas:

$$\vec{x}_i(t) = \vec{x}_i(t-1) + \vec{v}_i(t) \tag{4-3}$$

$$t = t + 1 \tag{4-4}$$

7) Go to step 2, and repeat until termination criteria reaches.

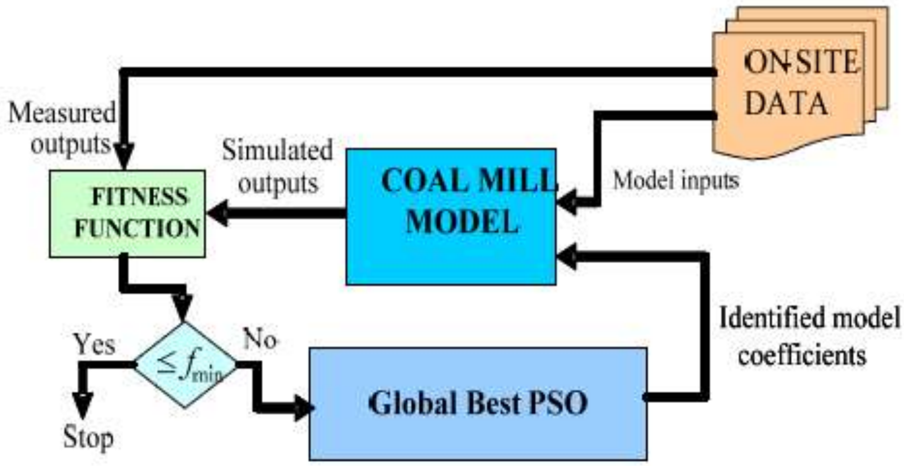

Figure 4.1: Schematic of the model's coefficients identification

4.3.3. DEMOS OF PSO

In order to demo the working process of the PSO, a simple problem is employed to illustrate the PSO performance. The task is of the problem is to find the value of 'a' and 'b' of the following function:

$$f(t) = a * \cos(t) + b * \sin(t) \qquad (4\text{-}5)$$

to minimize the error between the function values of the given curve as shown on Figure 4.1. Further restrictions of the parameters are given as follows: $t = [0 : 0.1 : 2\pi]$, $a \in [-10,10]$, and $a \in [-5,5]$.

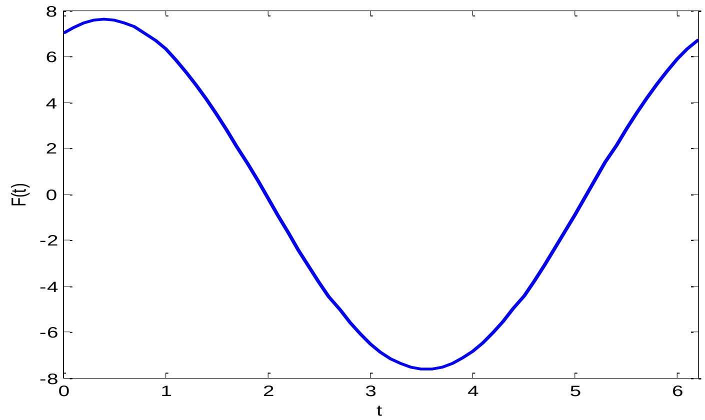

Figure 4.2: Given curve of the F(t) value

Since the aim of the problem is identify the 'a' and 'b' to minimize the different between their function values and the given curve, the cost function for the PSO to search is given as follows:

$$ObjF = \sum_{t=[0:0.1:2\pi]} \{[a * \cos(t) + b * \sin(t)] - F(t)\} \quad (4\text{-}6)$$

where F(t) are the given value of the curve as shown in Figure 4.2; a and b are the parameters that need to be identified by PSO.

List of PSO Properties	Value Setting
Number of iteration	1000
Swarm Size	40
Cognitive Acceleration c_1	2
Social Acceleration c_2	2
Value of velocity Weight at the beginning of the PSO ω_{start}	0.9
The fraction of maximum iterations for which the velocity weight is linearly varied	1.0

Value of velocity Weight at the end of the PSO ω_{end}	0.4
Maximum velocity $\bar{v}_{\max}$	10

Table 4.2: Properties setting of PSO

Setting the PSO properties as shown in Table 4.2, and let the PSO run for 1000 iterations, it founds the identified results for 'a' and 'b' are: $a=7$ and $b=3$.

The overall PSO running performance is shown in Figure 4.3. It converges at around 700 iterations, and takes 5.3 seconds to find the identified results. The evolutionary progress of the PSO is shown in Figure 4.4. The left column presents the evolutionary progress of the particles in the iteration 1, 100, and 1000, where it can be seen that all the particles fly towards the optimization point (7,3), and converged at 1000 iteration. The right column presents the evolutionary progress of the fitting curves process. In the iteration 1, 100, and 1000, the particle with best performance in the group of the current iteration is picked up, and applied to Equation (4-29) to draw the simulated curve (red line) against the given measured curve (blue line).

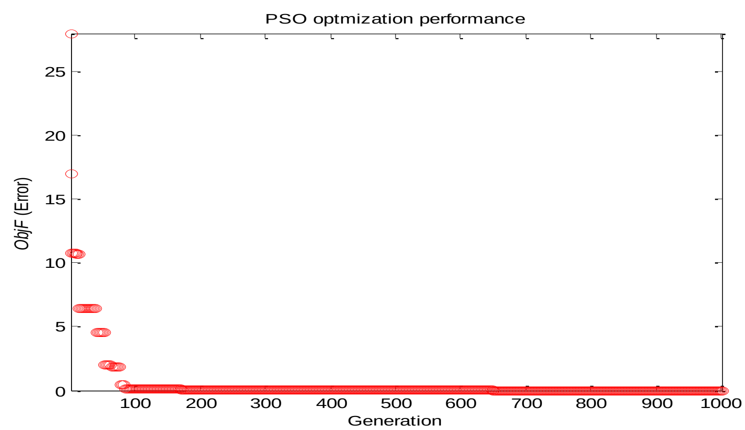

Figure 4.3: PSO running performance

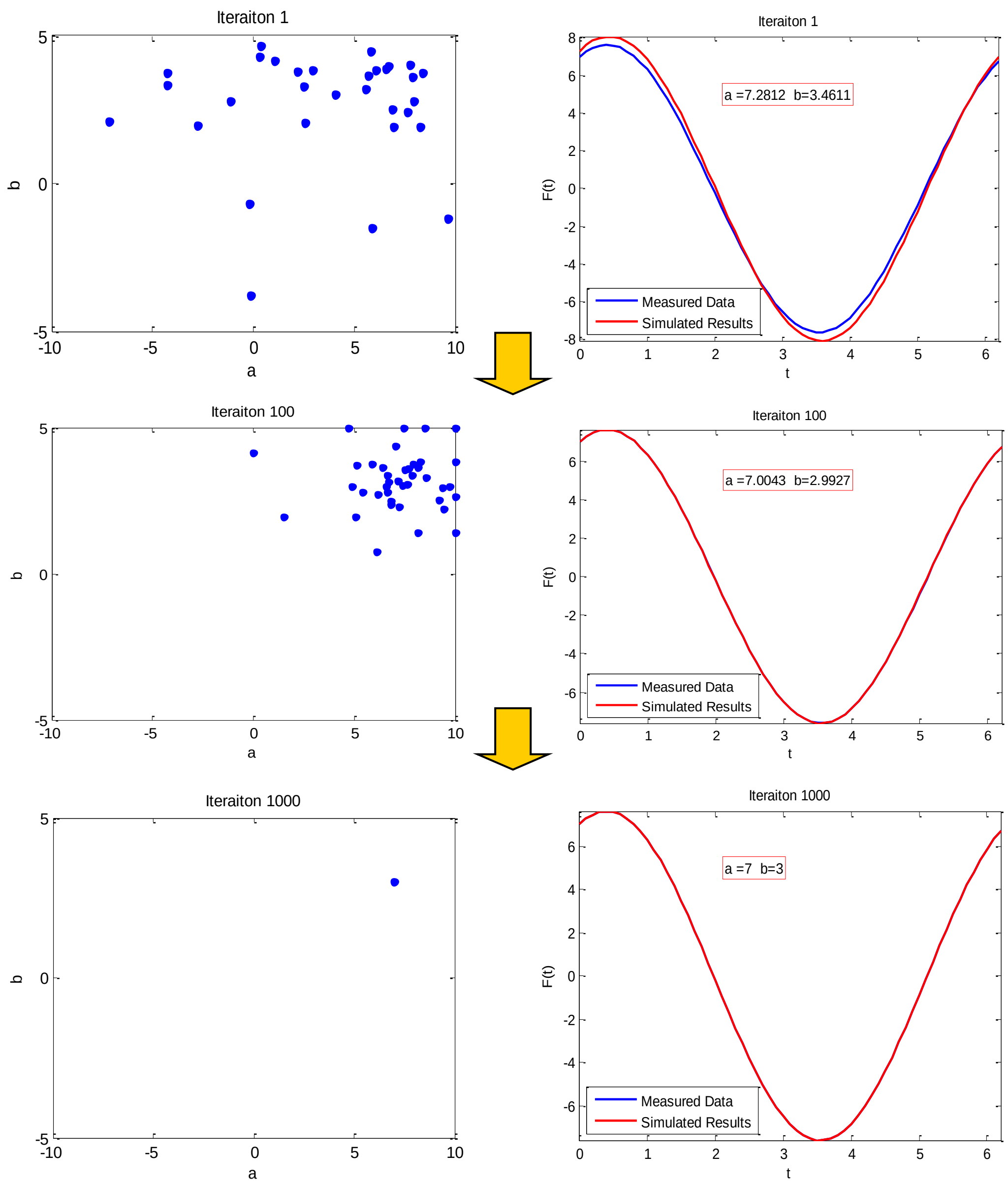

Figure 4.4: Evolution progress of the PSO

4.4. SUMMARY AND DISCUSSION

The chapter started from description of general intelligent optimization algorithms and explained what the main factors and functions are required. Then the chapter moved onto the newly born intelligence searching algorithm, PSO algorithm. An optimization/parameter identification example is employed to illustrate the working process of the PSO. From the simulation result, it shows that the PSO algorithm works well in identifying the parameters base on the measured data curve provided. The algorithm works very well, and the author anticipates this algorithm will provide great help to the project. The next challenge is to transform the optimization method to suit for dynamic process optimization for coal mill modelling and parameter identification.

5. MILL PARAMETER INDEFICATION USING PSO AND COMPARISON WITH THE RESULTS USING GAS

5.1. INTRODUCTION

Two parameter identification methods using intelligent algorithms have been described in Chapter 4. The algorithms have been implemented in Matlab, which will be used as the main tool for Tube-Ball mill unknown parameters identification. Then the results obtained using PSO has been compared with the results using GAs. This chapter will report the identification results and compare these two methods with multi sets of data collected from EDF Energy Cottam power station. The data sets cover different periods of mill operations. For example, initially the data covered a period of month; from the 1st of January 2007 until the 31st of January 2007; with a sampling period of 5 minutes. After 6 months new data were collected from EDF Energy. The data covered a period of 10 days; from the 27th of June 2007 until the 7th of July 2007; with sampling period of 5 seconds this time. After 3 months new data were collected from EDF Energy. The data covered a period of 2 days; 23rd of October 2007 and 25th of October 2007. A list of the data sets is provided in Appendixes.

The chapter starts from listing all the data sets to give an overall picture for what data sets are available for the task of this chapter. Parameter identification with a set of data is given and then the chapter moves onto model validation using different sets of data. Finally, the comparison for two different intelligent algorithms is presented.

5.2. MODEL UNKNOWN PARAMETER IDENTIFICATION

As a first step, four sets of sections data are chosen to represent the mill operation status. The on-site measurement mill data are organized in two groups. One group is used to identify the model parameters and the other to verify the identified results. For identification the following data were used:

- Section 1_1: 01/Jan/07 10:00:00 until 02/Jan/07 19:00:00
- Section 1_3: 09/Jan/07 08:00:00 until 11/Jan/07 16:00:00

For verification the data were used:

- Section 1_4: 21/Jan/07 00:00:00 until 22/Jan/07 23:55:00
- Section 2_10: 06/Jul/07 00:00:00 until 07/Jul/07 00:00:00

To obtain the unknown parameters or coefficients of the mill model, intelligent algorithms are adopted for the parameter identification. Two algorithms are investigated; they are Genetic Algorithms (GAs) and Particle Swarm Optimisation. The identification process using GAs can be illustrated by the block diagram shown in Figure 5.1.

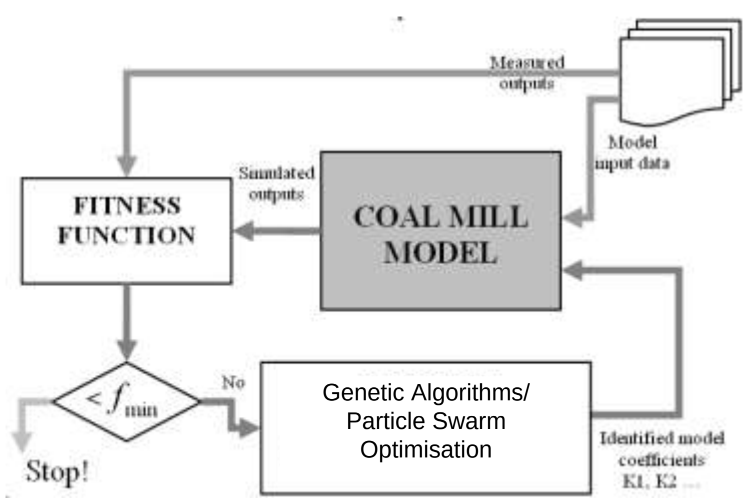

Figure 5.1: Schematic of the model's coefficients identification

One identification case is demonstrated and explained here. The model parameters are identified using the data set 1and the identified parameter values are listed in Table 5.1.

Table 5.1 The Identified Model Coefficients

K_1 = 0.00901453	K_2 = 0.001
K_3 = 0.00001	K_9 = 0.00405967
K_{10} = 0.0029524	K_{11} = 0.000374
K_{12} = 0.00013713	K_{13} = 5.460076
K_{14} = 0.02	K_{15} = 0.0013
K_{16} = 0.000091913	K_{17} = 0.14524
K_{18} = -0.812036	K_{19} = 0.01669
K_{20} = 0.000003256	

We had many discussions and meetings with engineers from Cottam power plant, considering the best selection for the boundaries. The final boundaries were proposed by the engineers based on their previous work and experience. The values that are shown above are not final but are updating all the time as the implemented software is running.

Using the data listed in the previous section, for the identification of the unknown parameters were carried out with the initial version of the Tube-Ball mill model. The results are shown in Figure 5.2-5.10.

The red curves are the measured data of the system outputs and the blue curves are simulated variables.

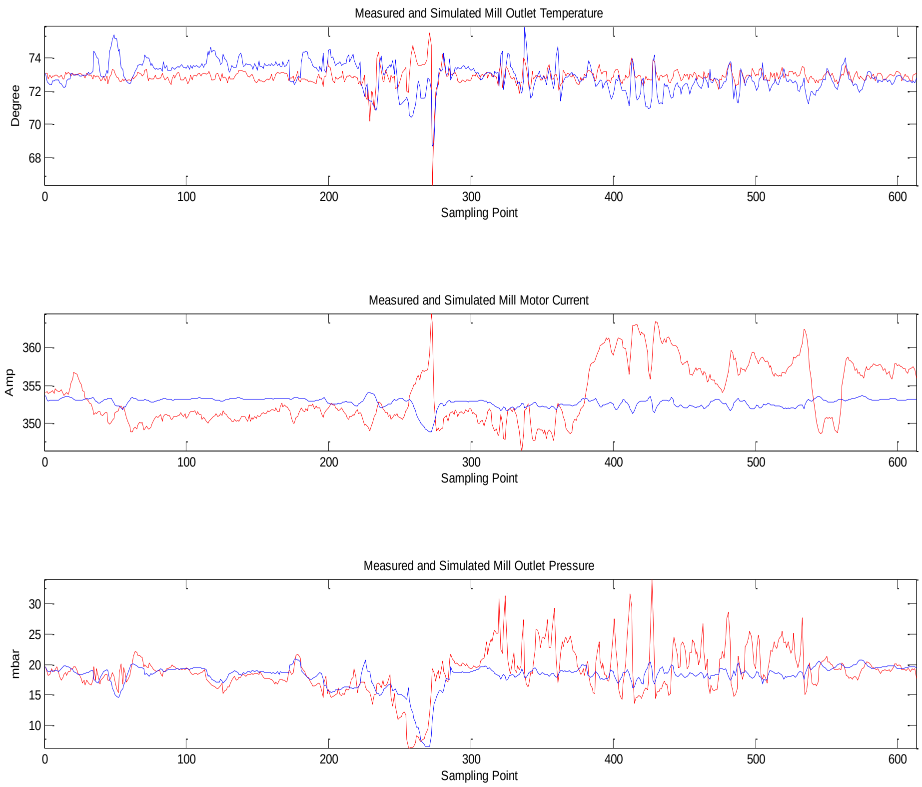

Figure 5.2: Case 1 of measured and simulated mill responses

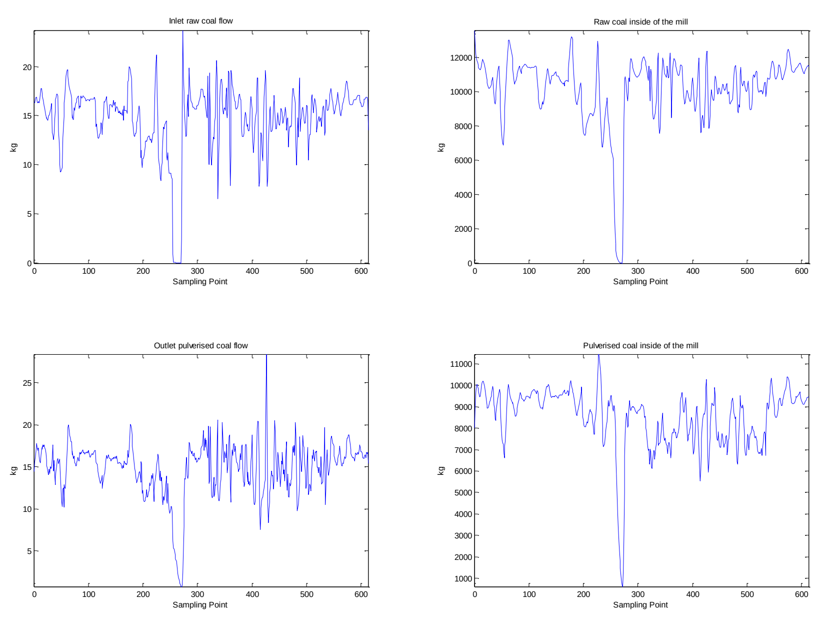

Figure 5.3: Case 1 of mill intermediate variables

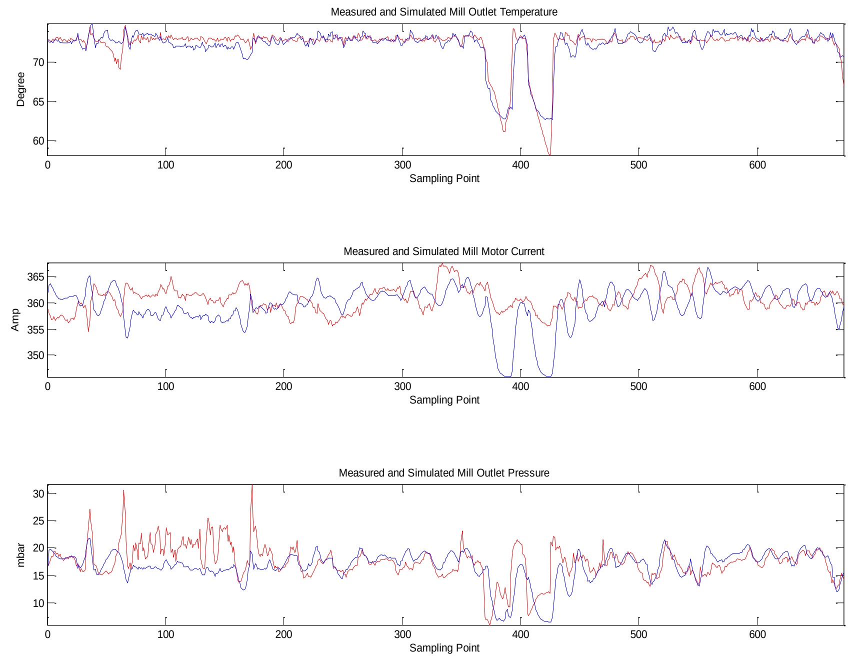

Figure 5.4: Case 2 of measured and simulated mill responses

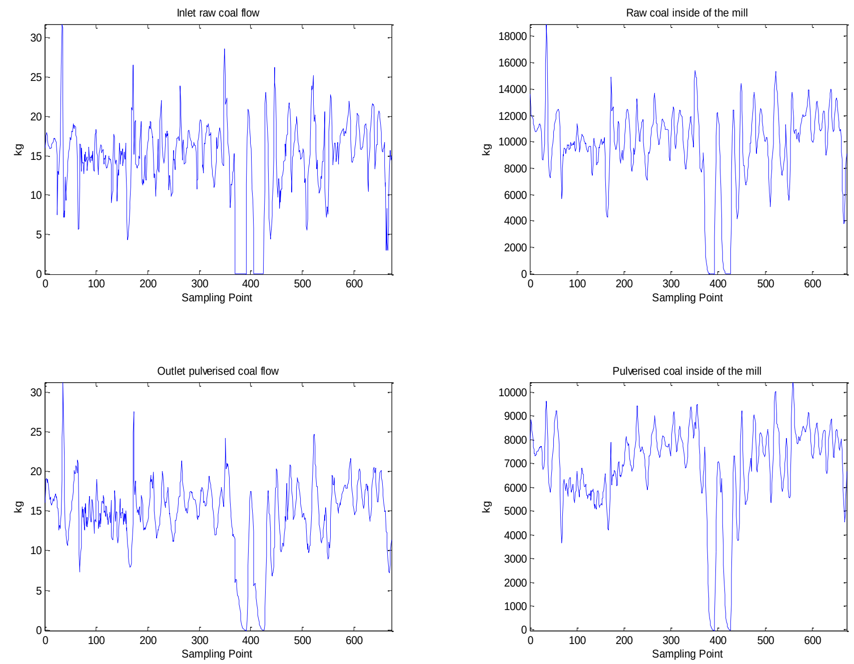

Figure 5.5: Case 2 of mill intermediate variables

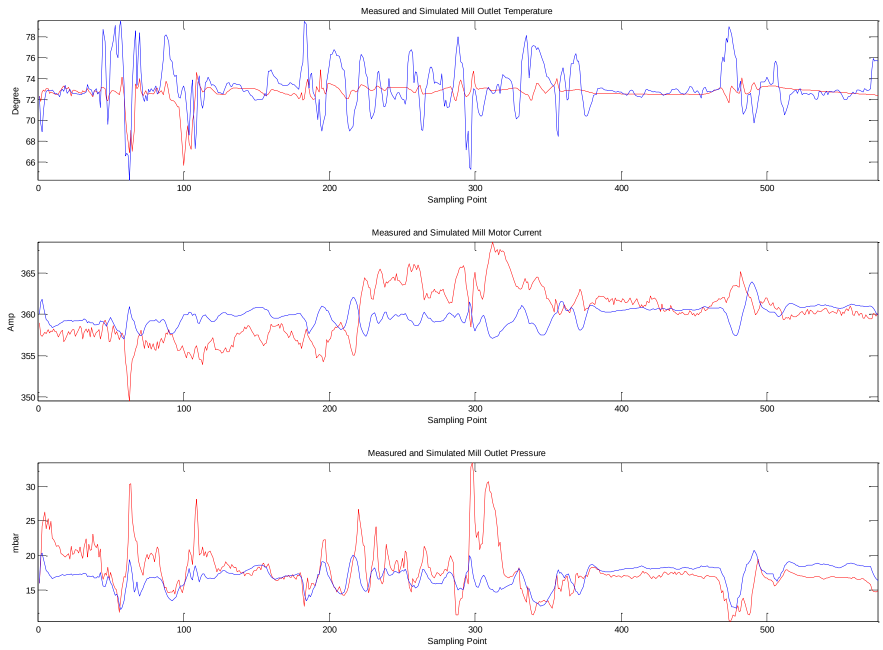

Figure 5.6: Case 3 of measured and simulated mill responses

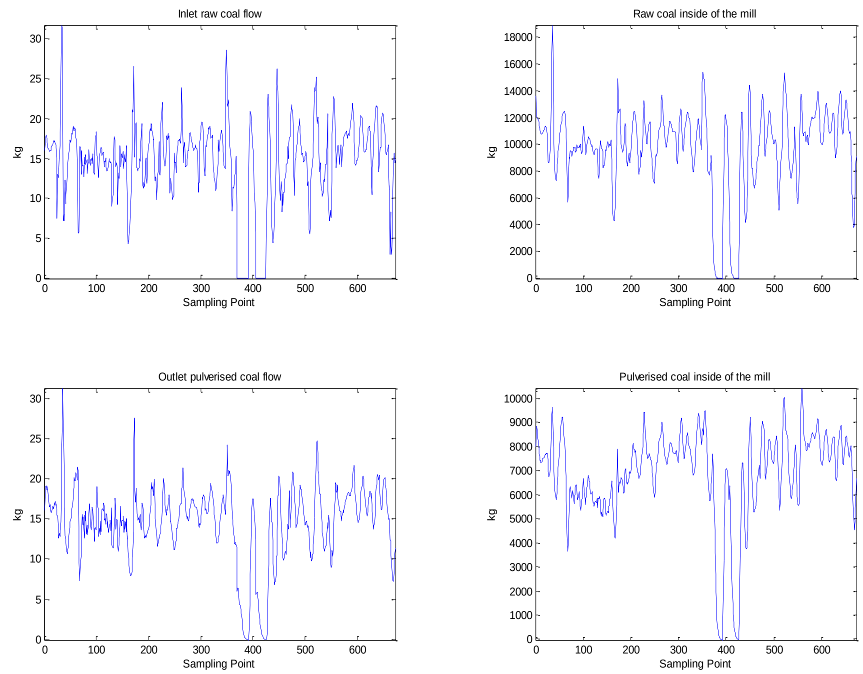

Figure 5.7: Case 3 of mill intermediate variables

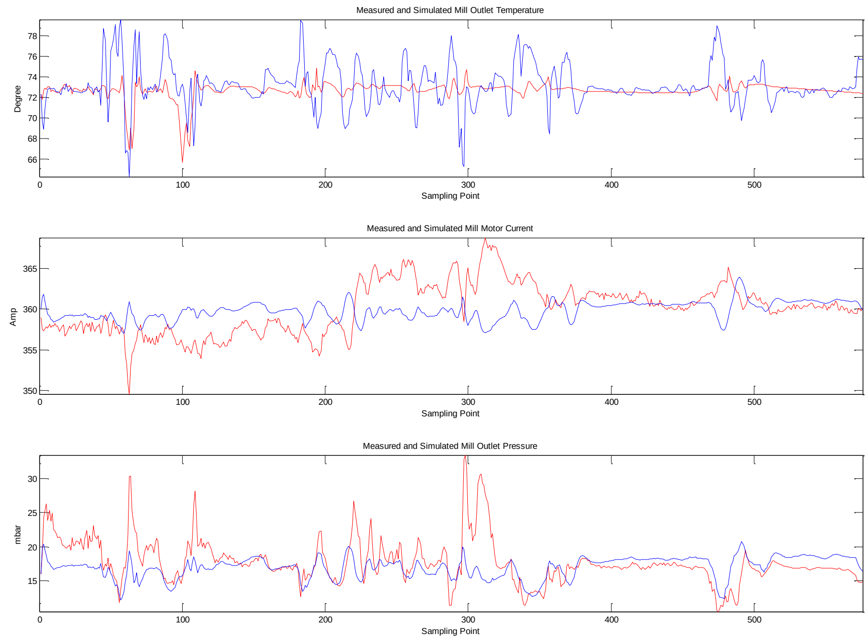

Figure 5.8: Case 4 of measured and simulated mill responses

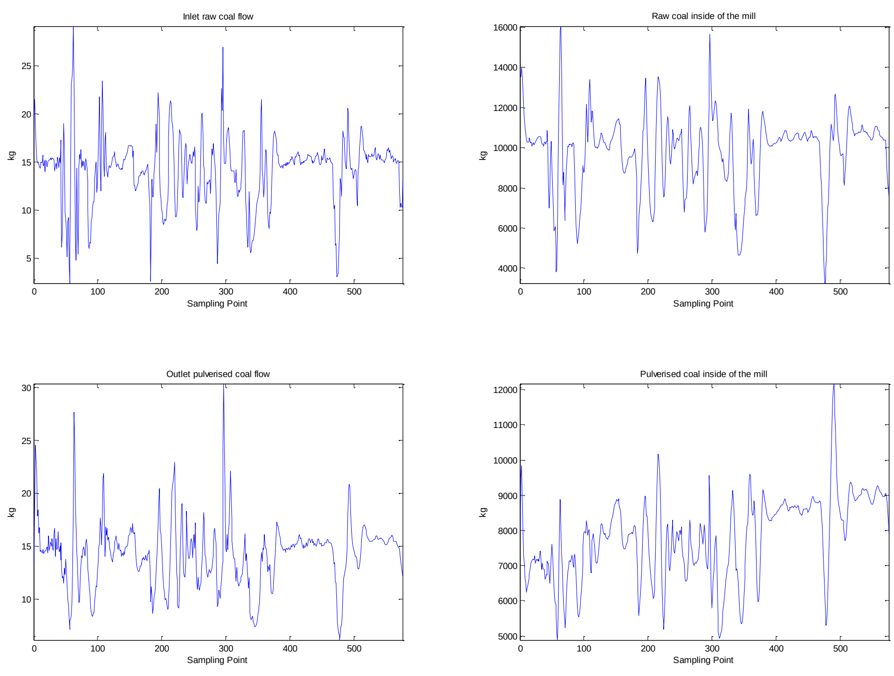

Figure 5.9: Case 4 of mill intermediate variables

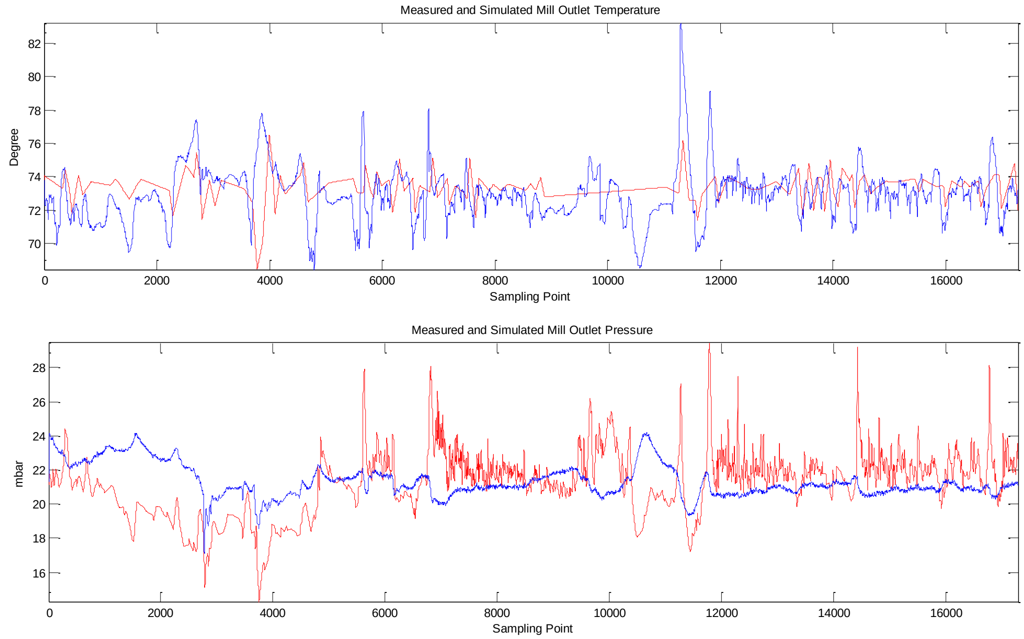

Figure 5.10: Case 5 of measured and simulated mill responses

The simulation results are presented in the Figures 5.2, 5.4, 5.6, 5.8 show the variables which can be measured from the current mill system so the model estimated values can compare with the measured values. The measurable variables include Mill Outlet Temperature (top figure), Mill Outlet Current (middle figure) and Mill Outlet Pressure (diff) (bottom figure). Figures 5.3, 5.5, 5.7, 5.9 display the immeasurable variables which are considered as the intermediate variables. Those variables give an indication for what is happening inside the mill.

In the figures, all the Figure a's present the comparisons between the systems measured mill outlet temperature and the model simulated mill outlet temperature. From the figure, it can be seen that simulated mill outlet temperature can follow the trends of variations in the measured mill outlet temperature well. However, at the middle of the data, the simulated mill outlet temperature vibrates away from the measured mill outlet temperature, and causes increased errors between the measured and estimated values. So this indicates that further improvement may be required.

In the figures, all the Figure b's presents the comparisons between the systems measured mill motor current and the model simulated mill motor current, which represents the mill load in an indirect manner. From the figure, it can be seen that the model simulated mill motor current can follow the general variation trends of the measured current. Again, some discrepancies can be seen in the diagram although they are in the tolerance range. Further work is also carried out for improvement.

In the figures, all the Figure c's present the comparisons between the systems measured mill outlet pressure and the model simulated mill inlet pressure. From the figure, it can be seen that the model simulated mill outlet pressure approaches to the measured mill inlet pressure until the middle of the data. The main problems observed from the results are that the simulated results are more violent in variations. This may be caused by the large sampling intervals. EDF Energy provided fast sampling rate data for the research team and the results improvement can be seen in the latter part of the chapter.

In other figures, the first row of the figure presents the model simulated raw coal flow rate inlet by feeders and the model simulated pulverized coal flow outlet by exhausters. The inlet raw coal flow rate values at around 18 kg/s (64.8 ton/h) in steady state period, and the outlet pulverized coal flow follows the trends of the inlet raw coal flow very well.

The second row of the figure presents the model simulated mass of raw coal and the mass of pulverized coal inside of the mill. In steady state working condition, the model predicts about 18 tons of raw coal and 9 tons of pulverized coal inside of the mill. These have been discussed with the combustion engineers. The engineers consider the figures are within their predicted range as there is no measurement available for those variables at the moment.

5.3. MODEL MODIFICATION FOR THE TUBE-BALL MILL (1)

The equations (3-17) and (3-18) are developed based on the working principle of a vertical spindle mill. The grinding wheels/mechanisms inside of a vertical spindle mill spin at high speed to grid raw coal which will be fed into grinding bowl. This rotating mechanism acts like a paddle spinning inside the mill and the mill product pressure ΔP_{mpd} is generated due to influences of aerodynamics. Equation (3-17) represents the dynamic characteristic of this mill produced pressure inside the mill, which is similar to a first order linear system and also the pulverized coal in mill and the raw coal fed into the mill contribute to the variation of the pressure.

From the working principle of a Tube-Ball mill (PF System Manual from EDF Energy), it is known that there is actually no rotation mechanism like paddles spinning inside of the mill. The mill product pressure can be ignored in this system. And from the air flow diagram shown in Figure 5.11, the mill outlet pressure is a compromised aerodynamic result among the mill inlet pressure, suction pressures generated by the Exhauster Fans A_1 and A_2, mass of raw coal inside of the mill and mass of pulverized coal inside of the mill. So the mill pressure model is modified and presented below in Equation (5-1).

$$\Delta \dot{P}_{out} = K_9 \cdot P_{E1} + K_{10} \cdot P_{E2} + K_{11} \cdot M_{pf} + K_{12} \cdot M_c \ldots$$
$$\ldots + K_{13} \cdot \Delta \dot{P}_{in} + K_{18} \cdot \Delta P_{out} \tag{5-1}$$

where P_{E1} is the mill A_1 exhauster motor current, P_{E2} is the mill A_2 exhauster motor current, $K_9 \sim K_{18}$ are the coefficients to be identified, and the other symbols representing the same variables are explained in Chapter 3, Mathematical Model of Tube Ball Mills.

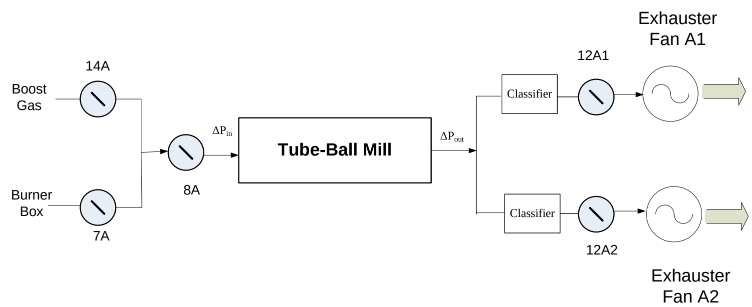

Figure 5.11: Sketch of the air flow in the tube ball mill

So using the data and doing the modifications to the tube ball mill model we can identified the unknown parameters. After the model has been modified, the simulation using the same data set has been re-conducted and the results are illustrated in Figures 5.12-5.15. As we can see from the results after the modification the results are better and the model simulated results are trends the variation of the measured results even closer. Further improvement is needed to achieve the best possible results.

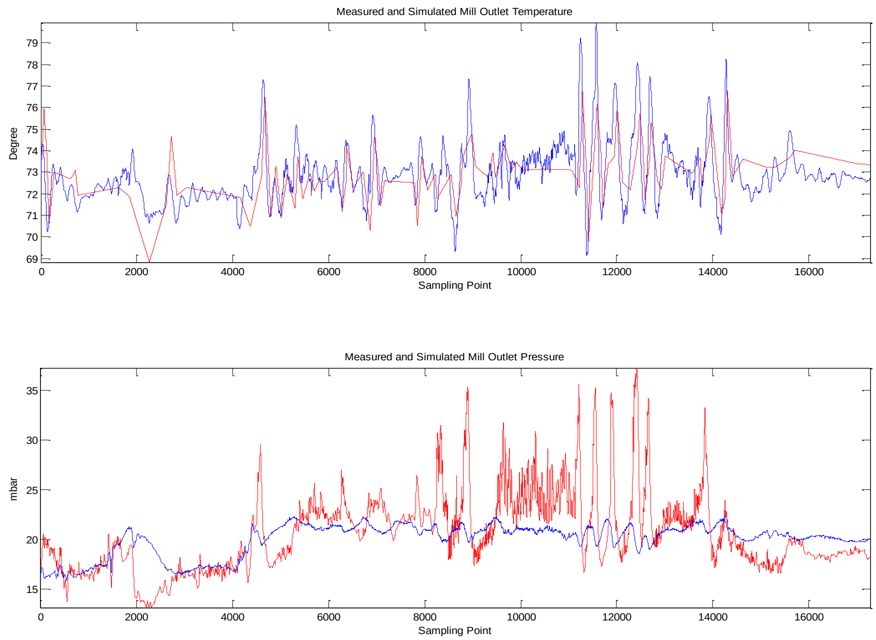

Figure 5.12: Measured and Simulated Results Case I (Figure 5.2)

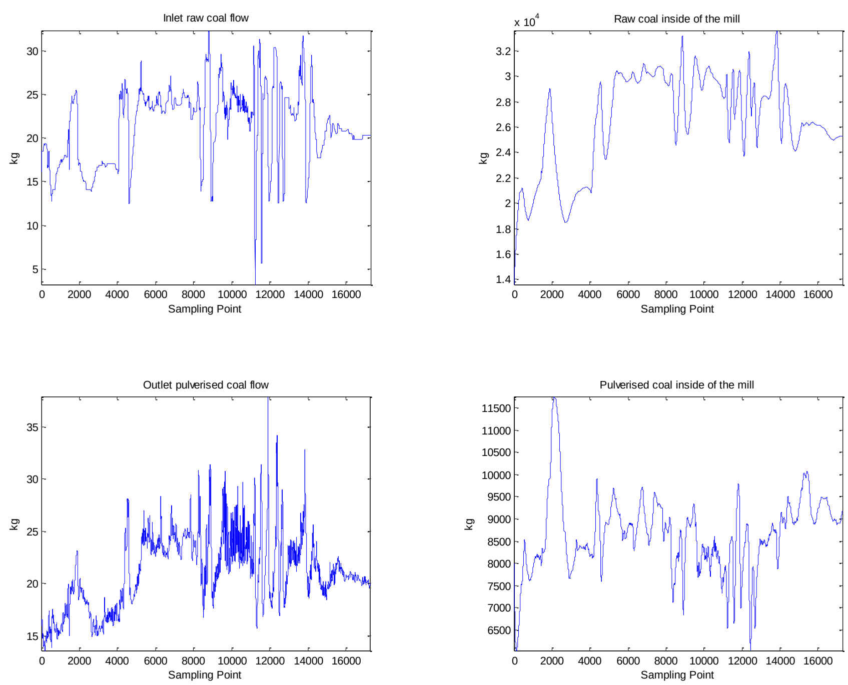

Figure 5.13: Intermediate variables for the Case I data

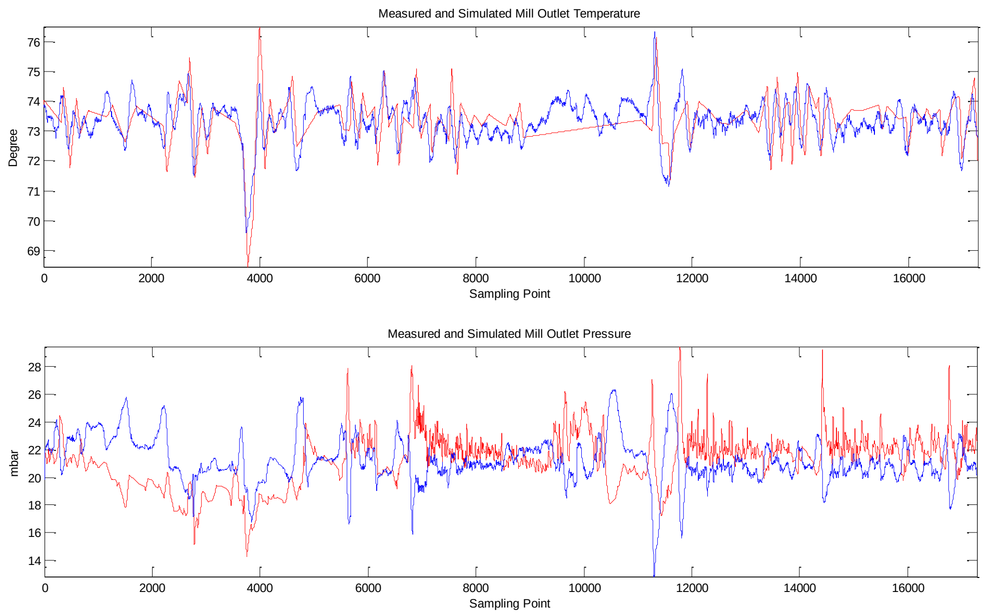

Figure 5.14: Measured and Simulated Results for Case 5

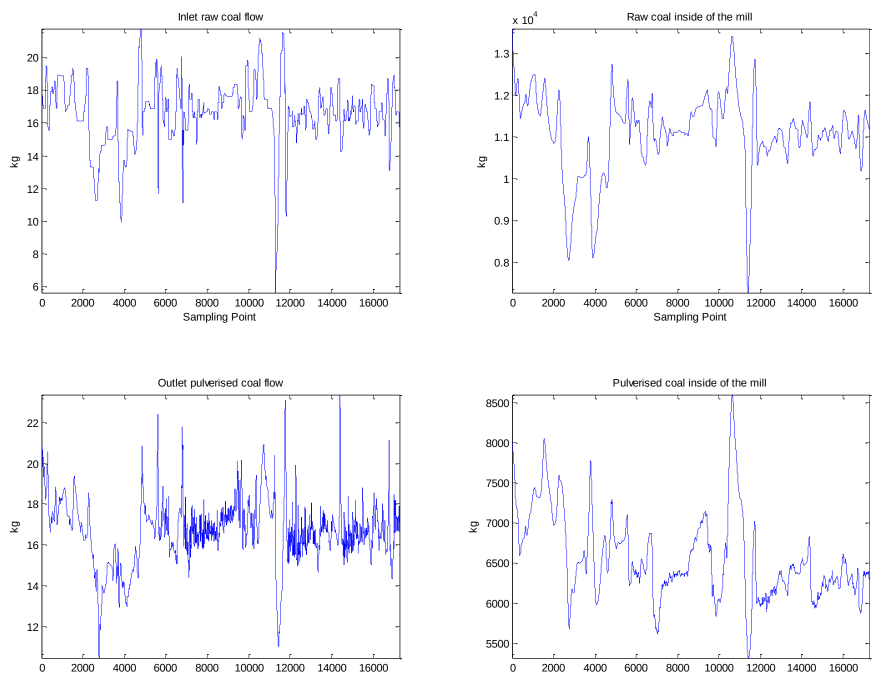

Figure 5.15: Intermediate variables for Case 5 study

5.4. MODEL MODIFICATION FOR THE TUBE-BALL MILL (2)

With the modified model, a consultation meeting was held on 4th February 2008 with the power plant engineers from EDF Energy and E.On Technology Centre. Based on the discussion at the meeting, further modification on the model has been performed for the purpose of improvement.

5.4.1. NEW EQUATION FOR ESTIMATING COAL FLOWING INTO THE MILL

Following the discussion, the zero values of actuation position of the feeders do not indicate coal feeders are off. A further conditional variable needs to be included to judge the situation of the feeder's operation; the mill feeder motor current is considered as the addition information to the raw coal inlet calculation. When the feeder motor is off (say the feeder motor current equals to 0 Amp or less than 1 Amp), zero value of the feeder actuation position (0%) represents the feeder is off. However, when the feeder motor is on (say the feeder motor current bigger than 1 Amp), zero value of the feeder actuation position (0%) represents the feeder is working on its minimum speed. So, two Boolean variables C_{f1} & C_{f2} are introduced into model for the modelling of the inlet coal flow W_c. The model equation is shown as follows:

$$W_c(t) = C_{f1}[K_{f1}A_{P1}(t) + 3.3] + C_{f2}[K_{f2}A_{P2}(t) + 3.3] \tag{5-2}$$

where

A_{P1} is the A1 Feeder Actuation Position (%)

A_{P2} is the A2 Feeder Actuation Position (%)

$K_{f1} = 32.60$ and $K_{f2} = 31.64$

$C_{f1}=1$ if mill A1 feeder current $P_{F1}>1\ Amp$, else $C_{f1}=0;$

$C_{f2}=1$ if mill A2 feeder current $P_{F2}>1\ Amp$, else $C_{f2}=0.$

A simulation result of the inlet coal flow estimated by equation (5-1) is shown in Figure 5.16. From the figure, we can see the A1 Feeder and A2 Feeder work together for some periods and then works alone by itself. By judging the value of the feeder motor currents, the inlet coal flow is estimated correctly, and it matches the estimations from the engineers in power plant.

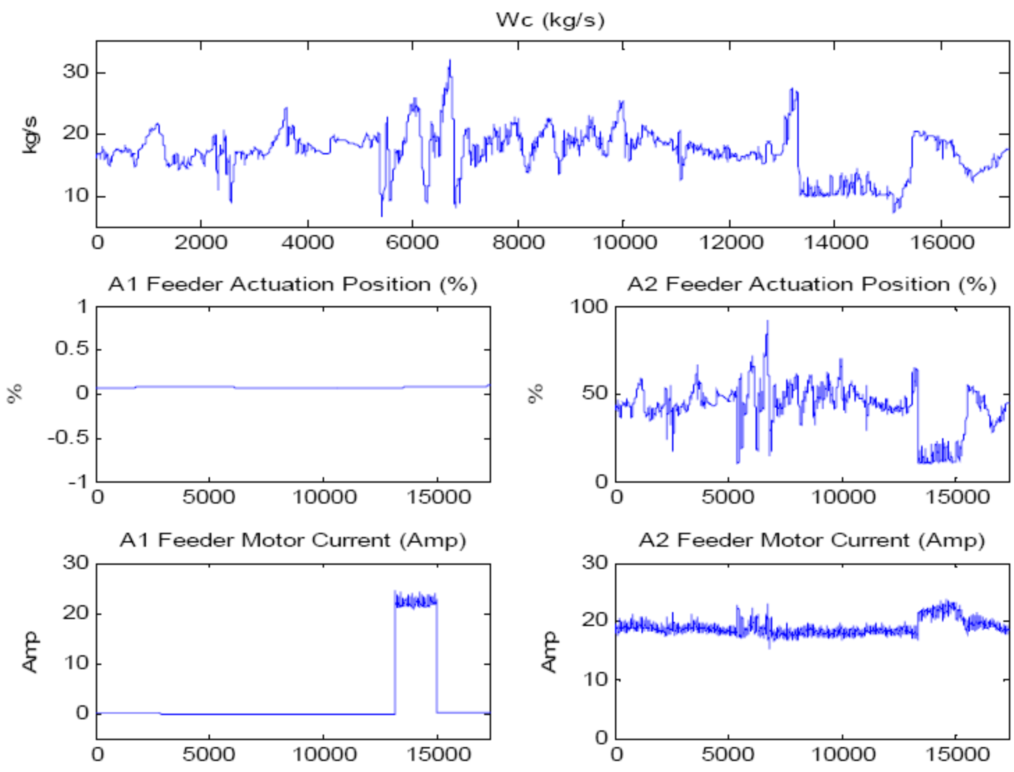

Figure 5.16: Inlet raw coal flow calculated by equation (5-2)

5.4.2. NEW EQUATION FOR PULVERISED COAL FLOW OUT THE MILL

Learning from the empirical formula of W_{pf} from E.ON, the equation for calculation of W_{pf} has now been modified. The threshold value of P_{E1} & P_{E2} are set to be 22 Amps, and the offset value C is set to be 0.9Kg/s based on the engineer's recommendation from their measurement.

$$W_{pf}(t) = K_{16}\Delta P_{out}(t) M_{pf}(t) + [C_{E1}P_{E2} + C_{E1}P_{E2}]K_{19} + 0.9 \tag{5-3}$$

where

$C_{E1} = 1$ if mill A1 Exhauster current $P_{E1} > 22\ Amp$, else $C_{E1} = 0$

$C_{E2} = 1$ if mill A1 Exhauster current $P_{E2} > 22\ Amp$, else $C_{E2} = 0$

5.4.3. FORMULA FOR CALCULATING AIR INTO THE MILL

Following the empirical air flow formula from E.ON, the inlet air flow is modified to be as shown below:

$$W_{air} = 12.42 \cdot \sqrt{\Delta P_{in\_Diff}} + 4.01 \tag{5-4}$$

where:

ΔP_{in_Diff} is the mill inlet differential pressure (mbar)

W_{air} is the mass flow rate of inlet air (kg/s)

A simulation value of the inlet air flow equation (5-2) is shown in Figure 5.17. The value of the air flow is around 20kg/s

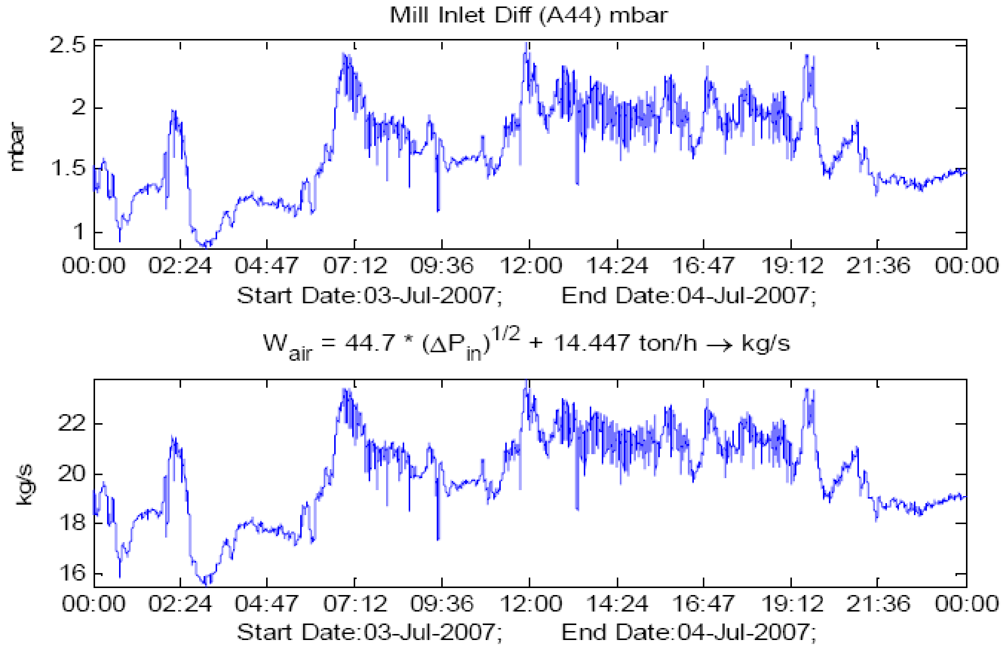

Figure 5.17: Calculated mass flow rate of inlet air

5.4.4. THE MODIFIED VERSION OF THE TUBE-BALL MILL MODEL

Based on simulation studies and consulting with the industry supervisors and engineers, the new version of the coal mill model is shown below:

$$W_{air} = 12.42 \cdot \sqrt{\Delta P_{in\_Diff}} + 4.01 \tag{5-5}$$

$$W_c(t) = C_{f1}[K_{f1}A_{P1}(t) + 3.3] + C_{f2}[K_{f2}A_{P2}(t) + 3.3] \tag{5-6}$$

$$W_{pf}(t) = K_{16}\Delta P_{out}(t)M_{pf}(t) + [C_{E1}P_{E2} + C_{E1}P_{E2}]K_{19} + 0.9 \tag{5-7}$$

$$\dot{M}_c(t) = W_c(t) - K_{15} M_c(t) \tag{5-8}$$

$$M_{pf}(t) = K_{15} \dot{M}_c(t) - W_{pf}(t) \tag{5-9}$$

$$\Delta \dot{P}_{out} = K_9 \cdot P_{E1} + K_{10} \cdot P_{E2} + K_{11} \cdot M_{pf} + K_{12} \cdot M_c + K_{13} \cdot \Delta P_{in\_Diff} + K_{18} \cdot \Delta P_{out} \tag{5-10}$$

$$\dot{T}_{out} = K_1 T_{in}(t) + K_2 W_{air}(t) - K_3 W_c(t) + K_{14} P(t) - K_{20} T_{out} T_{in} + K_{17} T_{out} \tag{5-11}$$

where:

A_{P1}: A1 feeder actuator position (%)

A_{P2}: A2 feeder actuator position (%)

ρ: Primary air density (kg/m^3)

M_c: Mass of coal in mill (kg)

M_{pf}: Mass of pulverized coal in mill (kg)

T_{out}: Outlet temperature of coal mill (^{o}C)

ΔP_{Out}: Mill outlet differential pressure (mbar)

ΔP_{mpd}: Mill product differential pressure (mbar)

W_{pf}: Mass flow rate of pulverized coal outlet from mill (kg/s)

P: Mill current (Amp)

ΔP_{In}: Mill inlet differential pressure (mbar)

W_c : Mass flow rate of coal into mill (kg/s)

T_{in} : Inlet temperature of coal mill (^oC)

W_{air} : Primary air flow rate into coal mill (kg/s)

P_{E1} : A1 Exhauster Motor Current (Amp)

P_{E2} : A2 Exhauster Motor Current (Amp)

C_{f1}, C_{f2}: A1 A2 feeders Boolean control coefficients

C_{E1}, C_{E2}: A1 A2 exhauster Boolean control coefficients

K_{f1}, K_{f2}: A1 A2 feeder coefficients

$K_1,...K_{20}$: Unknown coefficients to be identified

It can be seen from the results that the model simulated results for temperature can follow the trends of variation of the model measured results. The divergence of the two slopes and the difference between the simulated and measured points is very small. Only in some points there are big errors. These errors means there might be faults or fire in the mill's operation. We have discussed the results with on-site engineers and they accept the results as they expected.

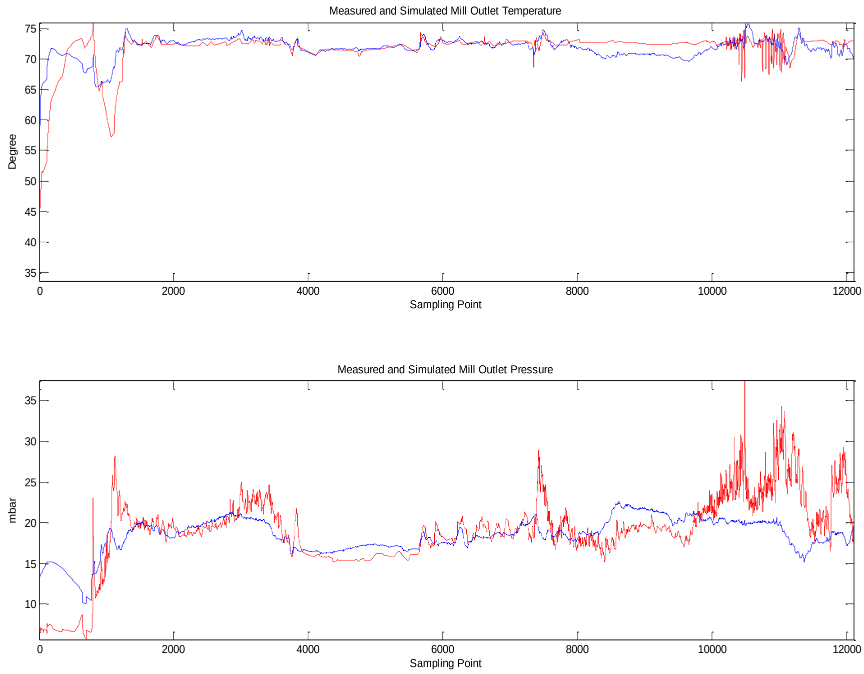

Figure 5.18: Measured and Simulated Results using the modified model

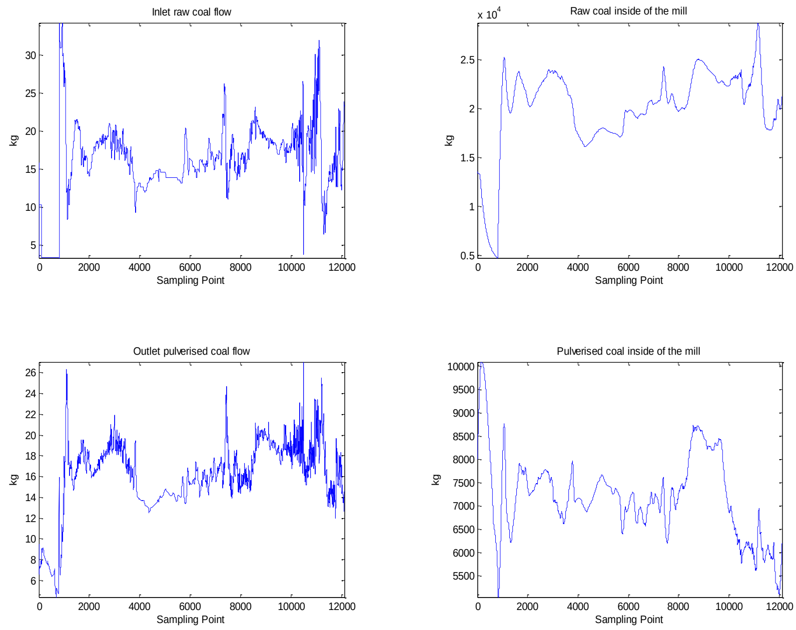

Figure 5.19: Intermediate variables of the mill using the modified model

5.5. PARAMETER IDENTIFICATION USING GENETIC ALGORITHMS

The simulation results suing PSO are presented in Figure 5.2 – 5.19. The figures show the variables which can be measured for the current mill system so the estimated values can compare with the measured values. Alongside with my PhD project, the research group has been using Genetic Algorithms for a few years for parameter identification. One of my objectives of the project is to study an alternative intelligent algorithm, Particle Swarm Optimization as described above. Although the satisfactory results are obtained, this section is to compare the merits of the two methods.

Figures 5.20-5.23 (Top) presents the comparisons between the systems measured mill outlet temperature and the model simulated mill outlet temperature. From the figure, it can be seen that simulated mill outlet temperature can follow the trends of variations in the measured mill outlet temperature well. However, at the middle of the data, the simulated mill outlet temperature vibrates away from the measured mill outlet temperature, and causes errors. Further improvement is required for further work.

Figures 5.20-5.23 (Bottom) presents the comparisons between the systems measured mill inlet pressure and the model simulated mill inlet pressure. From the figure, it can be seen that the model simulated mill inlet pressure approaches to the measured mill inlet pressure until the middle of the data. The main problems observed from the results are that the simulated results are more violent in variations.

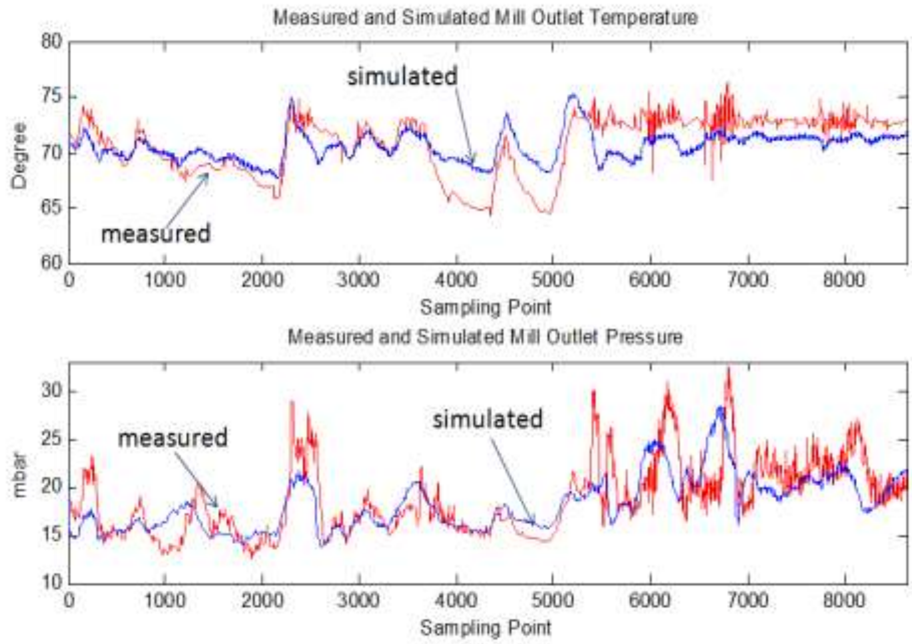

Figure 5.20: Measured and simulated output for the data collected on 9th March 2008, 00:00:00 ~ 12:00:00 (12 hours)

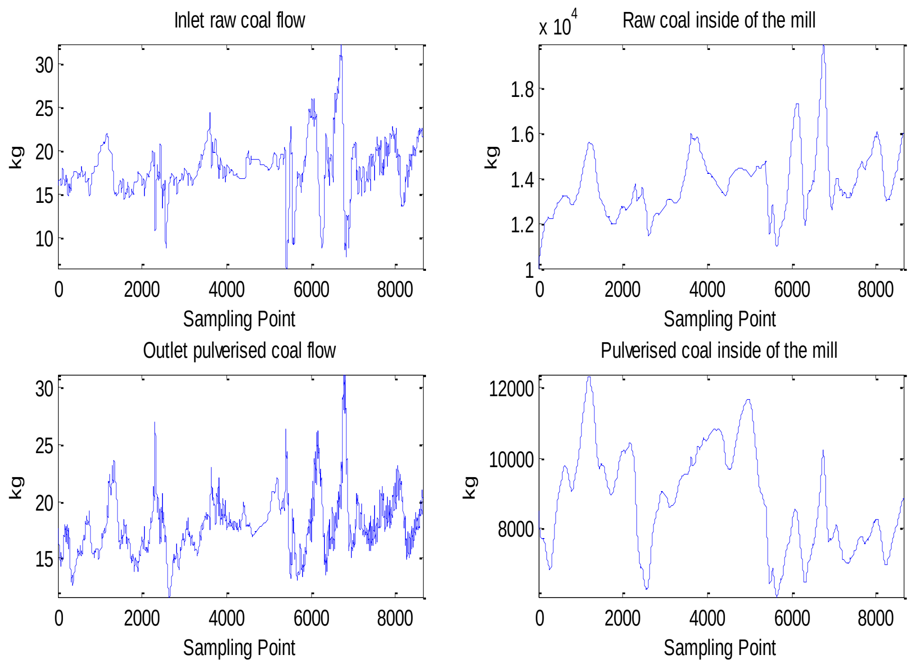

Figure 5.21: Model intermediate variables for the data collectedon 9th March 2008, 00:00:00 ~ 12:00:00 (12 hours)

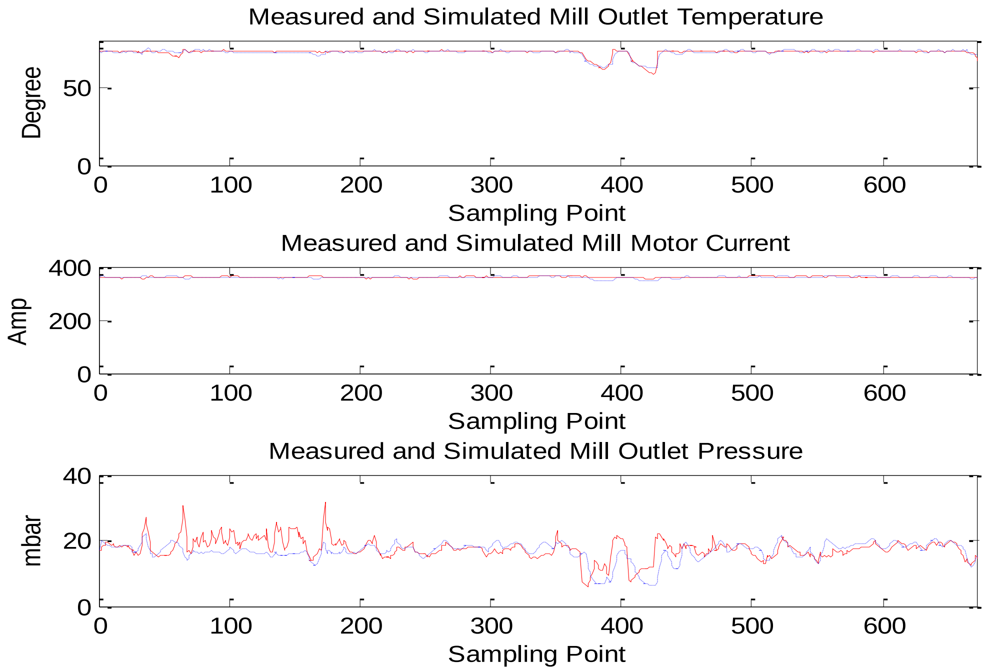

Figure 5.22: Measured (solid lines) and simulated (broken lines) using PSO

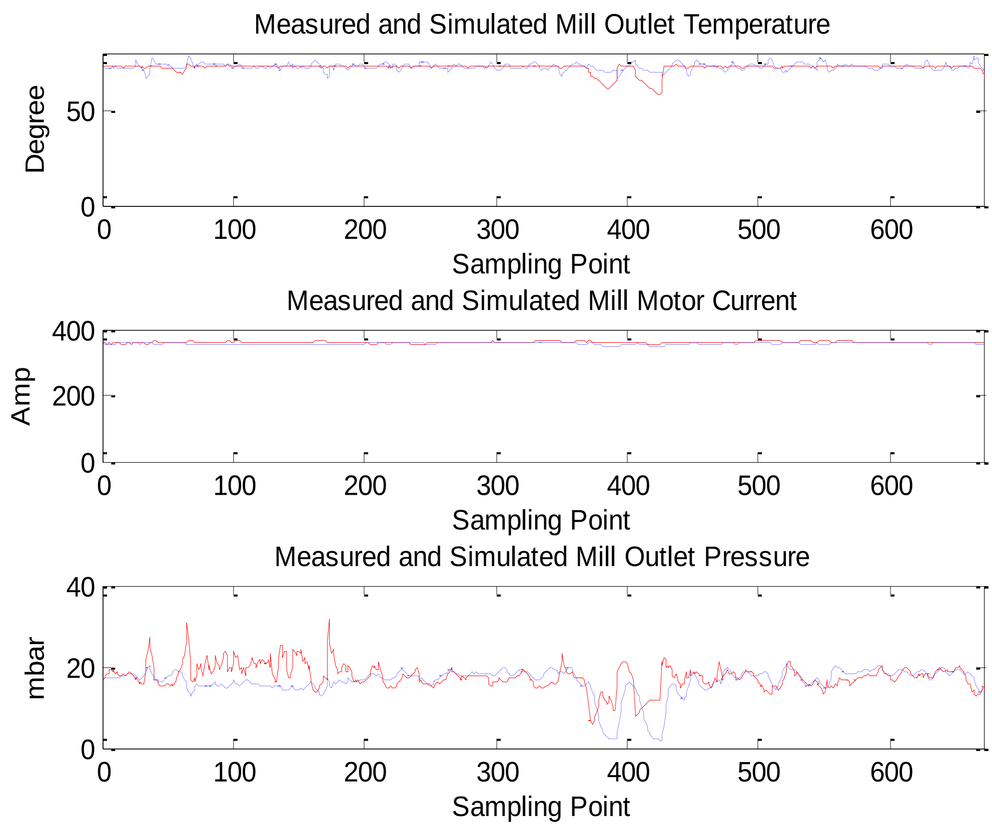

Figure 5.23: Measured (solid lines) and simulated (broken lines) using GA

Huge amount of simulation work using variation of data collected from the power station has been conducted. Comparing the results between PSO and GA, in general, using PSO the model simulated results are better than the GA. In PSO the model simulated results follow the trends of variation of the measured results. In GA the model simulated results follow the general variation of the measured results but at some points there is a striking discrepancy between the measured and simulated results. However, PSO is not as robust as GAs, that is, the results obtained by using PSO can be very good, however, and it often happens that no satisfactory results were obtained. The comparisons of typical cases are summarized in Table 5.1.

Table 5.2 Comparison between PSO and GA

	PSO (Particle Swarm Optimization)		**GA (Genetic Algorithms)**	
DATA 1: Section 1_1	**Iterations**	200	200	**Generations**
	Best Obj*F*(Error)	55.8376	65.8698	**Best Fitness Function**
	Time Elapsed (Mins)	269.4724	495.3864	**Time Elapsed (Mins)**
DATA 2: Section 1_2	**Iterations**	200	200	**Generations**
	Best Obj*F*(Error)	38.1208	43.1284	**Best Fitness Function**
	Time Elapsed (Mins)	164.8594	320.151	**Time Elapsed (Mins)**
DATA 3: Section 1_3	**Iterations**	200	200	**Generations**
	Best Obj*F*(Error)	62.4619	73.1884	**Best Fitness Function**
	Time Elapsed (Mins)	227.5758	598.469	**Time Elapsed (Mins)**

Table 5.2 shows the comparison between the two intelligent methods PSO and GA. First for both methods, the same data are use and the same numbers of generations/iterations were choosing. As we can see from results, the PSO is running faster, almost half of the time needed for the GA. The reason is that PSO is searching for the best unique solution and the GA is searching for a list of possible solutions. Also the Obj*F*(Error) is lower

than the Fitness Function Value. That means the PSO is closer to the optimum solution for model.

5.6. SUMMARY AND DISCUSSION

The initial model of the Tube-Ball mill was tested. Simulation results are shown based on data that were collected from EDF Energy. Afterwards all the modifications are presented with tested results and finishes with the final model.

The second part of this chapter is a comparison between 2 intelligent methods, PSO (Particle Swarm Optimization) and GA (Genetic Algorithms). From the test analysis the conclusion is that PSO performs better rather the GA. However, from my experience in using these two intelligent algorithms, PSO sometimes cannot give the convergent results, which is PSO may not be as stable or robust as GAs. This needs to be taken into consideration when the choice needs to be made between the two optimization methods.

6. MULTI-SEGMENT COAL MILL MODEL

6.1. INTRODUCTION

The mathematical model described in previous chapters is only suitable for the mill normal grinding process or the steady –state operation stage. A multi-segment mill model is derived to cover the whole milling process from start-up to shut-down.

6.2. START-UP AND SHUT-DOWN SEQUENCES

The start-up sequence for a typical coal milling process can be divided into six different operational stages (O1 – O6) as shown Figure 6.1.

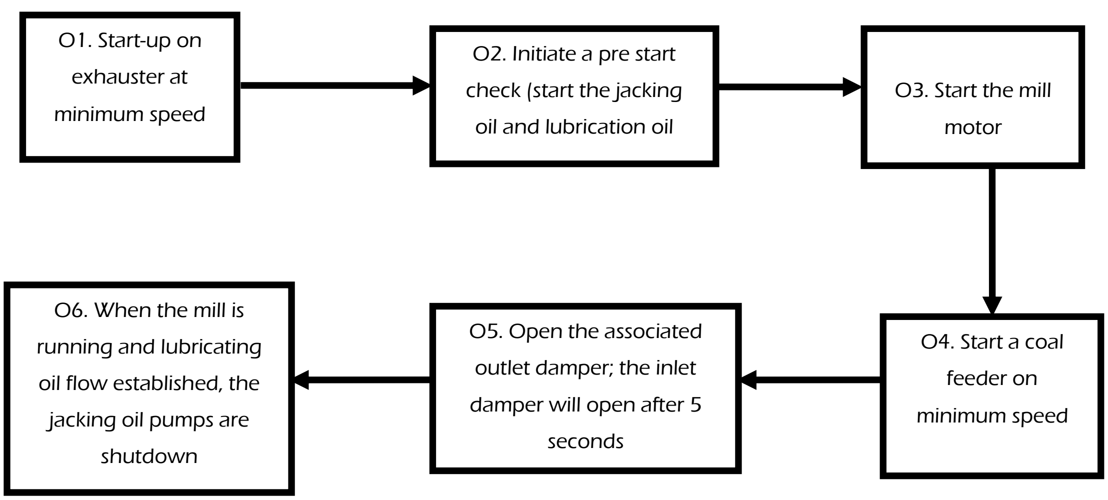

Figure 6.1: A typical start-up sequence

Similarly a typical coal mill shut-down sequence can be divided into five different operational stages (O7 - O11) as shown in Figure 6.2.

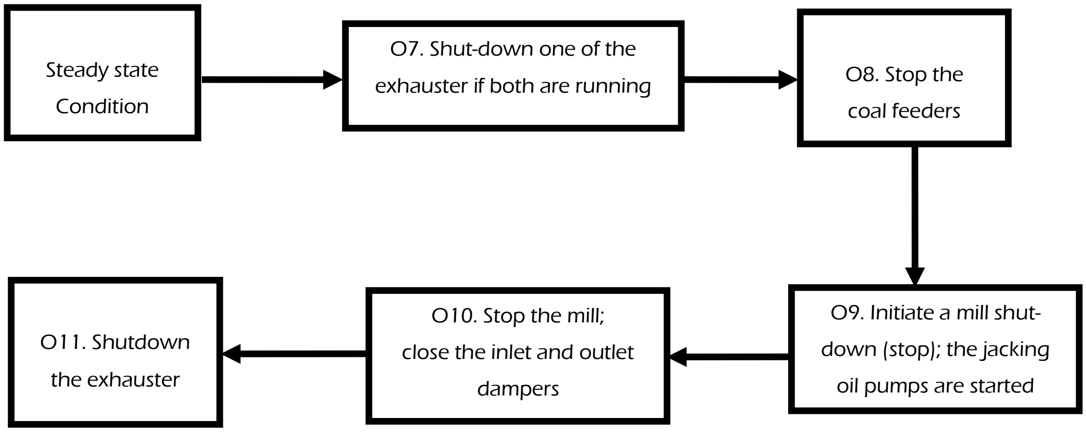

Figure 6.2: A typical shut-down sequence

The overall operational stages of a coal mill in the start-up and shut-down procedures can be divided into 11 operational stages. In order to develop the model for the whole milling process, it requires a signal/flag to tell which operational stage the system is during the operation periods of start-up and shut-down. However, there is no direct indicator logged into the database to give the information at Cottam Power Station. So the alternative signals of indirect variable values are considered, for example, A1 Feeder Motor Current A1723 and *etc* and the logical values of the plant operations, for example, Mill A I/L Damper Open D53, the system's operational stages can be identified and triggered for changes. Detailed descriptions are given below:

A. O1: Start one exhauster at the minimum speed to purge the system

This operation stage can be detected by comparing the values of the exhausters' motor currents. Because the offsets of current sensors exist, the value of exhausters' motor current logged is a very small value (e.g. 0.0111644649878144 Amp) rather than zero when the motor is off. For triggering this operational stage, the following conditions are desired:

- A1 Exhauster Motor Current ≥ 1 Amp; or
- A2 Exhauster Motor Current ≥ 1 Amp

An illustration of values variations of the two exhausters motor currents for starting-up are given in Figure 6.3, where P_E1 represents the A1 Exhauster Motor Current (A66), P_E2 represents the A2 Exhauster Motor Current (A73).

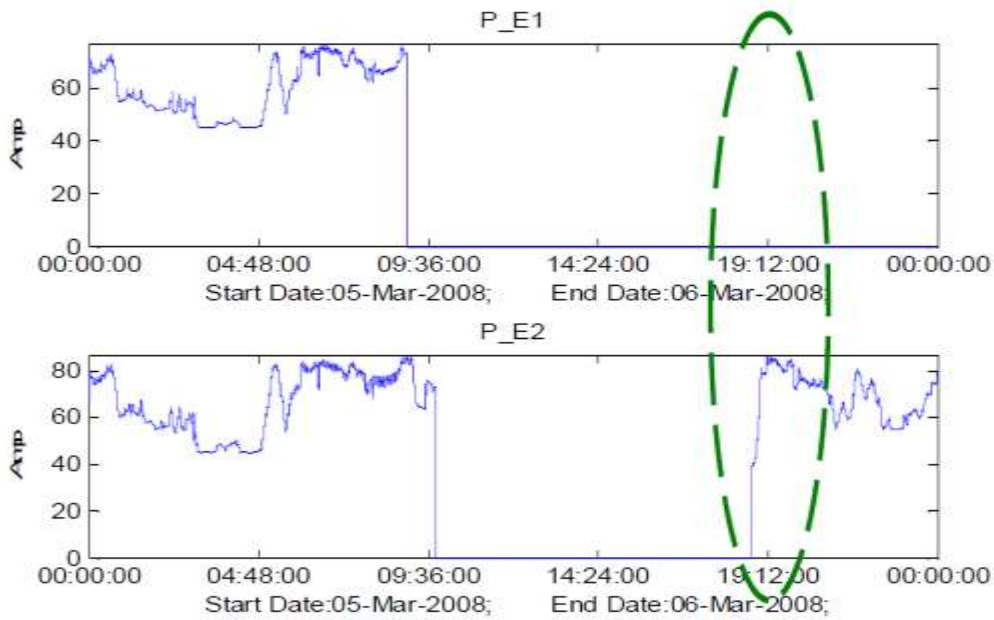

Figure 6.3: Values of A1 A2 Exhauster Motor Current at the starting-up stage

B. O2: Initiate the pre start checking process, then start the jacking oil and lubrication oil pumps

For triggering this operational stage, we can look at the values of the Boolean variables of Lube Oil PP DE CB Closed Buttons (e.g. D64) and J.O. Oil PP DE CB Closed Buttons (e.g. D68). However, for the modelling purpose, these operations do not influence the model equation directly. So the trigger of this step can be skipped.

C. O3: When the mill oil system are satisfactory and the inlet and outlet damper are closed, the mill motor starts

This operation stage can be detected by comparing the values of the mill motor current. Similar to O1, the value of 1Amp is used as the threshold to tell if the motor is on. For triggering this operational stage, the following condition is desired:

- Mill Motor Current P ≥ 1 Amp

An illustration of value variations of the mill motor current at starting-up is shown in Figure 6.4, where P represents the Mill Motor Current (A80).

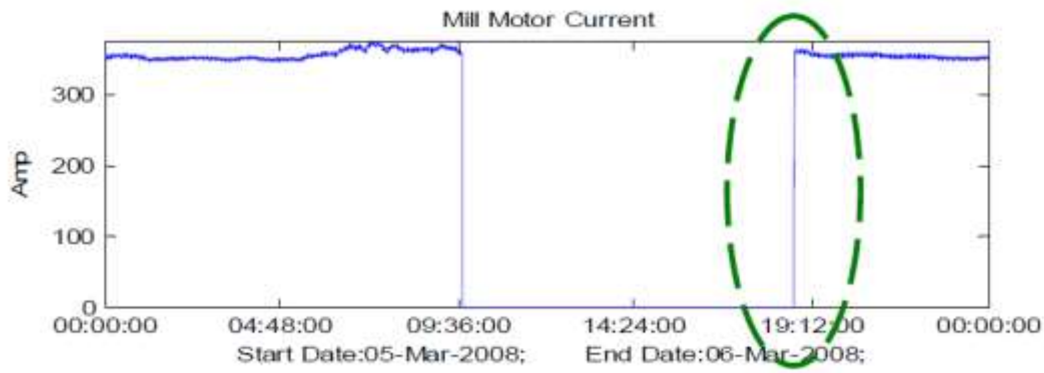

Figure 6.4: Values of mill motor currents while starting-up

D. O4: Start a coal feeder at the minimum speed

There are two feeders equipped at each coal mill to feed raw coal to the mill, which are named as A1 and A2 feeders. While at the stage of starting-up of the coal mill, it will start a coal feeder at a minimum speed initially, and then the second feeder may start later depending on the load demands. The operation stage of staring a coal feeder can be detected by comparing the values of the feeders' motor currents. Similar O1, the value of 1Amp is used as the threshold to tell if the motor is on. For triggering this operational stage, the following conditions are to be detected:

- A1 Feeder Motor Current ≥ 1 Amp; or

- A2 Feeder Motor Current ≥ 1 Amp

An illustration of values variations of the two feeders' motor currents while starting-up is shown in Figure 6.5, where P_F1 represents the A1 Feeder Motor Current (A1723), P_F2 represents the A2 Feeder Motor Current (A1733).

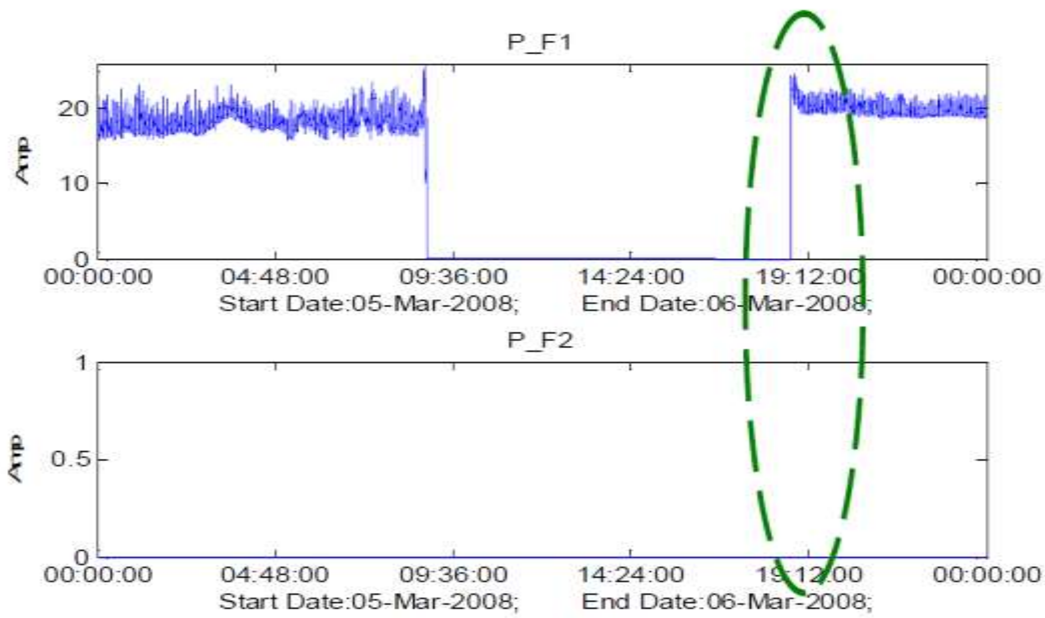

Figure 6.5: Values of A1 A2 feeders motor currents while starting-up

E. O5: Open the associated outlet damper; the inlet damper will open after 5 seconds

There are two outlet dampers, named 12A1 and 12A2, equipped in each coal mill, which are associated to the exhausters A1 and A2 and controlled independently. To detect the operation of the opening of the associated outlet dampers, the following conditions are to be held:

- Mill A1 O/L Damper Open (D55) = = 1, or
- Mill A2 O/L Damper Open (D57) = = 1

The inlet damper 8A is controlled by the sequence system and is opened when the mill is running and one outlet damper is open. To detect the operation of the opening of the inlet damper, the following condition is expected to be true:

- Mill A I/L Damper Open (D53) = = 1

An illustration of values variations of the three logical variables at the stage of the starting-up is shown in Figure 6.6, where D55 represents Mill A1 O/L Damper Open, D57 represents Mill A2 O/L Damper open and D53 represents Mill I/L Damper Open.

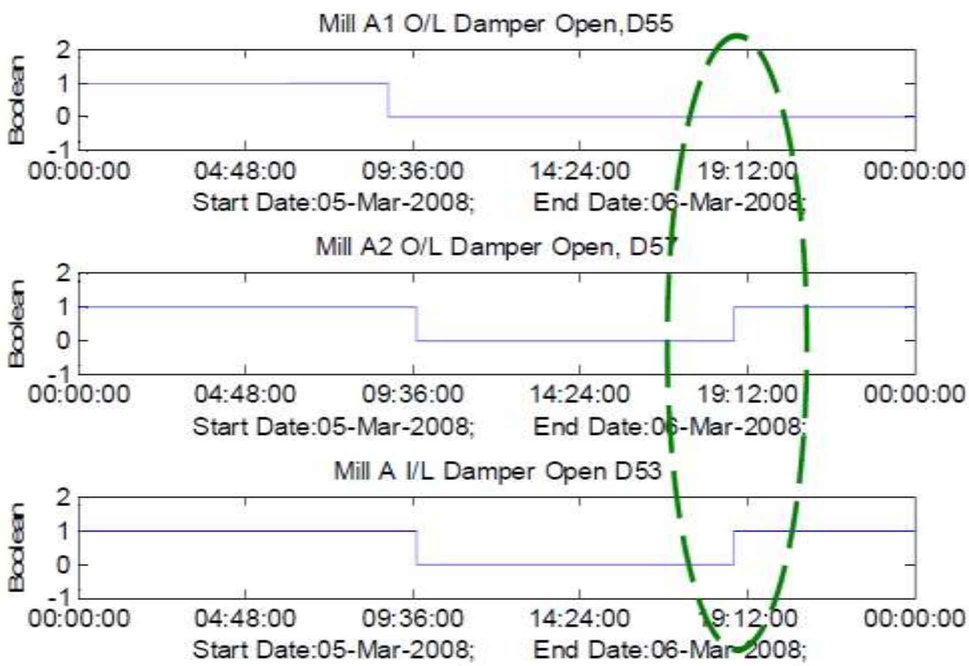

Figure 6.6: Values of A1 A2 feeders motor currents while starting-up

F. O6: When the mill is running and lubricating oil flow established, the jacking oil pumps are shutdown

This operation is the final step for the mill start-up sequence. The operation conditions of the lubrication oil pumps and the jacking oil pumps can be detected by looking at the values of the Boolean Variable of Lube Oil PP DE CB Closed Buttons (e.g. D64) and J.O. Oil PP DE CB Closed Buttons (e.g. D67) *etc*. However for the modelling purpose, this operation stage does not influence the model equation directly. So the trigger of this step can be skipped.

G. O7: Shutdown one of the exhausters if both of them are operating; the exhauster will purge at the maximum speed for 10 minutes and then stop

This operation is the first step of the mill shut-down sequence. Similar to O1, the operation stage can be detected by comparing the values of the exhausters' motor currents, wherein the following conditions are expected to be true:

- A1 Exhauster Motor Current ≤ 1 Amp; or
- A2 Exhauster Motor Current ≤ 1 Amp

An illustration of value variations of the two exhausters' motor current at the starting-up is given in Figure 6.7, where P_E1 represents the A1 Exhauster Motor Current (A66), P_E2 represents the A2 Exhauster Motor Current (A73).

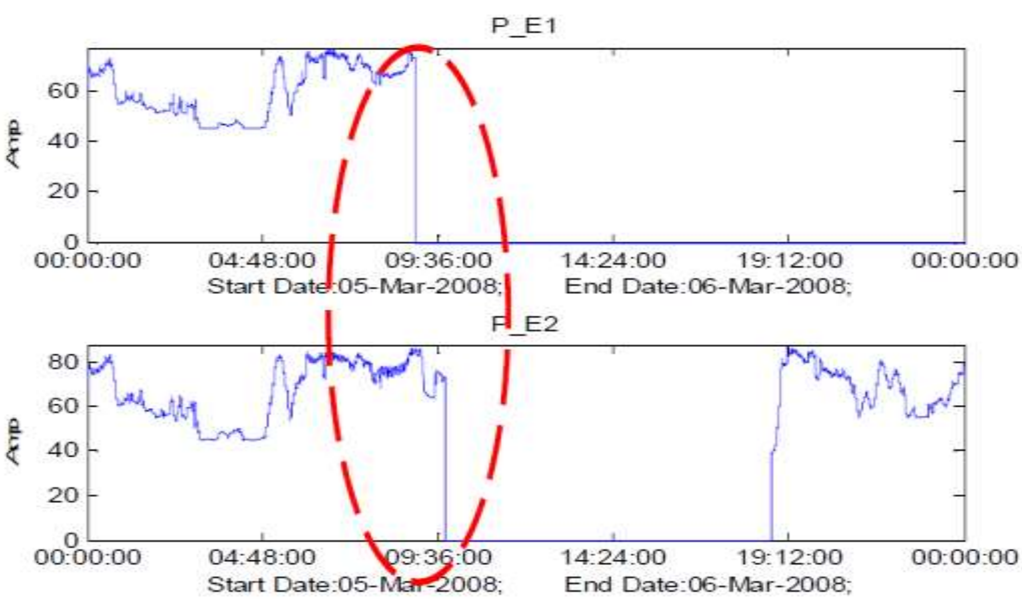

Figure 6.7: Values of A1 A2 exhausters' motor currents while shutting-down

H. O8: Stop the coal feeders

This operation is the second step of the mill shut-down sequence. It checks the operation condition of A1 and A2 feeders, and then it will stop any of coal feeders that were running. The operation stage of stopping a coal feeder can be detected by comparing the values of the feeders' motor currents. Similar to O1, the value of 1 Amp is used as the threshold to tell if the motor is off. For triggering this operational stage, the following conditions should be held:

- A1 Feeder Motor Current ≤ 1 Amp; or
- A2 Feeder Motor Current ≤ 1 Amp

An illustration of value variations of the two feeders' motor currents at the starting-up stage is given in Figure 6.8, where in P_F1 represents the A1 feeder Motor Current (A1723), P_F2 represents the A2 Feeder Motor Current (A1733).

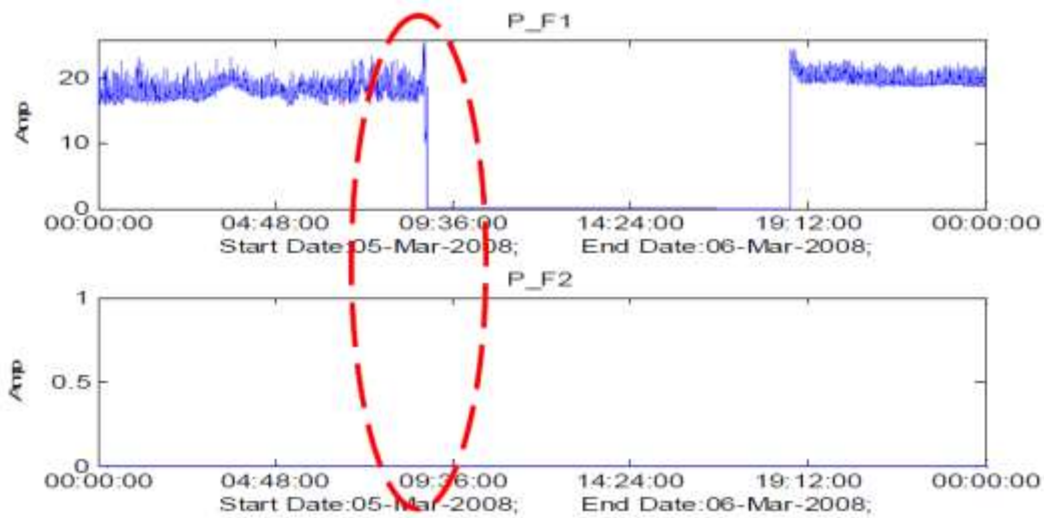

Figure 6.8: Values of A1 A2 feeders' motor currents while shutting-down

I. O9: Initiate a mill shut-down(stop); the jacking oil pumps start

Similar to O3, this operation stage can be detected by comparing the values of the mill motor current. For triggering this operational stage, the following condition is expected to be true:

- Mill Motor Current P $\leq$ 1 Amp.

An illustration of the values' variations of the mill motor current while starting-up are given in Figure 6.9, where P represents the Mill Motor Current (A80).

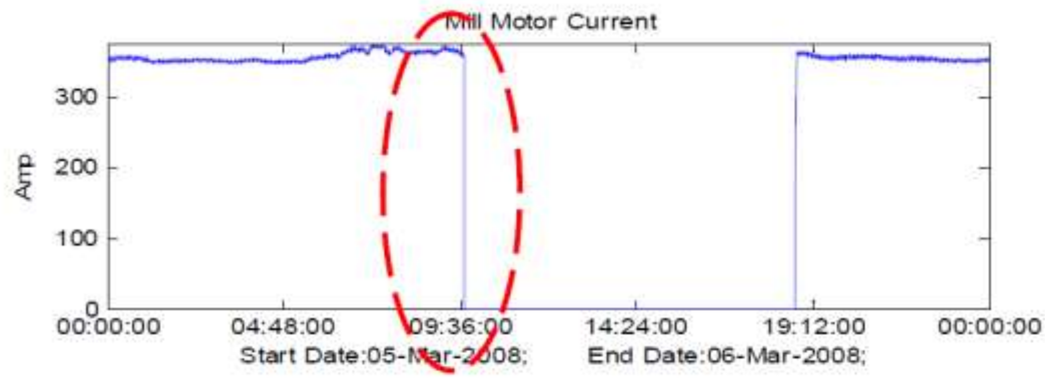

Figure 6.9: Values of mill motor currents while shutting-down

J. O10: When the jacking oil pressures are established, the mill stops and the inlet and outlet dampers are closed

Similar to O5, the trigger of the operation of the closures to the associated outlet dampers can be detected using the logical variables, which are shown as follows:

- Mill A1 O/L Damper Closed (D56) = = 1, or
- Mill A2 O/L Damper Closed (D58) = = 1

To detect the operation of the closing of the inlet damper, the following condition is expected to be true:

- Mill A I/L Damper Closed (D54) = = 1

An illustration of the values' variations of the three logical variables at the starting-up are given in Figure 6.10, where D56 represents Mill A1 O/L Damper Closed, D58 represents Mill A2 O/L Damper Closed, and D54 represents Mill I/L Damper Closed.

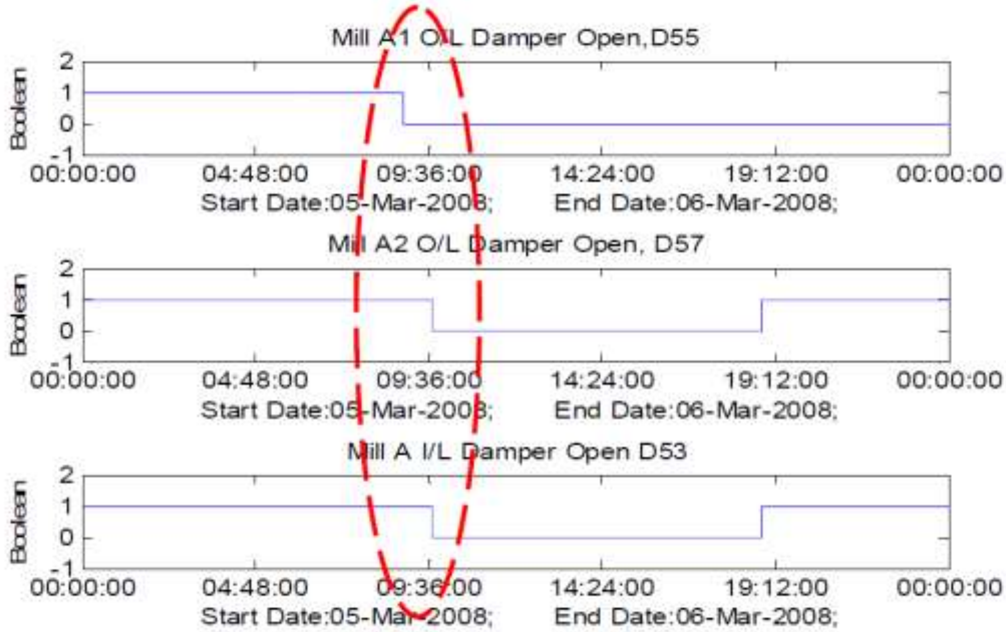

Figure 6.10: Values of A1 A2 feeder motor currents while shutting-down

K. O11: Shutdown the exhauster; the exhauster will purge at the maximum speed for 10 minutes and then stop.

This operation stage is the final step of the shut-down sequence. Similar to O7, the operation stage can be detected by comparing the values of the exhausters' motor currents, wherein the following conditions are desired to be true:

- A1 Exhauster Motor Current ≤ 1 Amp; and
- A2 Exhauster Motor Current ≤ 1 Amp

An illustration of the values' variations of the two exhausters' motor currents while starting-up are given in Figure 6.11, where P_E1 represents the A1 Exhauster Motor Current (A66), P_E2 represents the A2 Exhauster Motor Current (A73).

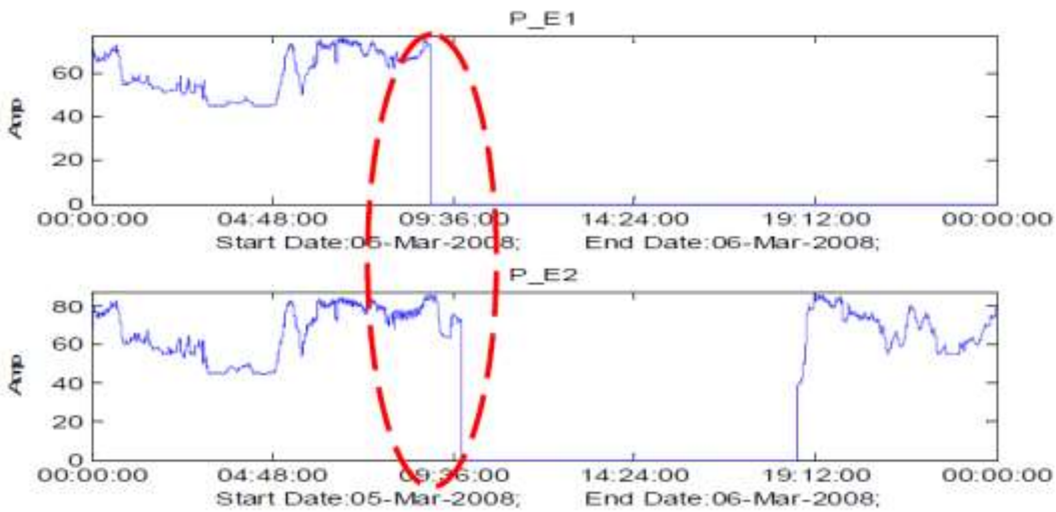

Figure 6.11: Values of A1 A2 exhauster' motor currents while shutting-down

6.3. MULTI-SEGMENT COAL MILL MATHEMATICAL MODEL

In the coal mill start-up and shut-down processes introduced in the previous sub-section, there are totally eleven different operation stages. For different operational stages, the coal mill system will be described by different mathematical equations. Grouping the working conditions of the coal mill system from the different operation stages, a multi-segment coal mill model is developed, the schematic diagram of which is shown in Figure 6.12. There are five different model segments, namely Model Segment I, Model Segment II, Model Segment III, Model Segment IV, Model Segment V. Detailed model equations for each segment are given below.

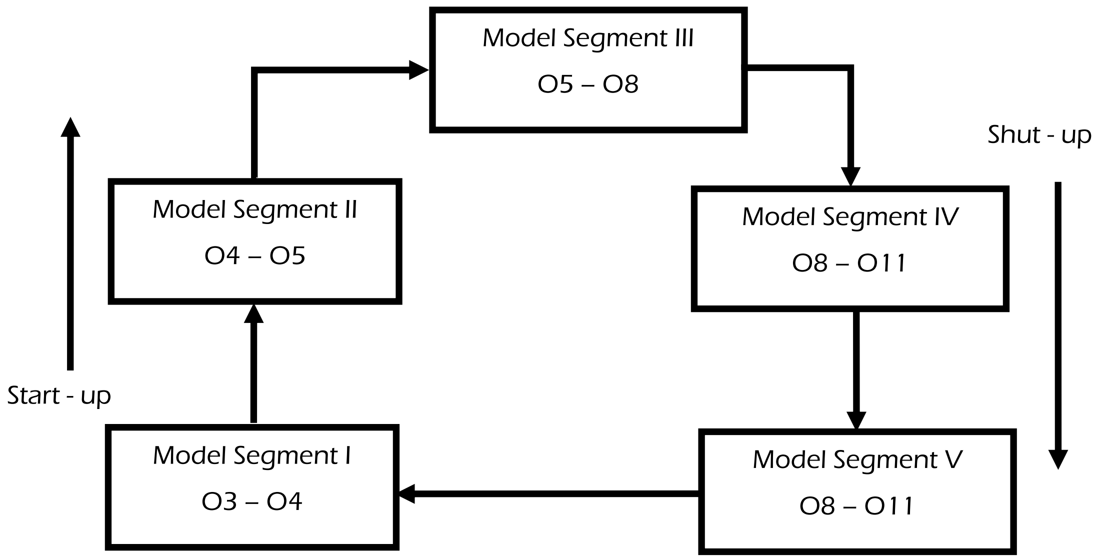

Figure 6.12: Multi-Segment Coal Mill Model

6.3.1. MODEL SEGMENT I

The duration of this model segment is valid from O3 to O4. In this duration, the coal mill feeders are off, so there is not any raw coal (W_c) coming into the coal mill, Equation I.2. At least one of the mill exhausters is on a this duration, however the outlet dampers (12A1 & 12A2) are all closed, so there is no pulverized coal (W_{pf}) outlet from the mill to the burner which can be described by Equation I.3. Similarly, the inlet damper (8A) is still closed in this duration; there is still no hot air (W_{air}) inlet into the coal mill as described by Equation I.1. As the inlet and outlet dampers are all closed, the mill body can treated as isolated, the mill outlet pressure become the atmosphere pressure and the mill outlet temperature varies to itself (Equations I.6 and I.7). The mill motor is on in this model segment, so that grinding has started. As no raw coal supplied into the mill, the raw coal remained in the coal mill from the last stage (M_c) reduces itself due to the grinding, and the pulverized coal inside of the mill (M_{pf}) increases itself consequently (

Equations I.4 and I.5). The whole sets of the model equations of Model Segment I are shown as follows:

$$W_{air}(t) = 0 \tag{1. 2}$$

$$W_c(t) = 0 \tag{3. 4}$$

$$W_{pf}(t) = 0 \tag{5. 6}$$

$$\dot{M}_c(t) = 0 - K_{15} \cdot M_c(t) \tag{7. 8}$$

$$\dot{M}_{pf}(t) = K_{15} \cdot M_c(t) \tag{9.10}$$

$$\Delta P_{out}(t) = 0 \tag{11.12}$$

$$\dot{T}_{out}(t) = 0 + K_{17} T_{out}(t) \tag{13.14}$$

where:

W_{air} : Primary air flow rate into coal mill (kg/s)

W_c : Mass flow rate of coal into mill (kg/s)

W_{pf} : Mass flow rate of pulverized coal outlet from mill (kg/s)

M_c : Mass of coal in mill (kg)

M_{pf} : Mass of pulverized coal in mill (kg)

ΔP_{out} : Mill outlet differential pressure (mbar)

T_{out} : Outlet temperature of coal mill (^{o}C)

K_{15}, K_{17} : Unknown coefficients to be determined

6.3.2. MODEL SEGMENT II

The duration of this model segment is valid from O4 to O5. In the duration, one of the mill feeders started running to feed raw coal into the mill for the grinding, wherein the raw coal flow rate (W_c) can be represent by Equation II.2 according to the previous research. In this duration, the inlet damper (8A) and outlet dampers (12A1 & 12A2) are still closed. Consequently, still there is no W_{air} inlet into the coal mill (Equation II.1), likewise there is no W_{pf} outlet from the mill (Equation II.3). Similarly to last segment, the mill body can be treated as isolated in segment II as well, the mill outlet pressure become zeros and the mill outlet temperature varies to itself (Equation II.6 and II.7). The mill motor is kept on running from the last segment, and the grinding is continued. As new raw coal supplied into the coal mill, Equations II.4 and II.5 represent the mass of raw coal (M_c) and mass of pulverized coal (M_{pf}). The whole sets of the model equations of Model Segment II are shown as follows:

$$W_{air}(t) = 0 \tag{15.16}$$

$$W_c(t) = C_{f1}[K_{f1}A_{P1} + 3.3] + C_{f2}[K_{f2}A_{P2} + 3.3] \tag{17.18}$$

$$W_{pf}(t) = 0 \tag{19.20}$$

$$\dot{M}_c(t) = W_c(t) - K_{15} \cdot M_c(t) \tag{21.22}$$

$$\dot{M}_{pf}(t) = K_{15}M_c(t) - 0 \tag{23.24}$$

$$\Delta P_{out}(t) = 0 \tag{25.26}$$

$$\dot{T}_{out}(t) = 0 + K_{17}T_{out}(t) \tag{27.28}$$

where:

A_{P1} : A1 feeder actuator position (%)

A_{P2} : A2 feeder actuator position (%)

K_{f1}, K_{f2} : A1 A2 feeder coefficients

C_{f1}, C_{f2} : A1 A2 feeders Boolean control coefficients

K_{15}, K_{17} : Unknown coefficients to be determined for Model Segment II

The other notations are same as previously stated in Segment I

6.3.3. MODEL SEGMENT III

The duration of this model segment is valid from O5 to O8. in this duration, the mill inlet damper (8A) and the outlet dampers (12A1 or 12A2) are opened; the mill motor is on; at least one of the mill feeder is on; similarly, at least one of the mill exhausters is on; This model segment represents the coal mill steady-state operation condition. Inheriting from previous research, the model equations for this segment are shown as follows:

$$W_{air}(t) = 12.42\sqrt{\Delta P_{in\_Diff}} + 4.01 \tag{29.30}$$

$$W_c(t) = C_{f1}[K_{f1}A_{P1} + 3.3] + C_{f2}[K_{f2}A_{P2} + 3.3] \tag{31.32}$$

$$W_{pf}(t) = K_{16}\Delta P_{Out}(t)M_{pf}(t) + [C_{E1}P_{E1} + C_{E2}P_{E2}]K_{19} + 0.9 \tag{33.34}$$

$$\dot{M}_c(t) = W_c(t) - K_{15} \cdot M_c(t) \tag{35.36}$$

$$\dot{M}_{pf}(t) = K_{15}M_c(t) - W_{pf}(t) \tag{37.38}$$

$$\Delta\dot{P}_{out}(t) = K_9P_{E1} + K_{10}P_{E2} + K_{11}M_{pf} + K_{12}M_c + K_{13}\Delta P_{in\_Diff} + K_{18}\Delta P_{Out} \tag{39.40}$$

$$\dot{T}_{out}(t) = K_1T_{in}(t) + K_2W_{air}(t) + K_{14}P(t) - K_3W_c(t) - K_{20}T_{out}T_{in} + K_{17}T_{out} \tag{41.42}$$

where

ρ : Primary air density (kg/m^3)

ΔP_{in} : Mill inlet differential pressure (mbar)

P_{E1} : A1 Exhauster Motor Current (Amp)

P_{E2} : A2 Exhauster Motor Current (Amp)

P : Mill motor current (Amp)

C_{E1}, C_{E2} : A1 A2 exhauster Boolean control coefficients

$K_1, ...K_{20}$: Unknown coefficients to identify in Segment III

The other notations are same as previous stated in Segment II.

6.3.4. MODEL SEGMENT IV

The duration of this model segment is valid from O8 to O10. In the duration, all the coal feeders are off, so the raw coal inlet flow rate W_c becomes zeros (Equation IV.2). All the other equipments are still operated as usual like the last model segment; the inlet damper 8A and the outlet dampers (12A1 or 12A2) are still opened; the mill motor is kept on running; at least one of the exhausters is kept on extracting pulverized fuel out. The model equations for this segment are shown as follows:

$$W_{air}(t) = 12.42\sqrt{\Delta P_{in\_Diff}} + 4.01 \tag{43.44}$$

$$W_c(t) = 0 \tag{45.46}$$

$$W_{pf}(t) = K_{16}\Delta P_{Out}(t)M_{pf}(t) + [C_{E1}P_{E1} + C_{E2}P_{E2}]K_{19} + 0.9 \tag{47.48}$$

$$\dot{M}_c(t) = W_c(t) - K_{15} \cdot M_c(t) \tag{49.50}$$

$$\dot{M}_{pf}(t) = K_{15} M_c(t) - W_{pf}(t) \tag{51.52}$$

$$\Delta \dot{P}_{out}(t) = K_9 P_{E1} + K_{10} P_{E2} + K_{11} M_{pf} + K_{12} M_c + K_{13} \Delta P_{in\_Diff} + K_{18} \Delta P_{Out} \tag{53.54}$$

$$\dot{T}_{out}(t) = K_1 T_{in}(t) + K_2 W_{air}(t) + K_{14} P(t) - 0 - K_{20} T_{out} T_{in} + K_{17} T_{out} \tag{55.56}$$

where

$K_1,...K_{20}$: Unknown coefficients to identify in Segment IV

The other notations are same as previous stated in Segment III.

6.3.5. MODEL SEGMENT V

The duration of this model segment is valid from O10 to O3. in the duration, all the coal mill equipments are off: the coal feeders are off; the mill motor is off; the exhausters are off; the inlet damper (8A) and the outlet dampers (12A1 & 12A2) are all closed. The coal mill system situates in the idle stage. As the inlet and outlet dampers are all closed, the mill body can be treated as isolated, the mill outlet pressure become zeros and the mill outlet temperature varies to itself (Equation V.6 and V.7). The whole set of model equations for this segment are shown as follows:

$$W_{air}(t) = 0 \tag{57.58}$$

$$W_c(t) = 0 \tag{59.60}$$

$$W_{pf}(t) = 0 \tag{61.62}$$

$$\dot{M}_c(t) = M_{c\_LastStage} \tag{63.64}$$

$$\dot{M}_{pf}(t) = M_{pf\_LastStage} \tag{65.66}$$

$$\Delta P_{out}(t) = 0 \tag{67.68}$$

$$\dot{T}_{out}(t) = 0 + K_{17} T_{out} \tag{69.70}$$

where

$M_{c\_LastStage}$: Mass of raw coal in mill from the last segment (kg)

$M_{pf\_LastStage}$: Mass of pulverized coal in mill from the last segment (kg)

K_{17} : Unknown coefficients to identify in Segment V

The other notations are same as previous stated in segment III.

6.4. PARAMATER IDENTIFICATION AND SIMULATION STUDY OF THE MULTI-SEGMENT MODEL

Three Start-up/shut-down data sets were collected from Cottam Power Station. Following the model parameter identification scheme as shown in Figure 5.1, the model parameters of the five segments are identified and listed in Table 6.1.

Parameters	Segment I	Segment II	Segment III	Segment IV	Segment V
K_1	N/A	0.01448386	0.6291708	0.17983636	N/A
K_2	N/A	N/A	0.00347259	0.00325034	N/A
K_3	N/A	N/A	0.264450089	N/A	N/A
K_9	N/A	N/A	0.022766272	0.01	N/A
K_{11}	N/A	N/A	5.8463E-05	4.02E-06	N/A
K_{12}	N/A	N/A	0.000144325	0.000419838	N/A
K_{13}	N/A	N/A	4.622867921	5.166732618	N/A
K_{14}	N/A	N/A	0.013445313	0.007214076	N/A
K_{15}	0.00031154	0.0003014	0.001102979	0.0011	N/A
K_{16}	N/A	N/A	4.60913E-05	4.5E-05	N/A
K_{17}	-0.0002333	-0.01	-0.02180219	0.028476639	-2.64E-05
K_{18}	N/A	N/A	-0.068402737	-1	N/A
K_{19}	N/A	N/A	0/01	0.01	N/A
K_{20}	N/A	N/A	0.0860919	0.003019315	N/A

Table 6.1: The identified model parameters of the five segment models

Three start-up/shut-down data sets collected from Cottam Power Station were selected for simulation study. The details of the data sets are given in Table 6.2

	Date Range
Data 1	16th Mar. 2008 00:00:00 ~ 17th Mar. 2008 00:00:00
Data 2	26th July 2008 00:00:00 ~ 27th July 2008 00:00:00
Data 3	28th July 2008 00:00:00 ~ 28th July 2008 00:00:00

Table 6.2: Data Sets employed for the simulation study

Using the parameters identified, the model simulation results are shown in Figures 6.13 ~ 6.18, in which, for the normal grinding stage, the key parameters K_{17} and K_{18} updating scheme is implemented which will be described in next section. The red curves are the measured data of the system outputs and the blue curves are simulated variables.

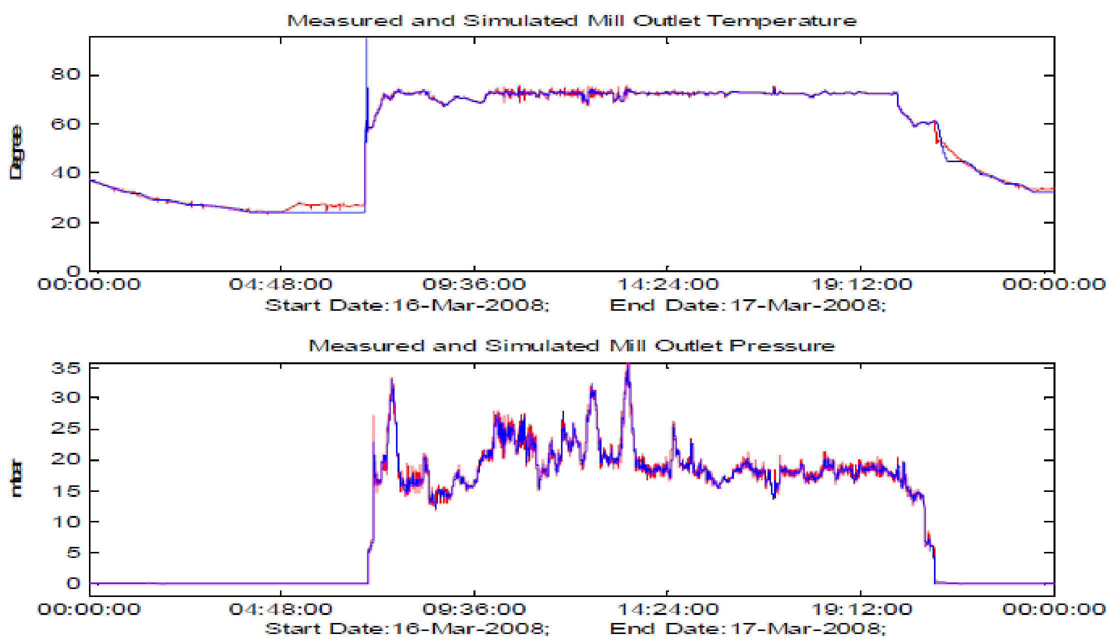

Figure 6.13: Model simulated and measured output using Data Set 1

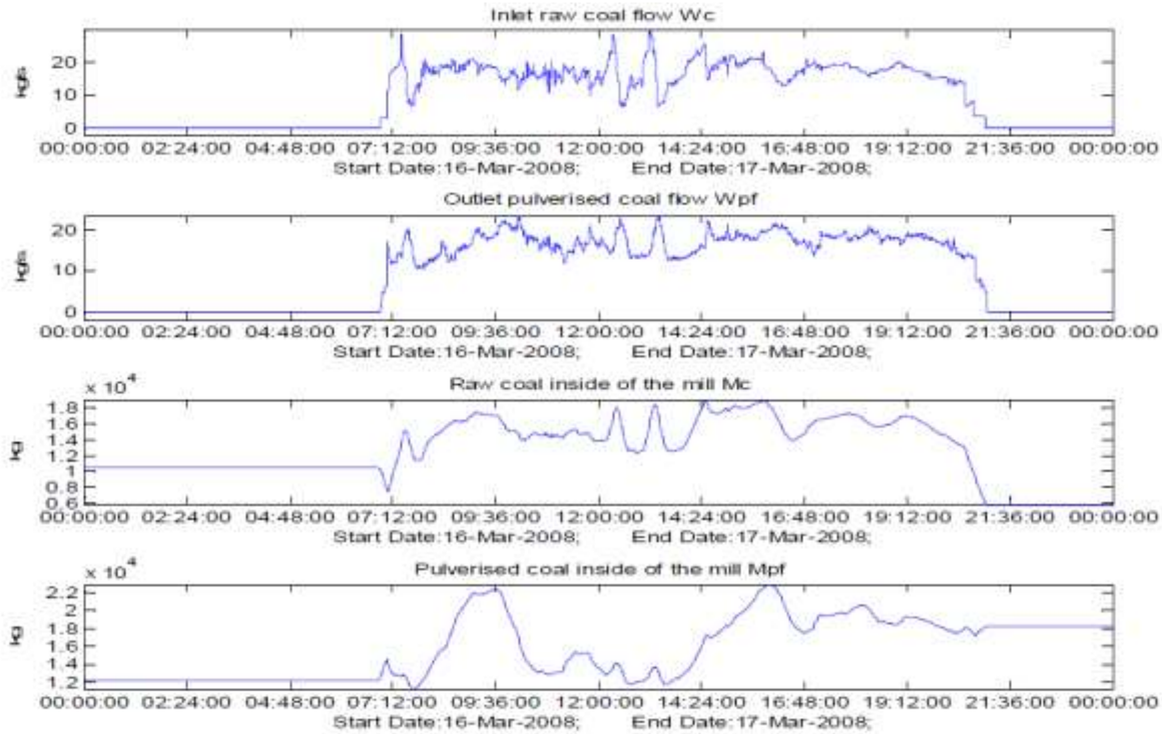

Figure 6.14: Model intermediate variables using Data Set 1

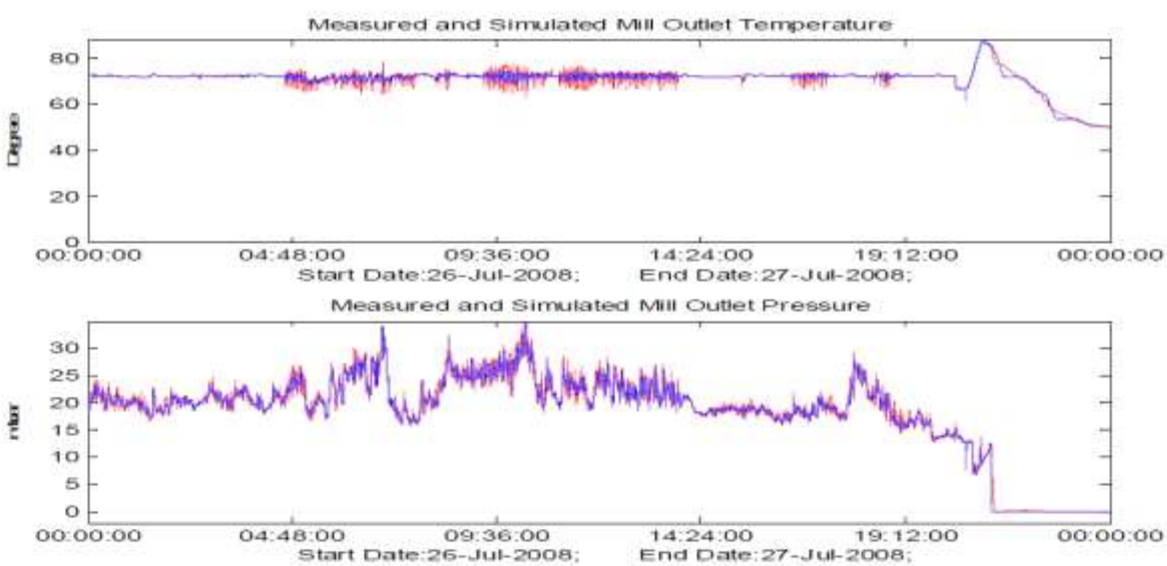

Figure 6.15: Model simulated and measured output using Data Set 2

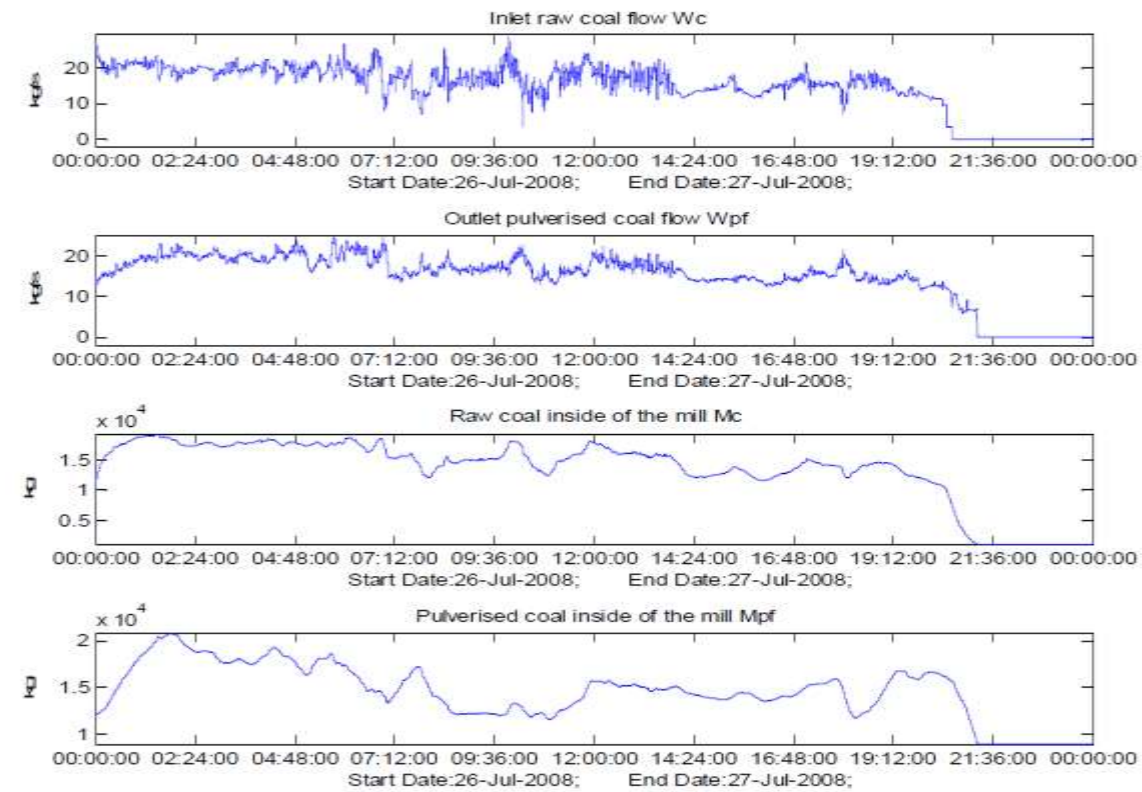

Figure 6.16: Model intermediate variables using Data Set 2

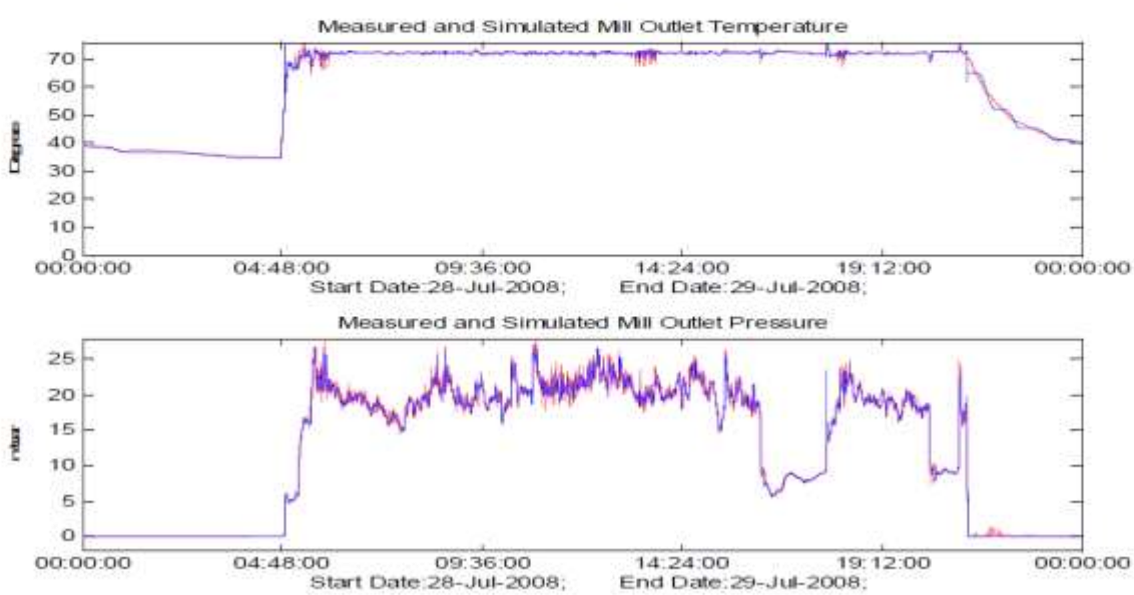

Figure 6.17: Model simulated and measured output using Data Set 3

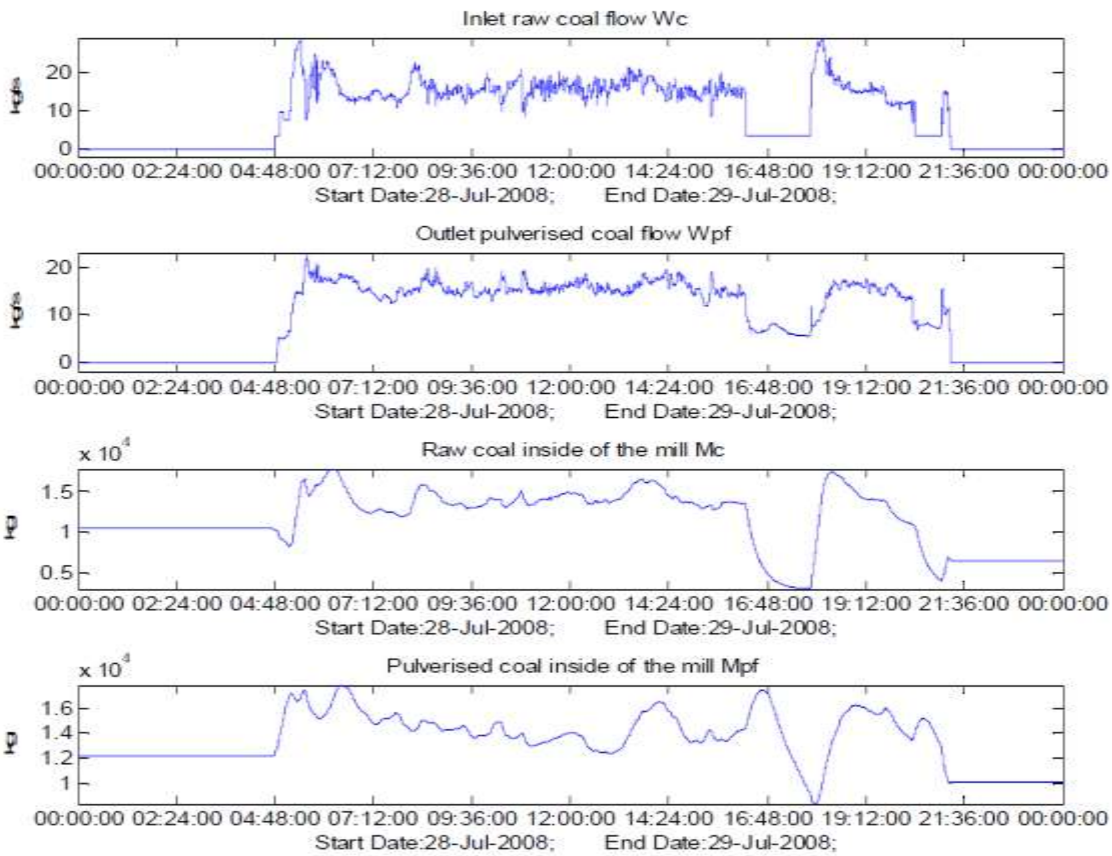

Figure 6.18: Model intermediate variables using Data Set 3

The simulation results indicated that the multi-segment mill model can capture the segment change flag/triggering signals and transfer the model from one segment to the next automatically. The simulated dynamic responses can follow the measured real mill data well. The model should be sufficient to represent the mill main characteristics and features. It can use for model based on-line condition monitoring.

6.5. MODEL BASED MILL CONDITION MONITORING AND FAULT DETECTION

With the mathematical model developed, there are two possible ways for mill condition monitoring and fault detection. The first is a direct observation method by comparing the measured data with the model predicted values. A big or sudden difference between the measured and predicted indicates that some unexpected or unwanted changes may have happened in the mill. To identify if a fault happened, a two step procedure could be applied in general:

Step1: re-identifying the mill parameters;

Step 2: observing the variation trend between the measured and predicted mill variable data values after the new mill parameters were reset. If the predicted values can follow the trend of the measured values, the mill operation conditions changed but no fault happens. If there is still a big gap between the measured and predicted values, it is very likely that a fault happens and an alarm should be raised.

For example, on 9th March 2008, it is noticed that the measured and the simulated data have a big discrepancy. The model parameters were updated in time but it did not reduce the gap in between the measured and simulated data as shown in Figure 6.19. This situation should be alerted as there is a high chance of a mill fault occurred. After discussion with the plant engineers, it is identified that a big choke of biomass was fed into the mill during that period of time. The mill was chocked with uneven blended biomass material. This may cause fires or an unexpected incident and will affect the combustion efficiency, so an alarm should be raised in this situation.

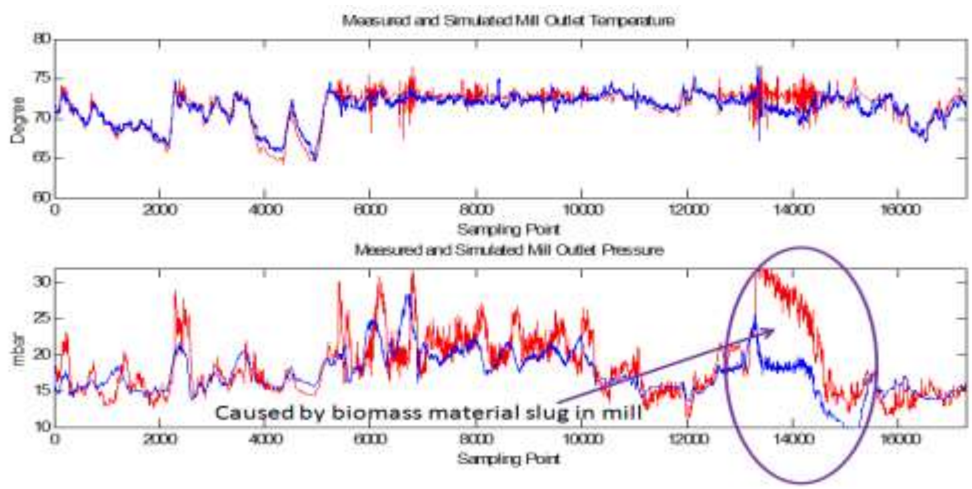

Figure 6.19: Comparing the measured and simulated mill outputs for the data collected on 9th March 2008, 00:00:00 ~ 24:00:00 (24 hours)

The above procedure also indicated another way of mill condition monitoring. Instead of monitoring the mill variable variations, we could update the mill parameters on-line and observe the variation trend of the mill parameters. From our simulation tests, only some model key parameter variations were influenced obviously by the mill operation condition variations. Through our analysis, a scheme is developed which will re-identify the key parameters related to T_{out} or ΔP_{out} on-line but with a longer sampling period compared with the data collection frequency. One example for this parameter observation scheme is given below.

For a particular period of mill operation, initially, the mill model parameters were identified using intelligent algorithms and the values of those parameters are listed in Table 6.3. Then $\hat{K}_{17}$ will update in every 3 or 5 minutes on-line (the updating frequency can be determined for different cases). Instead of observing the mill output variations, the parameter variations were observed. Any unusual changes in the key parameter will be observed and picked up. The simulation results for three different time periods are shown in Figures 6.20-22 drifted.

K1 = 0.008999456176758	K2 = 0.001000000000000	K3 = 0.000010000000000
K9 = 0.004076459761148	K10 = 0.002946259842502	K11 = 0.000374231947854
K12 = 0.000136976632433	K13 = 5.459980534489946	K14 = 0.020000000000000
K15 = 0.001300003051758	K16 = 0.000091967815298	K17 = -0.144579409664105
K18 = -0.807210866010111	K19 = 0.016689349863323	K20 = 0.000003245249092

Table 6.3. The identified model parameters

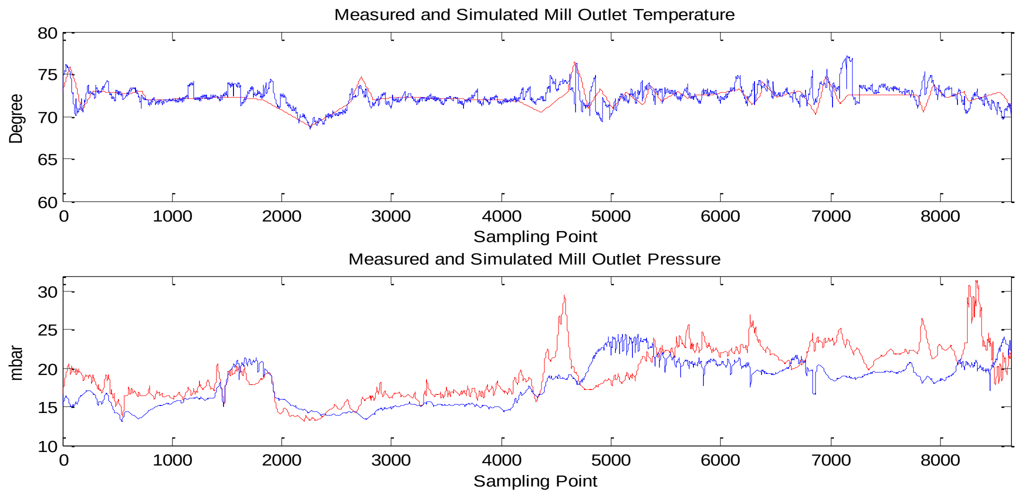

Figure 6.20: Model simulated outputs with $\hat{K}_{17}$ re-identified in every 5 minutes, with the data collected on 3rd July 2007, 00:00:00 ~ 12:00:00 (12 hours)

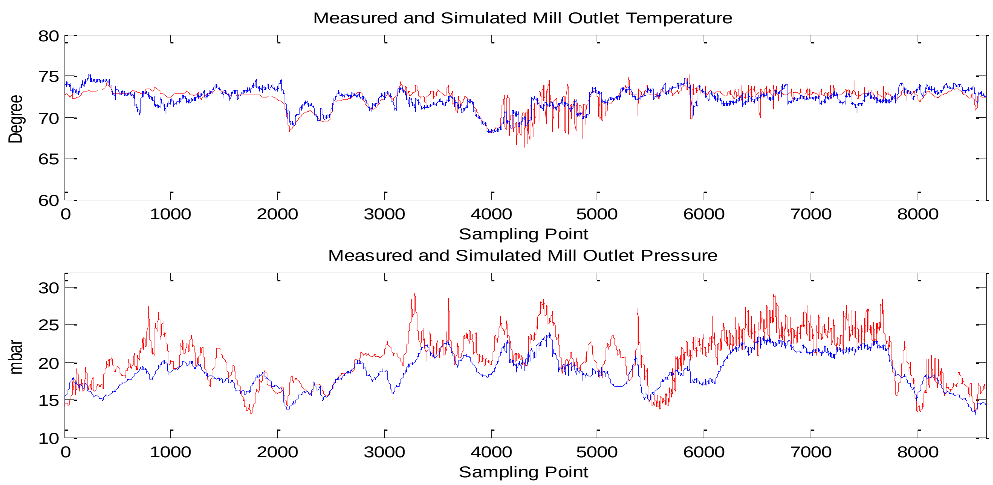

Figure 6.21: Model simulated outputs, with $\hat{K}_{17}$ re-identified in every 5 minutes, with the data collected on 2nd March 2008, 00:00:00 ~ 12:00:00 (12 hours)

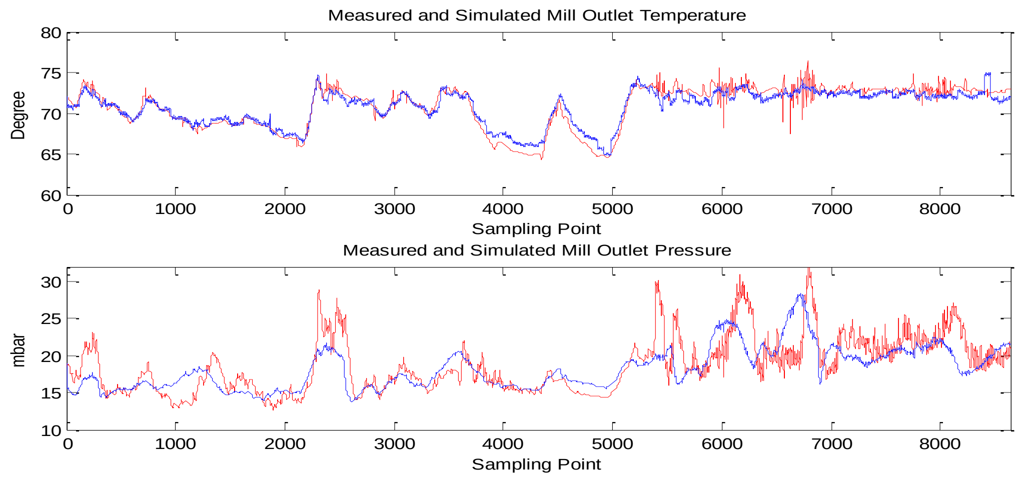

Figure 6.22: Model simulated outputs, with $\hat{K}_{17}$ re-identified in every 5 minutes, with the data collected on 9th March 2008, 00:00:00 ~ 12:00:00 (12 hours)

From the above results, it can be seen that the model simulated results follow the measured data more closely while $\hat{K}_{17}$ was updated in every 5 minutes. Also, the parameters change with time gradually but around the initially identified value.

If the value of $\hat{K}_{17}$ changes dramatically within a very short time period or drifted away from the initial value greatly, this may indicate that there is some sudden changes in the coal mill system or some unwanted or unexpected changes. One application for mill condition monitoring using the parameter updating scheme is to identify the biomass choking. For the simulation results shown in Figure 6.19, the parameter observation scheme is applied. The figure is redrawn with the parameter variations shown alongside the results. From Figure 6.22, we can see that the values of the $\hat{K}_{17}$ varies around -0.14 for the whole first 18 hours period, and the model simulated output of T_{out} for this first period of 18 hours matches the measured T_{out} very well. However, at around 18:30:00, the value of the $\hat{K}_{17}$ suddenly changed rapidly, and it changed very sharply. This sudden change in the parameter $\hat{K}_{17}$ is so obvious. This normally indicates that a big chunk of biomass materials were fed into the mill and was not blended properly. This has a potential to cause fires or other incidents so it should be reported and alarmed.

The scheme can also be used to identify the incident prior to its happening. A plugged incident happened on 4th Oct. 2007 at Cottam Power Station. The incident was analysed using this scheme. Model simulation results are presented in Figures 6.23-24. Monitoring the variations of the key parameters K17 and K18, it can be seen that the values of K17 and K18 move away from the average value for a "thinkable" time period before the incident in order to let the model simulated outputs follow the system measured outputs. These large offsets of K17 and K18 would become the featured pattern to indicate that mill operation condition is severely altered and an incident would be very likely to happen soon. It is also noticed that the intermediate variable of coal inside the mill increased greatly, which indicated that too much coal has been accumulated inside the mill. If the coal inside the mill and the parameter drifting can be noticed, this may be used to identify the incident earlier. The parameters were gradually drifted away from their nominal values for over 1.5 hours. If it can be identified earlier, the potential incident could be reported one hour earlier before the incident and the incident could be prevented. As only one set of incident data was obtained so more incident data are required to validate this prediction before any conclusions can be drawn.

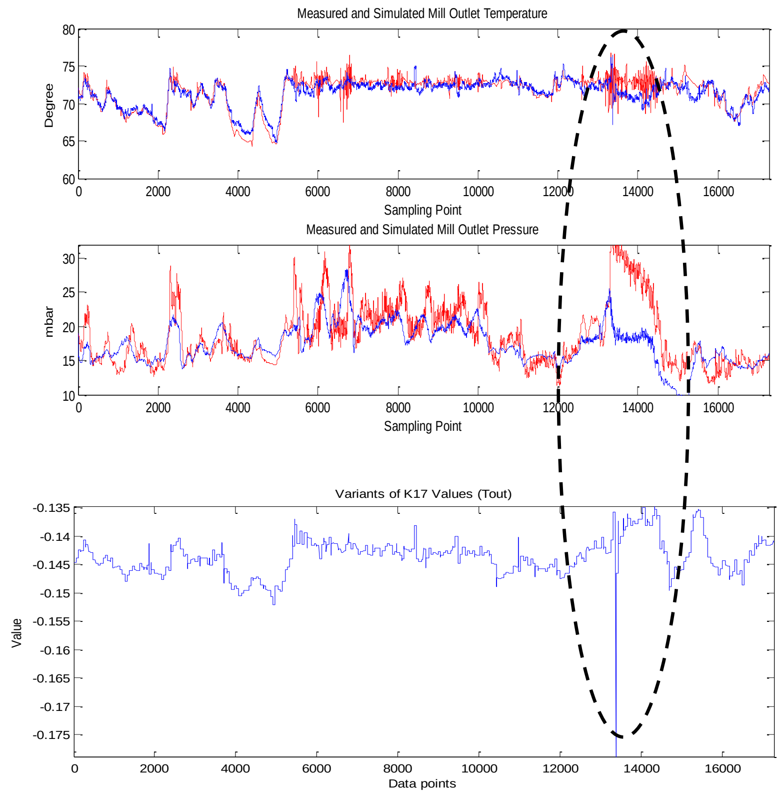

Figure 6.23: Model simulated outputs, with $\hat{K}_{17}$ re-identified in every 5 minutes, with the data collected on 9th March 2008, 00:00:00 ~ 24:00:00 (24 hours)

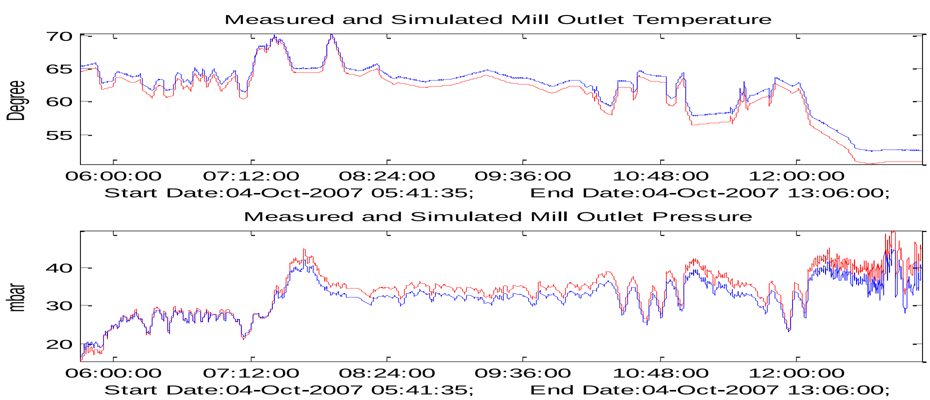

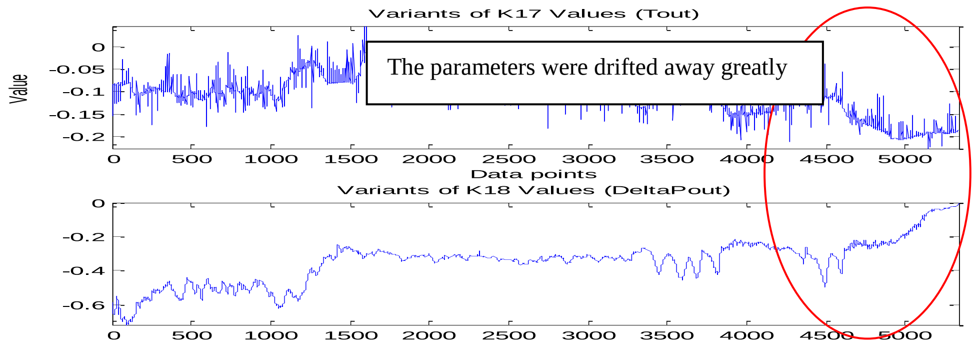

Figure 6.24: The simulation results for data obtained on the day of the incident happening

6.6. SUMMARY

The start-up and shut-down processes were briefly explained in the beginning of this chapter. For each process, the sequence was presented gradually. In the second part of this chapter, the multi-segment of the coal mill model was explained. There are 5 segments that were taken in count. Each segment was analyzed. From the simulation results using the on-site measurement data, the multi segment mill model work well to match all the operation stages.

7. SUMMARY AND RECOMMENDATION FOR FUTURE WORK

7.1. SUMMARY

The research project was carried out with the industrial support and supervision of EDF Energy and E.ON. The main contributions are summarized as follows:

- The pulverized coal mill mathematical model for E-Type vertical spindle mills has been analysed and refined which was developed through a previous research project.
- A multi-segment mathematical model for Tube-Ball mill is developed and the unknown parameters were identified using on-site measurement data from Cottam power plant, in which evolutionary computation techniques are adopted. The multi-segment model covers the whole milling process from the mill start-up to shut-down. The transition from one segment to another is determined/triggered with the signals/variations of the mill status specified in the mill operation procedure.
- The mill model has been verified by comparing the model predicted and measured mill variable values. Both off-line and on-line model validation has been carried out. The predicted mill outputs agree with the measured mill outputs well.
- Two associated computer programs were developed for mill parameter optimization and identification using intelligent algorithms. Two intelligent algorithms – Genetic Algorithms and Particle Swarm Optimization were

implemented, which can be used to search the best fitted values for all the unknown mill parameters.

7.2 RECOMMENDATIONS FOR FUTURE WORK

After the completion of the research project, the university will move further for modelling and safety monitoring of tube ball mills used at power plants. A software package will be developed for mill on-line implementation and condition monitoring. The software will have the following functions:

- Data logging/transferring from/to the power plant computer server via a particular network – cutlass
- Mill model real-time implementation
- Predicted and measured results display
- Operator-friendly software interface
- Condition monitoring functions
- Parameters updating

As this method only employs the currently available on-site measurement data without requiring any extra cost on hardware, this method is cost effective and it is easy for power plants to install.

The software will run independently from all the current power plant control software and will not interfere with any current plant operations. The current software can be installed and integrate with the existing software at Cottam Power Station to serve the purpose of mill condition and safety monitoring. Other power stations can also use the software; therefore, the software outcomes have the potential to benefit all coal fired power station operators in the UK and other countries.

REFERENCE

[1] A.E. Eiben, J.E. Smith, "Introduction to Evolutionary Computing", Springer, NY, 2003.

[2] Ahn, C. W., 2006. Advances in Evolutionary Algorithms - Theory, Design and Practice. Springer-Verlag.

[3] Armitage P., Methods of improving the performance of the John Thompson air swept suction tube ball mills and associated equipment, *EDF Energy Internal Report*, 1983.

[4] Austin, L., Luckie, P., Shoji, K., 1982a. An analysis of ball-and-race milling, part II: The Babcock E-1.7 Mill. Powder Technology 33 (1), 113–125.

[5] Austin, L., Luckie, P., Shoji, K., 1982b. An analysis of ball-and-race milling, part III: Scale-up to Industrial Mills. Powder Technology 33 (1), 127–134. 31

[6] Austin, L., Shah, J., Wang, J., Gallagher, E., Luckie, P., 1981. An analysis of ball-and-race milling, part I: The Hardgrove Mill. Powder Technology 29 (2), 263–275.

[7] Austin, L. G., 1971. Introduction to the mathematical description of grinding as a rate process. Powder Technology 5 (1), 1–17.

[8] Blach L., Wasniowski R., Wisniewski T., "Mathematical model and algorithms of optimal control of coal milling process in the bill mill", *MCIC Report (Metals and Ceramics Information Center),* pp.279-283, 1978

[9] Blankinship, S., 2004. Microwave measurement can optimize coal-fired boiler combustion. Power Engineering 108 (10), 7–8.

[10] Bollinger, K., Snowden, H., 1983. The experimental determination of coal mill models PAS-102 (6), 1473–1477.

[11] British Electricity International, *Modern Power Station Practice: incorporating modern power system practice* (3rd Edition (12 volume set) ed.), Pergamon, 1991

[12] CEGB. Modern Power Station Practice, volume 2. CEGB (Central Electricity Generating Board) Bankside House, London 1961

[13] Clerc M., Kennedy J., "The Particle Swarm-Explosion, Stability, and Convergence in a Multidimensional Somplex space", *IEEE Transaction on Evolutionary Computation*, vol. 6, p. 58-73, 2002

[14] Clerc Maurice, Particle Swarm Optimization, London: ISTE, 2006

[15] Coal Mill Manual from Innogy PLC

[16] Corti L., de Marco A. and Zizzo A., "Mathematical model of a coal mill", in *International Conference on Power Plant Simulation.* vol. 19-21 Nov. Cuernavaca; Morelos (Mexico DF), pp. 206-211, 1984.

[17] Dahl-Soerensen, M., Solberg, B., July 2009. Pulverized fuel control using biased flow measurements. In: Proceedings of the IFAC Symposium on Power Plants and Power Systems Control. Tampere, Finland. Department of Trade and Industry, January 2001. Pulverised fuel (pf) flow measurement and control methods for utility boilers. Technology Status Report 014, London, United Kingdom.

[18] 'Didcot A Dual-fired Power Station', Innogy plc journal, Innogy Plc.

[19] Dong-feng Wang,Pu Han Dao-Gang Peng. Optimal for ball mill pulverizing system and its application. Proceedings of the First International Conference on Machine Learning and Cybernetics.2002:2131-2136.

[20] Edlund, K., Børresen, S., Mølbak, T., Bendtsen, J., 2008. Introducing model predictive control for improving power plant portfolio performance. In: Proceedings of 17th IFAC World Congress. Seoul, Korea. 32

[21] Engelbrecht A.P., Computational Intelligence: John Wiley & Sons Ltd, pp. 185-209, 2001

[22] Fan, G. Q. and Rees, N. W., An intelligent expert system (KBOSS) for power plant coal mill supervision and control, *Control Engineering Practice*, vol. 5, pp. 101-108, 1997

[23] Fan, G., Rees, N., 24-30 November 1994. Modelling of verticle spindle mills in coal fired power plants. In: Proceedings of Electrical Engineering Congress. Sydney, Australia.

[24] Fan, G., Rees, N., Parker, D., August 1997. Analysis of coal mill dynamic characteristics under normal and abnormal operating conditions. In: Pro- ceeding of IFAC/CIGRE Symposium on Control of Power Systems and Power Plants. International Federation of Automatic Control, Beijing, China, pp. 487–493.

[25] Feoktistov, V., 2006. Differential Evolution - In Search of Solutions. Springer.

[26] Hamiane M., "Identification of a pulverized fuel mill from normal operating records using a multivariable polynomial matrix model", International Journal of Modeling and Simulation, vol. 20, pp 227-235, 2000

[27] J. Wei, J. Wang, P. Zachariades "On-Line Condition and Safety Monitoring of Pulverized Coal Mill Using a Model Based Pattern Recognition Technique", BCURA Project B85A-Report I, April 2007

[28] J. Wei, J. Wang, P. Zachariades "On-Line Condition and Safety Monitoring of Pulverized Coal Mill Using a Model Based Pattern Recognition Technique", BCURA Project B85A-Report II, October 2007

[29] J. Wei, J. Wang, P. Zachariades "On-Line Condition and Safety Monitoring of Pulverized Coal Mill Using a Model Based Pattern Recognition Technique", BCURA Project B85A-Report III, April 2008

[30] J. Wei, "Development of Power System Coal Mill and Aggregate Local Area Models using Evolutionary Computation Techniques", PhD Project Thesis, University of Liverpool, 2007

[31] Kennedy, J., Eberhart, R., *Swarm Intelligence*, Morgan Kaufmann Publishers, 2001.

[32] Kennedy, J., Eberhart, R., Particle swarm optimization. *IEEE international conference on Neural Network. Vol. 4*. IEEE Press, pp. 1942-1948, 1995.

[33] Kersting, F., 1984. Mathematical model of a roller mill for fuel grinding and drying in coal-fired power stations. Aufbereitungs-Technik 10, 563–571.

[34] Kitto, J., Stultz, S. (Eds.), 2005. Steam - its generation and use. The Babcock and Wilcox Company.

[35] Laudyn, D., Pawlik, M., Strzelczyk, F., 2007. Elektrownie. Wydawnictwo Naukowo - Techniczne, in Polish.

[36] Laux, S., Grusha, J., McCarthy, K., Rosin, T., 1999. Real time coal flow and particle size measurement for improved boiler operation. Tech. rep., Foster Wheeler Energy Corporation, TR-Tech Int. Oy.

[37] Ljung, L., July 2008. Perspectives on system identification. In: Proc. 17^{th} IFAC World Congress. Seoul, Korea, (Plenary session).

[38] McGriskin P., EDF Energy PF Code of Practice, 2004

[39] Neal, P. W., Waddington, J., Wilson, R., 1980. Determination of mill and 33 boiler characteristics and their effect on steam pressure control. Chem. Eng. Sci. 35 (10), 2107–2114.

[40] Palizban, H. A., O'Kelly, P. A., Rees, N. W., 1995. Practical optimal predic- tive control of power plant coal mills. In: IFAC Control of Power Plants and Power Systems.

[41] Parsopoulos K. E. and Vrahatis M. N., "Practical swarm optimizer in noisy and continuously changing environments", Artificial Intelligence and Soft Computing, vol. pp. 289-294, 2001

[42] Parsopoulos K. E., Plagianakos V. P., Magoulas G. D. and Vrahatis M. N., "Stretching technique for obtaining global minimizers through particle swarm optimization", in *Proc. Particle Swarm Optimization Workshop pp.22-29,* 2001

[43] Peet, W. J. and Leung, T. K. P., Dynamic simulation application in modern power plant control and design, Hong Kong, pp. 121-129, 1994.

[44] Price, K. V., Storn, R. M., Lampinen, J. A., 2005. Differential Evolution: A Practical Approach to Global Optimization. Springer-Verlag.

[45] Pulverized Fuel Systems Manual from *EDF Energy*.

[46] P. Zachariades, J. Wei, J Wang, "Development of a Tube-Ball Coal Mill Mathematical Model Using Intelligent Computation Techniques" The 13th International Conference on Automation and Computing, p.p. 47-52, 2007

[47] Rees, N. W. and Fan, G. Q., Modeling and control of pulverized fuel coal mills, *IEE Power & Energy Series 43: Thermal Power Plant Simulation and Control*, pp. 63-99, 2003.

[48] Rees, N., 1997. Advanced power plant control for large load changes and disturbances. In: Proceedings of the IFAC/CIGRE Symposium on Control of Power Systems and Power Plants, Beijing, China, 18-21 August.

[49] Robinson, G., 1985. A model of the transient operation of a coal pulveriser. Journal of the Institute of Energy 51, 51–63.

[50] Rothlauf, F., 2006. Representations for Genetic and Evolutionary Algo- rithms. Springer.

[51] Sato, K., Meguri, N., Shoji, K., Kanemoto, H., Hasegawa, T., Maruyama, T., March 1996. Breakage of coals in ring-roller mills .1. The breakage properties of various coals and simulation model to predict steady-state mill performance. Powder Technology 86 (3), 275–283. 34

[52] Shi Y., Eberhart R., and Chen Y., “Implementation of evolutionary fuzzy systems”, *IEEE Trans. Fuzzy Systems,* vol. 7(2), pp 109-119, 1999.

[53] Shi Y. and Eberhart R.., “Empirical study of particle swarm optimization”, in Proceedings of the IEEE Congress on Evolutionary Computation (CEC 1999), Piscataway, NJ., 1999

[54] Shoji, K., Meguri, N., Sato, K., Kanemoto, H., Hasegawa, T., Maruyama, T., SEP 1 1998. Breakage of coals in ring-roller mills Part 2. An unsteady-state simulation model. Powder Technology 99 (1), 46–52.

[55] Storn, R., Price, K., 1995. Differential evolution - a simple and efficient adaptive scheme for global optimization over continuous spaces. Tech. Rep. TR-95-012, ICSI.

[57] Su Hong, Chang Xiao-quan. The multi-sensor information fusion technology applied on the measurement of hole plate. Industrial instrument and automatic device.2004,5:20-22.

[58] Tian Liang, Zeng De-liang, Liu Ji-zhen. Data Merging based Deter Mination of the Optimal-load Operating Point of a Ball Mill[J]. JOURNAL OF ENGINEERING FOR THERMAL ENERGY AND POWER, 2004,19(2): 198-203.

[59] Ursem, R., Vadstrup, P., 2003. Parameter identification of induction motors using differential evolution. In: Proc. Congress on Evolutionary Compu- tation CEC ’03. Vol. 2. Canberra, Australia, pp. 790–796 Vol.2.

[60] Wang Lin, Multiple Sensor Information Fusion and its Application, Mater Degree Paper of North China Electric Power Uniersity2002：11-12.

[61] Wei J. L., Wang J., Wu Q. H., Oluwande G. and Boardman M., “Further study on coal mill modeling by machine learning based on on-site measurements”, *in Proc. of International Conference on System Engineering*, Coventry UK, Vol. II, pp 736-741, 2003.

[62] Wei, J. L., Wang, J., Wu, Q. H., September 2007. Development of a mul- tisegment coal mill model using an evolutionary computation technique. IEEE Transactions on Energy Conversion 22 (3), 718–727.

[63] Wei J. L., Wang J. and Wu Q. H., “Development of a Multi-Segment Coal Mill Model Using an Evolutionary Computation Technique”, *IEEE transaction on Energy Conversion*, vol 22, 885-896, 2007.

[64] Weston, Kenneth C., Energy Conversion, St. Paul, MN: West Pub. Co, c1992

[65] William M. Spears, “ Evolutionary Algorithms” , Springer, NY, 2000

[66] Y. G. Zhang, Q. H. Wu, J. Wang, G. Oluwande, D. Matts, X. X. Zhou. Coal Mill Modeling by Machine Learning Based on Onsite Measurements. IEEE TRANSACTION ON ENERGY CONVERSION, 2002, 17(4):549-556.

[67] Zhang Shu-qing, Deng Hong, Wang Yan-ling. Application and Improvement of D-S Evidential Reasoning Theory in Data Fusion. Journey of sensor technology, 2003 1 : 78-81

[68] Zhang Y. G., Wu Q. H., Wang J., Oluwande G., Matts D. and Zhou X. X., “Coal mill modeling by machine learning based on on-site measurements”, *IEEE Transactions on Energy Conversion*, vol. 17, pp 549-555, 2002.

APPENDIX 1 DATA LIST

1	Mill A Inlet Suction.	U1:A43
2	Mill A Inlet Diff	U1:A44
3	Mill A Desired Level	U1:A45
4	Mill A Mill Level	U1:A46
5	Firing Demand	U1:A47
6	Master Pressure MV	U1:A49
7	A1 Feeder Actuator Posn	U1:A52
8	A2 Feeder Actuator Posn	U1:A53
9	Mill A MILLDIFF Plugging Ratio	U1:A54
10	Mill A Inlet Pressure DV	U1:A56
11	Mill A Outlet Temp DV	U1:A58
12	Mill A Outlet Pressure	U1:A60
13	A1 Exhauster Motor Current	U1:A66
14	A1 Exhauster Target Current	U1:A67
15	Load Firing Demand (Same A79)	U1:A72
16	A2 Exhauster Motor Current	U1:A73
17	A2 Exhauster Target Current	U1:A74
18	Mill A A1 Exh Inlet Pressure	U1:A187
19	Mill A A1 Exh Outlet Pressure	U1:A188
20	Mill A A2 Exh Inlet Pressure	U1:A189
21	Mill A A2 Exh Outlet Pressure	U1:A190
22	Mill A Average Motor Current	U1:A195
23	Mill A A1 Feeder Actuator Position	U1:A1720
24	Mill A A1 Feeder Current	U1:A1723
25	Mill A A2 Feeder Actuator Position	U1:A1730

26	Mill A A2 Feeder Current	U1:A1733
27	Mill A Outlet Temp.	U1:A1765
28	Mill A Outlet Temp Error	U1:A1767
29	Mill A Outlet Temp DV	U1:A1768
30	Mill A Inlet Pressure	U1:A1769
31	Mill A Outlet Temp Error	U1:A1771
32	Mill A Outlet Temp DV	U1:A1772
33	Mill 9AB Boost Gas Temp	U1:A1773
34	Mill 9AB Boost Gas Temp DV	U1:A1774
35	Mill 9AB Boost Gas Temp Error	U1:A1776
36	Mill A A2 Exhauster Speed	U1:N154
37	Mill A Outlet Temp	U1:N155
38	Mill A A1 Exhauster Speed	U1:N159
39	Mill A Motor Amps	U1:N161
40	Mill A Inlet Temperature	U1:N170
41	Mill A Outlet Suction Pressure	U1:N173
42	Mill A Boost Gas Temperature	U1:N174